H-INFINITY OUTPUT-FEEDBACK CONTROL: APPLICATION TO UNMANNED AERIAL VEHICLE

by

JYOTIRMAY GADEWADIKAR

Presented to the Faculty of the Graduate School of

The University of Texas at Arlington in Partial Fulfillment

of the Requirements

for the Degree of

DOCTOR OF PHILOSOPHY

THE UNIVERSITY OF TEXAS AT ARLINGTON

May 2007

ACKNOWLEDGEMENTS

Enough can never be said to thank those who have supported me in this task. While working as a Research Assistant with Frank L. Lewis, I have attained a firsthand education in effective problem identification and solving, building coalitions, and navigating a rigorous work environment.

Dr. K. Subbarao's Co-Advising and guidance is the biggest factor for me to contribute the Unmanned Aerial Vehicle part of the dissertation. M. Abu-Khalaf gave invaluable support in my early endeavor to understand the language of the literature. A. Bhilegaonkar was instrumental in implementation support. I would like to thank A. Tiwari, P. Dang, K. Srinath, P. Ballal, and D. Vrabie for giving responsible teaching assistance for Capstone Control System Design Course. I would like to acknowledge my committee members who took time and honored my request to be a part this dissertation.

My parents, and my wife have willingly sacrificed much so that I could afford to spend time to complete these studies. P. Jain, N. Sisodia, V. Agrawal, and T. Pagarani were the four pillars of unquestioning support and trust beyond any fair expectations.

This research was supported by NSF grant ECS-0501451 and ARO grant W91NF-05-1-0314

February 22, 2007

ABSTRACT

H-INFINITY OUTPUT FEEDBACK CONTROL: APPLICATION TO UNMANNED AERIAL VEHICLE

Publication No. _____

Jyotirmay Gadewadikar, PhD.

The University of Texas at Arlington, 2006

Supervising Professor: Frank L. Lewis

This dissertation presents new necessary and sufficient conditions for static output-feedback control of linear time-invariant systems using the H-Infinity approach. Simplified conditions are derived which only require the solution of two coupled matrix design equations. It is shown that the static output-feedback H-Infinity solution does not generally yield a well-defined saddle point for the zero sum differential game; conditions are given under which it does.

This work presents a simplified parameterization of all H-Infinity static state-feedback controllers in terms of a single algebraic Riccati equation and a free parameter matrix. As a special case, necessary and sufficient conditions for the existence of an H-Infinity static output feedback gain are given.

This work also proposes three numerically efficient solution algorithms for the coupled design equations to determine the static output-feedback gain. In two of the algorithms an initial stabilizing gain is not needed. Correctness of these algorithms is proved. These algorithms also give flexibility to relatively weight control input and system performance.

Application to Unmanned Aerial Vehicle exemplifies the power of the theory developed. This work give a procedure for designing compensators of specified structure for shaping the closed loop response that uses H-infinity output-feedback design techniques. The method developed takes advantage of the wealth of experience in aerospace control design. This work also presents the implementation of L_2 Gain Bounded Static Output-Feedback control on Electromechanical Systems. Finally some future applications are explored including wireless networks.

TABLE OF CONTENTS

LIST OF ILLUSTRATIONS

CHAPTER 1

INTRODUCTION

The static output-feedback control, H-Infinity design and parameterization of all stabilizing controllers are three of the most researched and written about issues in modern control. This dissertation brings H-Infinity Design, Output-feedback, parameterization, and iterative design applications together. Achieved theoretical contributions in H-Infinity design techniques are presented. Chapter 1 gives a brief overview and background. In chapter 2, we show that the H-Infinity approach can be used for static output-feedback design to yield a simplified solution procedure that only requires the solution of *one* associated Riccati equation and a coupled gain matrix condition. This explains and illuminates the results in Kucera and de Souza (1995). That is, H-Infinity design provides more straightforward design equations than optimal control, which requires solving three coupled equations.

In chapter 3, we present a parameterization of all stabilizing H-Infinity controllers for continuous-time systems in terms of a single ARE and a free parameter matrix. The form of the result is simple and can be used to select the parameter matrix to satisfy additional design criteria. The result is used to develop necessary and sufficient conditions for existence of a solution to the H-Infinity static output feedback problem for continuous-time systems.

Chapter 4 presents three numerically efficient solution algorithms for the coupled design equations to determine the static output-feedback gain. In two of the algorithms an initial stabilizing gain is not needed. Correctness of these algorithms is proved. These algorithms also give flexibility to relatively weigh control input and system performance. Chapter 5 gives methods to design the controllers for Unmanned Aerial Vehicles (UAVs). Chapter 6 presents the application of L_2 gain bounded output-feedback controller on an electro-mechanical system. In chapter 7 some future applications are explored which includes wireless networks.

We have three objectives. First, we give necessary and sufficient conditions for OPFB with H-Infinity design. Second, we show parameterization of all stabilizing H-Infinity controllers. Third, we suggest less restrictive numerical solution algorithms. F-16 design examples drawn from the popular literature are included to show the power of the approach.

1.1 Review of Related work and Motivation

1.1.1 Review of Static Output-Feedback

The use of output feedback allows flexibility and simplicity of implementation. Moreover, in practical applications, full state measurements are not usually possible. The restricted-measurement static output-feedback (OPFB) problem is of extreme importance in practical controller design applications including flight control in Stevens and Lewis (2003), manufacturing robotics in Kim and Lewis (1998), and elsewhere where it is desired that the controller have certain pre-specified desirable structure, e.g., unity gain outer tracking loop and feedback only from certain available sensors. A

survey of OPFB design results is presented (Syrmos *et al.*, 1994). Finally, though many theoretical conditions have been offered for the existence of OPFB, there are few good solution algorithms. Most existing algorithms require the determination of an *initial stabilizing gain*, which can be extremely difficult.

It is well known that the OPFB optimal control solution can be prescribed in terms of three coupled matrix equations (Lewis and Syrmos, 1995), namely two associated Riccati equations and a spectral radius coupling equation. A sequential numerical algorithm to solve these equations is presented in Moerder and Calise (1985). OPFB stabilizability conditions that only require the solution of two coupled matrix equations are given (Trofino-Neto and Kucera, 1993, Kucera and Desouza, 1995, and Geromel and Peres, 1985). Some recent LMI approaches for OPFB design are presented in El Ghaoui *et al.* (1997), Geromel *et al.* (1998), and Cao *at al.*, (1998). These allow the design of OPFB controllers using numerically efficient software, e.g., the MATLAB LMI toolbox (Gahinet *et al.*, 1995). However several problems are still open, most of the solution algorithms are hard to implement (Lewis, 1995), are difficult to solve for higher order systems, may impose numerical problems and may have restricted solution procedures such as the initial stabilizing gain requirements.

1.1.2 Review of H-Infinity Design

H-Infinity design has played an important role in the study and analysis of control theory since its original formulation in an input-output setting in Zames (1981). It is well known that, through conservative, they provide better response in the presence of disturbance than H_2 optimal techniques. State-space H-Infinity solutions were

rigorously derived for the linear time-invariant case that required solving several associated Riccati equations in Doyle *et al.* (1989). Later, more insight into the problem was given after the H-Infinity linear control problem was posed as a zero-sum two-player differential game (Basar *et al.*, 1991). A thorough treatment of H-Infinity design is given in Knobloch *et al.*, (1993), which also considers the case of OPFB using *dynamic* feedback.

Static OPFB design, as opposed to dynamic output feedback with a regulator, is suitable for the design of aircraft controllers of prescribed structure. Recently H-Infinity design has been considered for static OPFB, Hol and Scherer (2004) addressed the applicability of matrix-valued sum-of-squares (sos) techniques for the computations of LMI lower bounds. Prempain and Postlethwaite (2004) presented conditions for a static output loop shaping controller in terms of two coupled matrix inequalities.

1.1.3 Review of Parameterization

The parameterization of all stabilizing controllers and the static output-feedback control problems are two of the most researched and written about issues in modern control. Static output feedback is indeed a special case of the former problem where the controller gain is restricted to lie in some subspace. The computation of optimal H-Infinity controllers of prescribed order and of static output feedback controllers are non-convex problems, and so are difficult to confront.

The parameterization of all stabilizing polynomial controllers was first given by Youla et al. (1976), and Kucera (1975, 1979) in terms of solutions to a Diophantine equation. The H-Infinity approach (Doyle, Glover, Khargonekar, and Francis, 1989)

has shown its effectiveness in the design of controllers for modern systems in aerospace, vehicle, automotive, industrial systems, and elsewhere. A parameterization of H-Infinity dynamic compensators for the state feedback and full information cases was given by Zhou (1992) in terms of the Hamiltonian matrix and the Youla-Kucera parameterization. A parameterization of all fixed-order H-Infinity dynamic compensators was given by Iwasaki and Skelton (1995) in terms of covariance control and the Lyapunov matrix. A parameterization of all dynamic H-Infinity controllers was given by Mita *et al.* (1998) in terms of two coupled algebraic Riccati equations (ARE). Zeren and Ozbay (2000) provided a solution in terms of linear fractional transformations and algebraic Riccati equations. A technique provided by Campos-Delgado and Zhou (2003) uses norm-constrained stable transfer matrices and a two-stage numerical search procedure. An LMI approach for the computation of optimal H_∞ controllers of prescribed order is given by Hol and Scherer (2004). Henrion, Kucera, and Molina-Cristobal (2005) use the Youla-Kucera parameterization to provide a method for designing low order compensators by simultaneous optimization over the numerator and denominator of the compensator. Application is made to H-Infinity control.

The book by Colaneri, Geromel, and Locatelli (1997) provides a unifying point of view for optimal H_2 and H-Infinity control for linear systems. Parameterization of full information controllers is given, both for static state feedback and dynamic feedback. Parameterization of dynamic output feedback controllers is given in terms of solutions to two algebraic Riccati equations. LMI solutions are also given. Nonlinear

H-Infinity design has been presented in Isidori and Astolfi (1992), which derives a dynamic output feedback regulator in terms of coupled Hamilton-Jacobi equations. A parameterization of nonlinear dynamic output feedback H-Infinity controllers was given there and also by Astolfi (1993), and Yang *et al.* (1996) in terms of nonlinear coupled Hamilton-Jacobi equations. A summary of H_∞ design is given by Knobloch, Isidori, and Flockerzi (1993), which considers disturbance attenuation, full information regulators, and nonlinear H-Infinity techniques including observers.

A survey of static output feedback control is given by Syrmos et al. (1997). Conditions often involve two Riccati equations coupled by a spectral radius condition (Lewis and Syrmos, 1995). Covariance assignment techniques (Hotz and Skelton, 1987, and Skelton and Iwasaki, 1993) involve coupled Lyapunov equations on subspaces. A parameterization of all static output feedback gains is given by Yasuda *et al.* (1993) in terms of such equations. LMI approaches have been presented by Iwasaki and Skelton (1995), where a parameterization was also presented. In Colaneri, Geromel, and Locatelli (1997), & Geromel, de Souza, and Skelton (1998), a parameterization of static output feedback gains is given in terms of the blocks of a symmetric matrix derived from coupled matrix inequalities. Also provided is a condition in terms of a matrix and its inverse. A numerical procedure is given to determine these quantities. LMI conditions for optimal and H-Infinity static output feedback are given by Shaked (2003).

Solutions to the parameterization of all stabilizing controllers and the output feedback problems are generally complex, depending for instance on coupled Riccati

equations, LMIs, or on a matrix and its inverse belonging to some sets. Moerder and Calise (1985) presented an algorithm for computing the optimal H_2 static output feedback gain that is in standard use, along with a convergence proof. This algorithm is extended and used for aircraft control design in Stevens and Lewis (2003). An initial stabilizing output-feedback gain is needed, which is difficult to determine for practical systems. Recent results address these issues. Jen-Te Yu (2004) provides a solution for the optimal static output feedback problem in terms of two AREs plus a projective coupling condition, but the AREs are standard ones involving state feedback, not output feedback. An algorithm is presented that requires an initial stabilizing state feedback gain, which is easy to find using standard LQR methods. Yang and Moore (2004) give an algorithm for static output feedback based on alternating projections.

A solution to the H-Infinity static output feedback problem is given by Gu and Misra (1994) for a restricted class of systems in terms of a *single* ARE and a related negative definiteness condition. Trofino-Neto and Kucera (1993) solve the static output feedback problem using inverse optimal control in terms of a single ARE projected onto nullspace perpendicular of C and a free parameter matrix. Astolfi and Colaneri (2000, 2001) present results in terms of a single ARE plus a condition holding over the nullspace of C. This is also recast as a pair of LMI with a nonlinear coupling equation. In Astolfi and Colaneri (2000b) this approach was used to give a parameterization of all static output feedback controllers, and in (Astolfi and Colaneri (2000, 2002, 1993) the results were generalized to nonlinear systems.

Geromel and Peres (1985) give a sufficient condition for a stabilizing static output feedback in terms of a single ARE with a free parameter matrix, plus a condition on the form of the gain matrix. A computational algorithm is proposed. Kucera and de Souza (1995) provide necessary and sufficient conditions for stabilizing static output feedback control using these constructions. Gadewadikar *et al.*, extend these conditions to obtain necessary and sufficient conditions for the existence of an H-Infinity static output feedback control. Geromel *et al.* (1989) provide similar results for the discrete-time case for decentralized feedback and output feedback. De Souza and Xie (1992) provide for the discrete-time case a parameterization of all stabilizing H-Infinity controllers in terms of similar constructions, and use that result to solve the H-Infinity static output feedback problem for discrete systems.

1.2 Mathematical Preliminaries and Notations

Over the years a terminology for H-Infinity Control has been developed. This section describes the basic concepts and background material related to analysis and control of linear systems using H-Infinity techniques. More details are described in B. Francis's Lecture Notes in Mathematics (Mosca *et al.*, 1990).

1.2.1 Norms for Signals and Systems

We consider systems which are linear, time-invariant, causal and finite dimensional. In the time domain an input-output model for such a system has the form of a convolution function.

$$y(t) = \int_{-\infty}^{\infty} g(t-\tau)u(\tau)d\tau$$

Such a system has an equivalent state-space model

$$\dot{x}(t) = Ax(t) + Bu(t),$$

$$y(t) = Cx(t) + Du(t)$$

Where *A, B, C, D* are real matrices of appropriate size.

Let $G(s)$ denote the system transfer matrix

$$G(s) = D + C(sI - A)^{-1}B$$

Another popular notation is the packed-matrix notation given by

$$G(s) = \begin{bmatrix} A & B \\ C & D \end{bmatrix}$$

Note that

$$\begin{bmatrix} A & B \\ C & D \end{bmatrix}$$

is a block matrix, not a transfer function.

One way to describe the performance control system is in terms of the size of certain signals of interest. Next section describes several ways of defining a signal's size, i. e. several norms of the signals. For simplicity, all signals are assumed to be scalar-valued. We consider signal mapping $(-\infty, \infty)$, for simplicity they are assumed to be piecewise continuous.

L_p-norm, $1 \le p < \infty$: The L_p norm of a signal $u(t)$ is

$$\|u\|_p = \left(\int_{-\infty}^{\infty} |u(t)|^p \, dt \right)^{1/p} \tag{1.1}$$

L_∞-norm

$$\|u\|_\infty = \sup_t |u(t)| \tag{1.2}$$

Norms for Systems

We introduce norms for a stable transfer function *G*:

H_p -norm, $1 \le p < \infty$

$$\|G\|_p = \left(\int_{-\infty}^{\infty} |G(j\omega)|^p \, d\omega \right)^{1/p} \tag{1.3}$$

H-Infinity -norm

$$\|G\|_\infty = \sup_\omega |G(j\omega)| \tag{1.4}$$

More generally H_∞ denotes the space of bounded analytic functions in the open right half-plane.

1.2.2 Hamiltonian Matrix Notation

The solution to the H-Infinity Control problem contains Algebraic Riccati Equations; the following Hamiltonian matrix notation (Knobolch *et al.*, 1993) is introduced to simplify solution representation. Consider the following riccati equation

$$A^T P + PA + Q - PBR^{-1}B^T P = 0 \tag{1.5}$$

The stabilizing solution of this equation is denoted by $P = Ric(H)$ where H is

$$H = \begin{bmatrix} A & -BR^{-1}B^T \\ -Q & -A^T \end{bmatrix} \text{ and } (A - BR^{-1}B^T P) \text{ is stable.}$$

1.2.3 Two-Port Block Diagram Representation

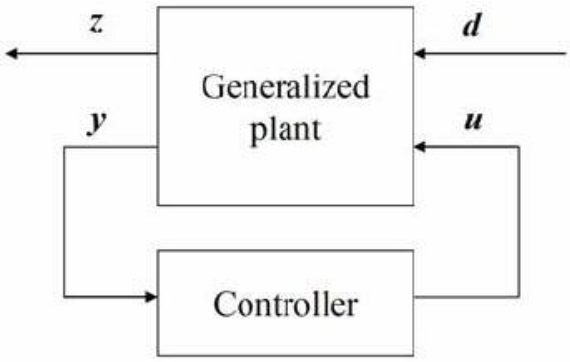

Figure 1.1 Two port block diagram

The two port diagram shown represents a variety of problems of interest. The diagram contains two main blocks, the plant and the controller. The plant section has two inputs and two outputs. The plant inputs are classified as control inputs and the disturbance. The control input, u is the output of the controller, which become the input to the actuators driving the plant. The disturbance, *d(t)* is actually a collection of exogenous inputs. The main distinction between *d(t)* and *u(t)* is that controller can not manipulate exogenous inputs. The plant outputs are also characterized into two groups. The first group *y(t)*, are signals that are measured and feedback. These become input to the controller. The second group, *z(t)* are the performance outputs. These are all the signals we are interested in controlling or regulating.

1.2.4 Interpreting H-Infinity Design Problems

H-Infinity control problems can be formulated in many ways, here is the most simplified interpretation of the problem is to find controller for the generalized plant such that Infinity norm of the transfer function relating exogenous input *d(t)* to

performance output *z(t)* is minimum (consider the two port diagram in Figure 1.1). The minimum gain is denoted by γ^*. If the norm for an arbitrary stabilizing controller is $\gamma > \gamma^*$ then system is L_2 gain bounded. To solve the H-Infinity problem we start with a value of γ and reduce it until γ^* is achieved.

CHAPTER 2

H-INFINITY OUTPUT FEEDBACK

This chapter presents new necessary and sufficient conditions for H-Infinity output-feedback design. Section 2.1 establishes system definitions with input, performance output, and disturbance notations; output-feedback stabilizability and detectability are discussed as well. Next section formulates bounded L_2 gain design problem in the context of output feedback control. Section 2.3 builds the foundation blocks for the main results; here intermediate mathematical analysis is presented to simplify the derivations of the main necessary and sufficient conditions in section 2.4. Finally section 2.5 presents the optimality conditions *i.e.* conditions of existence of well defined game theoretic solution are derived.

2.1 System Description and Definitions

Consider the linear time-invariant system of Figure 2.1 with control input *u(t)* output *y(t)*, and disturbance *d(t)* given by

$$\dot{x} = Ax + Bu + Dd\ ,\ y = Cx \tag{2.1}$$

and a performance output *z(t)* that satisfies

$$\|z(t)\|^2 = x^T Q x + u^T R u\ ,\ y = Cx\ ,$$

for some positive matrices $Q \geq 0$ and $R > 0$. It is assumed that *C* has full row rank, a standard assumption to avoid redundant measurements.

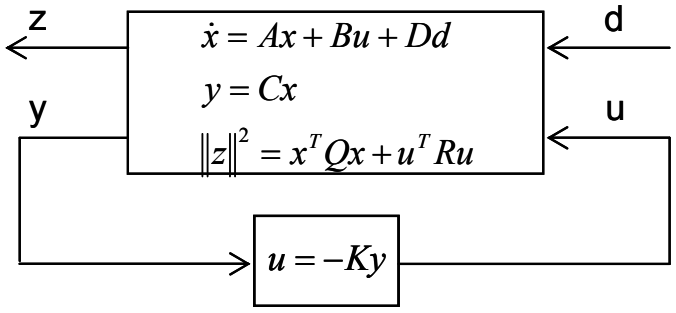

Figure 2.1 System Description H-Infinity Output Feedback

By definition the pair *(A, B)* is said to be stabilizable if there exists a real matrix *K* such that $A - BK$ is (asymptotically) stable. The pair (A, C) is said to be detectable if there exists a real matrix L such that $A - LC$ is stable. System (2.1) is said to be output feedback stabilizable if there exists a real matrix K such that $A - BKC$ is stable.

2.2 Bounded L_2 Gain Design Problem

The System L_2 gain is said to be *bounded or attenuated by* γ if

$$\frac{\int_0^\infty \|z(t)\|^2 dt}{\int_0^\infty \|d(t)\|^2 dt} = \frac{\int_0^\infty (x^T Qx + u^T Ru)dt}{\int_0^\infty (d^T d)dt} \le \gamma^2 \tag{2.2}$$

Defining a constant output-feedback control as

$$u = -Ky = -KCx \tag{2.3}$$

it is desired to find a constant output-feedback gain *K* such that the system is stable and the L_2 gain is bounded by a prescribed value γ.

2.3 Intermediate Mathematical Analysis

To find a constant output-feedback gain K as described in previous section, one may define the value functional given by Equation (2.4)

$$
\begin{aligned}
& J(K,d) \\
&= \int_0^\infty (x^T Q x + u^T R u - \gamma^2 d^T d)\, dt \\
&= \int_0^\infty [x^T (Q + C^T K^T R K C) x - \gamma^2 d^T d] dt,
\end{aligned}
\tag{2.4}
$$

the corresponding Hamiltonian is defined as

$$
\begin{aligned}
& H(x, V_x, K, d) \\
&= \frac{\partial V}{\partial x}^T [(A - BKC)x + Dd] + x^T (Q + C^T K^T R K C) x - \gamma^2 d^T d
\end{aligned}
\tag{2.5}
$$

with co-state $\frac{\partial V}{\partial x}$. It is known that for linear systems the value functional *V(x)* is quadratic and may be taken in the form $V = x^T P x > 0$ without loss of generality. We shall do so throughout the chapter.

Two lemmas simplify the presentation of our main Theorem 2.1 which solves this OPFB control problem. Lemma 2.1 is a mathematical description of Hamiltonian *H*, Equation (2.5) at given predefined disturbance *d**, Equation (2.6) and gain *K**, Equation (2.7). It shows that if the gain *K** exists the Hamiltonian takes on a special form.

Lemma 2.1: For the disturbance defined as

$$
d^*(t) = \frac{1}{\gamma^2} D^T P x\,, \tag{2.6}
$$

if there exists K^* satisfying

$$
K^* C = R^{-1}(B^T P + L), \tag{2.7}
$$

for some matrix *L*, then one can write

$$H(x, V_x, K^*, d^*) =$$
$$x^T[PA + A^T P + Q + \frac{1}{\gamma^2} PDD^T P - PBR^{-1}B^T P + L^T R^{-1} L]x. \tag{2.8}$$

Remark. The meaning of d^* and K^* and the special Hamiltonian $H(x, V_x, K^*, d^*)$ will be discussed later. The existence of K^* satisfying Equation (2.7) is addressed in Theorem 1.

Proof : Introduce a quadratic form *V(x)*

$$V = x^T Px > 0. \tag{2.9}$$

Then $\frac{\partial V}{\partial x} = 2Px$, and substitution in Equation (2.5) will give

$$\begin{aligned} &H(x, V_x, K, d) \\ &= 2x^T P[(A - BKC)x + Dd] + x^T (Q + C^T K^T RKC)x - \gamma^2 d^T d \end{aligned} \tag{2.10}$$

Note that, $H(x, V_x K, d)$ is globally concave in *d*. To find a maximizing disturbance set $0 = \frac{\partial H}{\partial d} = 2D^T Px - 2\gamma^2 d$. This defines the maximizing or worst case disturbance (2.6). Substitute Equation (2.6) into Equation (2.10) to get

$$\begin{aligned} &H(x, V_x, K, d^*) \\ &= 2x^T P[(A - BKC)x + D\frac{1}{\gamma^2} D^T Px] \\ &+ x^T (Q + C^T K^T RKC)x - \gamma^2 \left(\frac{1}{\gamma^2} D^T Px\right)^T \frac{1}{\gamma^2} D^T Px \\ &= x^T [P\ A + A^T P + Q + \frac{1}{\gamma^2} PDD^T P - \\ &PBKC - C^T K^T B^T P + C^T K^T RKC]x \end{aligned}$$

Completing the squares yields

$$
\begin{aligned}
&H(x, V_x, K, d^*) \\
&= x^T [PA + A^T P + Q + \frac{1}{\gamma^2} PDD^T P - PBR^{-1} B^T P \\
&+ (KC - R^{-1} B^T P)^T R(KC - R^{-1} B^T P)]x
\end{aligned} \tag{2.11}
$$

Substituting the gain defined by Equation (2.7) into Equation (2.11) yields Equation (2.8)

$$
\begin{aligned}
&H(x, V_x, K^*, d^*) \\
&= x^T [PA + A^T P + Q + \frac{1}{\gamma^2} PDD^T P - PBR^{-1} B^T P + \\
&(R^{-1} B^T P + R^{-1} L - R^{-1} B^T P)^T R(R^{-1} B^T P + R^{-1} L - R^{-1} B^T P)]x
\end{aligned}
$$

Or

$$
\begin{aligned}
&H(x, V_x, K^*, d^*) \\
&= x^T [PA + A^T P + Q + \frac{1}{\gamma^2} PDD^T P - PBR^{-1} B^T P + L^T R^{-1} L]x.
\end{aligned}
$$

The next Lemma expresses the Hamiltonian for any K and $d(t)$ in terms of the Hamiltonian for K^* and $d^*(t)$.

Lemma 2.2: Suppose there exists K^* so that Lemma 2.1 holds, then for any $x(t)$, K and $d(t)$ one can write

$$
\begin{aligned}
&H(x, V_x, K, d) \\
&= H(x, V_x, K^*, d^*) \\
&+ x^T [L + R(K - K^*)C]^T R^{-1} [L + R(K - K^*)C]x \\
&- x^T [L^T R^{-1} L]x - \gamma^2 \left\| d - d^* \right\|^2
\end{aligned} \tag{2.12}
$$

for K^* satisfying Equation (2.7), d^* satisfying Equation (2.6).

Proof: Now one has for any $x(t)$, K, $d(t)$, and a quadratic form $V(x)$ defined by Equation (2.9)

$$H(x,V_x,K,d) = \\ 2x^T P[(A-BKC)x+Dd] + x^T(Q+C^T K^T RKC)x - \gamma^2 d^T d \tag{2.13}$$

whence, one may derive

$$\begin{aligned} &H(x,V_x,K,d) \\ &= x^T\ [PA + A^T P + Q + \frac{1}{\gamma^2} PDD^T P - PBR^{-1}B^T P + L^T R^{-1} L]x \\ &+ x^T[-PBKC - C^T K^T B^T P + C^T K^T RKC - \frac{1}{\gamma^2} PDD^T P + PBR^{-1}B^T P - L^T R^{-1} L]x \\ &+ x^T 2PDd - \gamma^2 d^T d \end{aligned}$$

or

$$\begin{aligned} &H(x,V_x,K,d) \\ &= H(x,V_x K^*,d^*) \\ &+ x^T[-PB(KC - R^{-1}B^T P) - C^T K^T(B^T P - RKC) - L^T R^{-1} L]x \\ &+ x^T[-\frac{1}{\gamma^2} PDD^T P]x + x^T 2PDd - \gamma^2 d^T d \end{aligned} \tag{2.14}$$

Substituting $R^{-1}(B^T P + L) = K^* C$, $R^{-1}B^T P = K^* C - R^{-1}L$, $B^T P = RK^* C - L$, and $PB = C^T (K^*)^T R - L^T$ into the first term in square brackets yields, after some manipulations

$$\begin{aligned} &x^T[-PB(KC - R^{-1}B^T P) - C^T K^T(B^T P - RKC) - L^T R^{-1} L]x \\ &= x^T[C^T(K-K^*)^T R(K-K^*)C]x \\ &+ x^T[L^T R^{-1} L + C^T(K-K^*)^T L + L^T(K-K^*)C - L^T R^{-1} L]x \end{aligned}$$

The result contains non-square terms. One must change these into square form and study the contribution in order to reach any conclusion, therefore complete the square to see that

$$x^T[L^T R^{-1} L + C^T (K - K^*)^T L + L^T (K - K^*)C - L^T R^{-1} L]x$$
$$= x^T[\{L^T + C^T (K - K^*)^T R\}R^{-1}\{L + R(K - K^*)C\}$$
$$- C^T (K - K^*)^T RR^{-1} R(K - K^*)C - L^T R^{-1} L]x$$

Therefore one has

$$x^T[-PB(KC - R^{-1}B^T P) - C^T K^T (B^T P - RKC) - L^T R^{-1} L]x$$
$$= x^T[\{L^T + C^T (K - K^*)^T R\}R^{-1}\{L + R(K - K^*)C\} - L^T R^{-1} L]x \quad (2.15)$$

Consider now the remaining three terms on the right-hand side of Equation (2.14). One has $d^* = \frac{1}{\gamma^2} D^T Px$, so that

$(d^*)^T = \frac{1}{\gamma^2} x^T PD$, $x^T PD = \gamma^2 (d^*)^T$, and $\gamma^4 d^* (d^*)^T = x^T [PDD^T P]x$. Therefore one can show

$$x^T[-\frac{1}{\gamma^2} PDD^T P]x + x^T 2PDd - \gamma^2 d^T d = -\gamma^2 \|d - d^*\|^2 \quad (2.16)$$

Substituting now Equations (2.16) and (2.15) into (2.14) yields Equation (2.12).

Remarks:

1. According to the proof and the form of the Hamiltonian in Equation (2.12), *d*(t)* given by Equation (2.6) can be interpreted as a worst-case disturbance since the equation is negative definite in $\|d - d^*\|$.
2. The form (2.12) of the Hamiltonian does not allow the interpretation of *K** defined by Equation (2.7) as a minimizing control. More shall be said about this subsequently.

2.4 Necessary and Sufficient Conditions

Theorem 2.1. Necessary and Sufficient Conditions for H-infinity Static OPFB Control:

Assume that $Q \geq 0$ and (A, $\sqrt{Q}$) is detectable. Then system defined by Equation (2.1) is output-feedback stabilizable with L_2 gain bounded by γ , if and only if

i. *(A, B)* is stabilizable and *(A, C)* is detectable

ii. There exist matrices K^* and L such that

$$K^* C = R^{-1}(B^T P + L) \tag{2.17}$$

where $P>0$, $P^T = P$, is a solution of

$$PA + A^T P + Q + \frac{1}{\gamma^2} PDD^T P - PBR^{-1}B^T P + L^T R^{-1} L = 0 \tag{2.18}$$

Proof:

Sufficiency. To prove sufficiency first note that Lemma 2.1 shows that $H(x, V_x, K^*, d^*) = 0$ if (ii) holds. It is next required to show bounded L_2 gain if (ii) holds. From Lemma 2.1 and Lemma 2.2, one has for any *K, x(t),* and *d(t)*

$$\begin{aligned} & H(x, V_x, K, d) \\ & = x^T [L + R(K - K^*)C]^T R^{-1} [L + R(K - K^*)C]x \\ & - x^T [L^T R^{-1} L]x - \gamma^2 \left\| d - d^* \right\|^2 \end{aligned} \tag{2.20}$$

Note that one has, along the system trajectories, for $u = -Ky = -KCx$

$\frac{dV}{dt} = \frac{\partial V}{\partial t} + \frac{\partial V}{\partial x}^T \dot{x} = \frac{\partial V}{\partial x}^T (Ax + Bu + Dd) = \frac{\partial V}{\partial x}^T [(A - BKC)x + Dd]$, so that from Equation (2.5)

$$H(x,V_x,K,d)=\frac{dV}{dt}+x^T(Q+C^TK^TRKC)x-\gamma^2d^Td \tag{2.21}$$

With Equations (20) and (21)

$$\begin{aligned}&x^T[L+R(K-K^*)C]^TR^{-1}[L+R(K-K^*)C]x\\&-x^T[L^TR^{-1}L]x-\gamma^2\|d-d^*\|^2\\&=\frac{dV}{dt}+x^T(Q+C^TK^TRKC)x-\gamma^2d^Td.\end{aligned}$$

Selecting $K= K^*$, for all $d(t)$, and x(t)

$$\begin{aligned}&\frac{dV}{dt}+x^T(Q+C^TK^TRKC)x-\gamma^2d^Td=\\&-x^T[L^TR^{-1}L]x-\gamma^2\|d-d^*\|^2\le 0.\end{aligned} \tag{2.22}$$

Integrating this equation yields

$$V(x(T))-V(x(0))+\int_0^T[x^T(Q+C^TK^TRKC)x-\gamma^2d^Td]\,dt\le 0 \tag{2.22}$$

Selecting $x(0)=0$ and noting that non-negativity implies $V(x(T))\ge 0 \quad \forall T$, one obtains

$$\int_0^T x^T(Q+C^TK^TRKC)x\,dt\le\gamma^2\int_0^T d^Td\,dt \tag{2.24}$$

for all $T>0$, so that the L_2 gain is less than γ.

Finally, to prove the stability of the closed-loop system, letting $d(t)=0$ in Equation (2.22) one has

$$\frac{dV}{dt}\le -x^T(Q+C^TK^TRKC)x\le -x^TQx\,. \tag{2.25}$$

Now detectability of (A, $\sqrt{Q}$) shows that the system is locally AS with Lyapunov function *V(x)*.

Necessity. To prove necessity, suppose that there exists an output feedback gain K that stabilizes the system and satisfies L_2 gain $< \gamma$. It follows that $A_c \equiv A - BKC$ is stable. Since $A - BKC = A + \overline{L}C = A + B\overline{K}$, then (i) follows.

Consider the equation

$$A_c{}^T P + PA_c + \frac{1}{\gamma^2} PDD^T P + Q + C^T K^T RKC = 0. \tag{2.26}$$

From Knobloch, Isidori, & Flockerzi, 1993, Theorem 2.3.1, closed-loop stability and L_2 gain boundedness implies that Equation (2.26) has a unique symmetric solution such that $P \geq 0$. Rearranging Equation (2.26) and completing the square will yield.

$$\begin{aligned} & PA + A^T P + Q + \frac{1}{\gamma^2} PDD^T P - PBR^{-1} B^T P \\ & + (KC - R^{-1} B^T P)^T R(KC - R^{-1} B^T P) \\ & = 0. \end{aligned} \tag{2.27}$$

Equation (2.18) is obtained from Equation (2.27) for the gain defined by Equation (2.17) and (ii) is verified.

Note that Equation (2.26) is a Lyapunov equation referred to the output *z(t)*, since $\|z(t)\|^2 = x^T Qx + u^T Ru$. Moreover, this theorem reveals the importance of the

Hamiltonian $H(x,V_x,K^*,d^*)$ since the equation $H(x,V_x,K^*,d^*)=0$ must hold for a stabilizing OPFB with bounded H-infinity gain. Note further that if *C=I, L=0*, this theorem reduces to known results for full state variable feedback.

2.5 Existence of Game Theoretic Solution

The form of Equation (2.12) does not allow the interpretation of *(K*, d*)* as a well-defined saddle point. The purpose of this section is to study when the two policies are in saddle point equilibrium for static output-feedback H_∞ . This means one has a Nash equilibrium in the game theoretic sense as discussed in Basar *et al.*, 1991, so that the H_∞ OPFB problem has a unique solution for the resulting *L.* In fact, this is the case when Theorem 2.1 is satisfied with *L=0*, as we now show using notions from two-player, zero-sum differential game theory (Knobloch *et al.*, 1993, and Basar *et al.*, 1991). The minimizing player controls *u(t)* and maximizing player controls *d(t).*

Theorem 2.2: Existence of Well-Defined Game Theory Solution

(K,d*)* is a well-defined game theoretic saddle point corresponding to a zero-sum differential game if and only if L is such that

$$M \equiv L^T(K-K^*)C + C^T(K-K^*)^T L + C^T(K-K^*)^T R(K-K^*)C \geq 0 \tag{2.28}$$

when $K \neq K^*$.

Note that this is always true if *L=0*.

Proof:

Equation (2.12) becomes

$$H(x,V_x,K,d) =$$
$$H(x,V_x,K^*,d^*) + x^T[L + R(K-K^*)C]^T R^{-1}[L + R(K-K^*)C]x$$
$$- x^T[L^T R^{-1} L]x - \gamma^2 \|d - d^*\|^2$$

$$H(x,V_x,K,d)$$
$$= H(x,V_x,K^*,d^*) + x^T[L + R(K-K^*)C]^T R^{-1}[L + R(K-K^*)C]x$$
$$- x^T[L^T R^{-1} L]x - \gamma^2 \|d - d^*\|^2$$
$$= H(x,V_x,K^*,d^*) + x^T L^T R^{-1} Lx +$$
$$x^T L^T (K-K^*)Cx + x^T[R(K-K^*)C]^T R^{-1} Lx +$$
$$x^T[R(K-K^*)C]^T R^{-1}[R(K-K^*)C]x - x^T[L^T R^{-1} L]x - \gamma^2 \|d - d^*\|^2$$

$$H(x,V_x,K,d) = H(x,V_x,K^*,d^*) + x^T Mx - \gamma^2 \|d - d^*\|^2, \qquad (2.29)$$

under the condition defined by Equation (2.28), one has

$$H(x,V_x,K^*,d) \le H(x,V_x,K^*,d^*) \le H(x,V_x,K,d^*) \qquad (2.30)$$

or

$$\frac{\partial^2 H}{\partial u^2} > 0, \qquad \frac{\partial^2 H}{\partial d^2} < 0, \qquad (2.31)$$

at (K*, d*). It is known that a saddle point at the Hamiltonian implies a saddle point at the value function *J* when considering finite-horizon zero sum games. For the infinite horizon case, the same strategies remain in saddle point equilibrium when sought among the class of stabilizing non-anticipative strategies (Basar and Oldser, 1998). Therefore, this implies that

$$\frac{\partial^2 J}{\partial u^2} > 0, \quad \frac{\partial^2 J}{\partial d^2} < 0, \qquad (2.32)$$

which guarantees a game theoretic saddle point.

Remarks:

1. To complete the discussion in the Remarks following Lemma 2, note that Theorem 2 allows the interpretation of K^* defined by Equation (2.7), when L=0, as a minimizing control in a game theoretic sense. It is important to understand that introducing L in Theorem 1 provides the extra design freedom nedded to provide *necessary and sufficient* conditions for the existence of the H-infinity OPFB solution.
2. If $L \neq 0$, then there may exist a saddle point in some cases. However counter-examples are easy to find.

CHAPTER 3

H-INFINITY STATE FEEDBACK PARAMETERIZATION

This chapter presents a parameterization of all stabilizing H_∞ controllers for continuous-time systems in terms of a single ARE and a free parameter matrix. The form of the result is simple and can be used to select the parameter matrix to satisfy additional design criteria. Chapter is organized as follows; Sections 3.1 and 3.2 are introductory. Section 3.3 presents main results. In section 3.4 the result is used to develop necessary and sufficient conditions for existence of a solution to the H-Infinity static output feedback problem for continuous-time systems.

3.1 System Description and Definitions

Consider the Linear Time-Invariant (LTI) system in Figure 3.1

$$\dot{x} = Ax + Bu + Dd\ ,\ y = Cx \tag{3.1}$$

$$x \in R^n, u \in R^m, y \in R^p$$

and a performance output $z(t)$ that satisfies

$$\|z(t)\|^2 = x^T Q x + u^T R u\ , \tag{3.2}$$

with $Q^T = Q \geq 0$, $R^T = R > 0$. It is assumed that C has full row rank, a standard assumption to avoid redundant measurements.

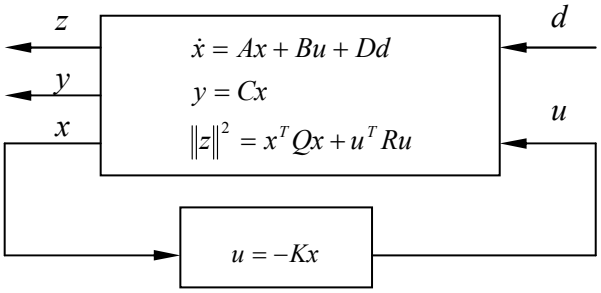

Figure 3.1 System Description H-Infinity State-Feedback

The System L_2 gain is said to be bounded or attenuated by γ if

$$\frac{\int_0^\infty \|z(t)\|^2 dt}{\int_0^\infty \|d(t)\|^2 dt} = \frac{\int_0^\infty (x^T Qx + u^T Ru)dt}{\int_0^\infty (d^T d)dt} \le \gamma^2 \tag{3.3}$$

for any non-zero energy-bounded disturbance input d. Call γ^* the minimum gain for which this occurs. For linear systems, there are explicit formulae to compute γ^*, see, e.g., Chen (2000). Throughout this paper we shall assume that γ is fixed and $\gamma > \gamma^*$.

3.2 Bounded L_2 Gain Design Problem Statement

Defining a constant state-feedback control as

$$u = -K_s x, \tag{3.4}$$

it is desired to find the state-variable feedback (SVFB) gain K_s such that the closed-loop system $A_{cs} \equiv A - BK_s$ is asymptotically stable and the L_2 gain is bounded by a prescribed value $\gamma > \gamma^*$.

3.3 Parameterization

The following main theorem shows necessary and sufficient conditions for the parameterization of all stabilizing H-Infinity static state-feedback gains. It provides a simpler parameterization than most other results in the literature.

Theorem 3.1 – Parameterization of all H_∞ SVFB gains

Assume that ($A, Q^{1/2}$) is detectable. Then K_s is a state feedback that stabilizes system (3.1) and guarantees L_2 gain bounded by $\gamma > \gamma^*$, if and only if there exists a parameter matrix L such that

$$K_s = R^{-1}(B^T P + L), \tag{3.5}$$

where $P = P^T \geq 0$, is a solution to

$$PA + A^T P + Q + \frac{1}{\gamma^2} PDD^T P - PBR^{-1}B^T P + L^T R^{-1} L = 0 \tag{3.6}$$

Proof:

Necessity:

Suppose that there exists a state-feedback gain K_s that stabilizes the closed loop system $A_{cs} \equiv A - BK_s$ and satisfies L_2 gain bounded by γ. Consider the equation

$$PA_{cs} + A_{cs}{}^T P + \frac{1}{\gamma^2} PDD^T P + Q + K_s{}^T R K_s = 0 \tag{3.7}$$

Considering the definition (3.2), from Knobloch *et al.*(1993), Theorem 2.3.1, closed-loop stability and L_2 gain boundedness implies that Equation (3.7) has a unique symmetric solution such that $P \geq 0$. Rearranging Equation (3.7) and completing the square will yield

$$PA + A^T P + Q + \frac{1}{\gamma^2} PDD^T P - PBR^{-1}B^T P + (K_s - R^{-1}B^T P)^T R(K_s - R^{-1}B^T P) = 0. \tag{3.8}$$

Substituting the gain defined by (3.5) in (3.8) yields (3.6).

Sufficiency:

Define $\overline{Q} \equiv Q + K_s{}^T RK_s + \frac{1}{\gamma^2} PDD^T P$ and $\widetilde{Q} \equiv Q + K_s{}^T RK_s$. Suppose that (3.5) and (3.6) hold, then (3.7) follows, so that

$$PA_{cs} + A_{cs}{}^T P + \overline{Q} = 0. \tag{3.9}$$

We claim that detectability of $(A, Q^{1/2})$ implies detectability of $(A_{cs}, \overline{Q}^{1/2})$. For, note that detectability of $(A, Q^{1/2})$ implies that $A - \widetilde{L}Q^{1/2}$ is stable for some $\widetilde{L}$. One can write

$$A - \widetilde{L}Q^{1/2} = A_c - \overline{L}\overline{Q}^{1/2} \tag{3.10}$$

for $\left(\overline{Q}^{1/2}\right)^T \equiv \left[\left(Q^{1/2}\right)^T \quad (R^{1/2}K)^T \quad \left(\frac{1}{\gamma}\right)PD\right]$ and $\overline{L} \equiv \left[\widetilde{L} \quad -BR^{-1/2} \quad 0\right]$. It follows that if pair $(A, Q^{1/2})$ is detectable then pair $(A_c, \overline{Q}^{1/2})$ is detectable as well. Moreover $\overline{Q} \geq 0$, and $P \geq 0$. Therefore, using the Lyapunov stability criteria (Wonham, 1985), Lemma 12.2, Equation (3.9) implies closed-loop stability. Finally for $z = [Q^{1/2}x \quad R^{1/2}u]^T$ one has $z^T z = x^T \widetilde{Q} x$, and

$$PA_{cs} + A_{cs}{}^T P + \frac{1}{\gamma^2} PDD^T P + \widetilde{Q} = 0, \tag{3.11}$$

and system L_2 gain bounded-ness then follows from Van der Schaft (1992), Theorem 2.

3.4 Applications to Output Feedback Design

A special case of this result shows when there exists a static output feedback (OPFB) gain F that stabilizes the system (3.1) with bounded L_2 gain. OPFB requires a restricted form of the gain matrix K_s that has C as a right divisor. Define the control input for OPFB as

$$u = -Fy = -FCx = -K_s x$$

which yields the closed-loop system $A_0 \equiv (A - BFC)$ Equations for OPFB design are generally complicated, consisting of three coupled matrix equations, as given in Lewis and Syrmos (1995), Moerder and Calise (1985), and Jen Te Yu (2004).

The next result provides simplified equations for OPFB design. The Corollary holds for a prescribed matrix Q and follows directly from Theorem 1.

Corollary 3.1- Existence of H-Infinity OPFB for a given *Q*

Consider a specified $Q \geq 0$ such that $(A, Q^{1/2})$ is detectable, and a specified value of $\gamma > \gamma^*$. Then there exists an OPFB gain F such that $A_0 \equiv (A - BFC)$ is asymptotically stable with bounded L_2 gain if and only if there exists a parameter matrix L such that

$$FC = R^{-1}(B^T P + L), \tag{3.12}$$

where $P = P^T \geq 0$, is a solution to

$$PA + A^T P + Q + \frac{1}{\gamma^2} PDD^T P - PBR^{-1}B^T P + L^T R^{-1} L = 0 \tag{3.13}$$

The next result gives necessary and sufficient conditions for the existence of a stabilizing OPFB with bounded L_2 gain. It follows from Corollary 1 by setting $Q = C^T C$. It is a refinement of the result in Kucera and de Souza (1995), and extends that result to solve the H-Infinity OPFB problem.

Corollary 3.2- Existence of H-Infinity OPFB

For a given $\gamma > \gamma^*$, there exists an OPFB gain such that $A_0 \equiv (A - BFC)$ is asymptotically stable with L_2 gain bounded by γ if and only if:

i. (A, C) is detectable

and there exist matrices L and $P = P^T \geq 0$ such that:

ii. $FC = R^{-1}(B^T P + L)$.

iii. $$PA + A^T P + C^T C + \frac{1}{\gamma^2} PDD^T P - PBR^{-1}B^T P + L^T R^{-1} L = 0 \quad (3.14)$$

Proof:

Necessity:

To prove necessity, set $Q = C^T C$, $K_s = FC$ and proceed with the necessity proof of Theorem 1. Note further that $(A - BFC)$ stability implies (A, C) detectability.

Sufficiency:

Suppose that (i), (ii) and (iii) hold, then the sufficiency proof of Theorem 1 holds with $Q = C^T C \geq 0$.

Remarks.

Note that under the special form $Q = C^T C$, the performance output is given by

$$\|z\|^2 = \|y\|^2 + \|u\|^2,$$

Note that a stabilizability condition on (A, B) is hidden in the assumption of existence of a solution $P = P^T \geq 0$ to (3.14).

CHAPTER 4

SOLUTION ALGORITHMS

Chapters 2 and 3 established the existence of the H-Infinity Design Conditions. This chapter presents three approaches to find the H-Infinity Design Solution using output-feedback. These approaches are Algebraic Riccati Equation Based Iterative Numerical Algorithms to achieve predefined disturbance attenuation.

4.1 Solution Algorithm I

Most existing iterative algorithms for OPFB design require the determination of an initial stabilizing gain, which can be very difficult for practical systems.

The following algorithm is proposed to solve the two coupled design equations in Theorem 2.1. Note that it does not require an initial stabilizing gain since, in contrast to Kleinman's Algorithm, 1968 and the algorithm of Moerder and Calise, 1985, it uses a Riccati equation solution, not a Lyapunov equation, at each step.

Algorithm:

1. Initialize: Set *n=0,* $L_0 = 0$, and select γ , Q and R.

2. *n-th* iteration: solve for P_n in

$$P_n A + A^T P_n + Q + \frac{1}{\gamma^2} P_n D D^T P_n - P_n B R^{-1} B^T P_n + L_n{}^T R^{-1} L_n = 0 \qquad (4.1)$$

   Evaluate gain and update L

$$K_{n+1} = R^{-1}(B^T P_n + L_n)C^T (CC^T)^{-1} \tag{4.2}$$

$$L_{n+1} = RK_{n+1}C - B^T P_n \tag{4.3}$$

3. Check Convergence: If K_{n+1} and K_n are close enough to each other, go to 4 otherwise set $n = n+1$ and go to 2.
4. Terminate: Set K= K_{n+1}

Note that this algorithm uses well-developed techniques for solving Riccati equations available, for instance, in MATLAB.

Lemma 4.1:

If this algorithm converges, it provides the solution to (2.17) and (2.18).

Proof:

Clearly at convergence (2.18) holds for P_n. Note that substitution of Equation (4.2) into Equation (4.3) yields.

$$L_{n+1} = R[R^{-1}(B^T P_n + L_n)C^T (CC^T)^{-1}]C - B^T P_n$$

Defining $C^+ = C^T (CC^T)^{-1}$ as the right inverse of C one has

$$L_{n+1} = (B^T P_n + L_n)C^+ C - B^T P_n$$
$$L_{n+1} = -B^T P_n (I - C^+ C) + L_n C^+ C$$

At convergence $L_{n+1} = L_n \equiv L$, $P_n \equiv P$ so that

$$0 = L(I - C^+ C) + B^T P(I - C^+ C)$$
$$0 = (B^T P + L)(I - C^+ C)$$

$$B^T P + L = (B^T P + L)C^+ C$$

This guarantees that there exists a solution K^* to (3.17) given by $K = R^{-1}(B^T P + L)C^+$.

4.2 Design Example: F-16 Normal Acceleration Regulator Design using Solution Algorithm I

In aircraft control design, it is very important to design feedback control regulators of prescribed structure for both stability augmentation systems (SAS) and control augmentation systems (CAS) (Stevens and Lewis, 2003). Therefore, static OPFB design is required. This example shows the power of the proposed static H-Infinity OPFB design technique, since it is easy to include model dynamics, sensor processing dynamics, and actuator dynamics, but no additional dynamics (e.g. regulator) are needed.

The OPFB design algorithm presented is applied to the problem of designing an output-feedback normal acceleration regulator for the F-16 aircraft in Stevens and Lewis (2003, Section 5.4). The control system is shown in Figure 4.1, where n_z is the normal acceleration, r is the reference input in g's, and the control input $u(t)$ is the elevator actuator angle. To ensure zero steady-state error an integrator has been added in the feed-forward path, this corresponds to the compensator dynamics. The integrator output is ε. The short period approximation is used so the aircraft states are pitch rate q and angle of attack α. Since alpha measurements are quite noisy, a low pass filter with the cutoff frequency of 10 *rad/s* is used to provide filtered measurements α_F of the angle of attack. An additional state δ_e is introduced by the elevator actuator.

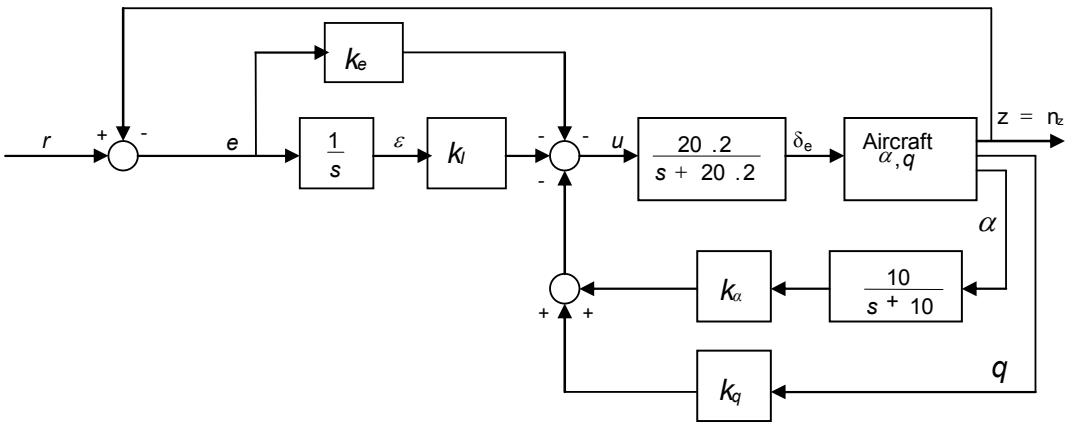

Figure 4.1 G Command System

The state vector is:

$x(1) = \alpha$: Angle of attack.

$x(2) = q$: Pitch Rate.

$x(3) = \delta_e$: Elevator Actuator.

$x(4) = \alpha_F$: Filtered measurement of angle of attack.

$x(5) = \varepsilon$: Integral Controller.

The measurement outputs are $y = [\alpha_F \quad q \quad e \quad \varepsilon]^T$.

We use the short period approximation to the F-16 dynamics linearized about the nominal flight condition described in Stevens and Lewis (2003), Table 3.6-3 (502 ft/s, level flight, dynamic pressure of 300 psf, $x_{cg} = 0.35\bar{c}$) and the dynamics are augmented to include the elevator actuator, angle-of-attack filter, and compensator dynamics. The result is

with

$$A = \begin{bmatrix} -1.01887 & 0.90506 & -0.00215 & 0 & 0 \\ 0.82225 & -1.07741 & -0.17555 & 0 & 0 \\ 0 & 0 & -20.2 & 0 & 0 \\ 10 & 0 & 0 & -10 & 0 \\ -16.26 & -0.9788 & 0.4852 & 0 & 0 \end{bmatrix}$$

$$B = \begin{bmatrix} 0 \\ 0 \\ 20.2 \\ 0 \\ 0 \end{bmatrix}, D = \begin{bmatrix} 0 \\ 0 \\ 1 \\ 0 \\ 0 \end{bmatrix}, C = \begin{bmatrix} 0 & 0 & 0 & 57.2958 & 0 \\ 0 & 57.2958 & 0 & 0 & 0 \\ -16.26 & -0.9788 & 0.4852 & 0 & 0 \\ 0 & 0 & 0 & 0 & 1 \end{bmatrix}$$

The factor of 57.2958 is added to convert angles from radians to degrees.

The control input is $u = -Ky = -[k_\alpha \quad k_q \quad k_e \quad k_I]y$. It is required to select the output-feedback feedback gains to yield stability with good closed-loop response. Note that k_α and k_q are feedback gains, while k_e and k_I are feed-forward gains. This approach allows the adjustment of both for the best bounded L_2 gain performance. The algorithm presented above was used to design an H-Infinity pitch-rate regulator for a prescribed value of γ.

For the computation of the output feedback gain K it is necessary to select Q and R. Using the algorithm described above for the given γ, Q, and R the control gain K is easily found using MATLAB in a few seconds. If this gain is not suitable in terms of time responses and closed-loop poles, the elements of Q and R can be changed and the

design repeated. After repeating the design several times we selected the design matrices as

$$Q = \begin{bmatrix} 264 & 16 & 1 & 0 & 0 \\ 16 & 60 & 0 & 0 & 0 \\ 1 & 0 & 0 & 0 & 0 \\ 0 & 0 & 0 & 0 & 0 \\ 0 & 0 & 0 & 0 & 100 \end{bmatrix}, \quad R = [0.1]$$

which yields the feedback matrix

$$K = \begin{bmatrix} 0 & -0.1778 & 12.4336 & 31.7201 \end{bmatrix}.$$

The resulting closed-loop poles are at

$$s = -28.3061,\ -1.4974 \pm 1.2148\mathrm{i},\ -3.1809,\ -10.$$

The resulting gains are applied to the system, and a unit step disturbance *d(t)* is introduced in simulations to verify robustness of the design. The resulting time responses shown in Figures 4.2 and 4.3 are very good. Note that, though we designed an H_∞ regulator, the structure of the static OPFB controller with the prescribed loops also guarantees good tracking.

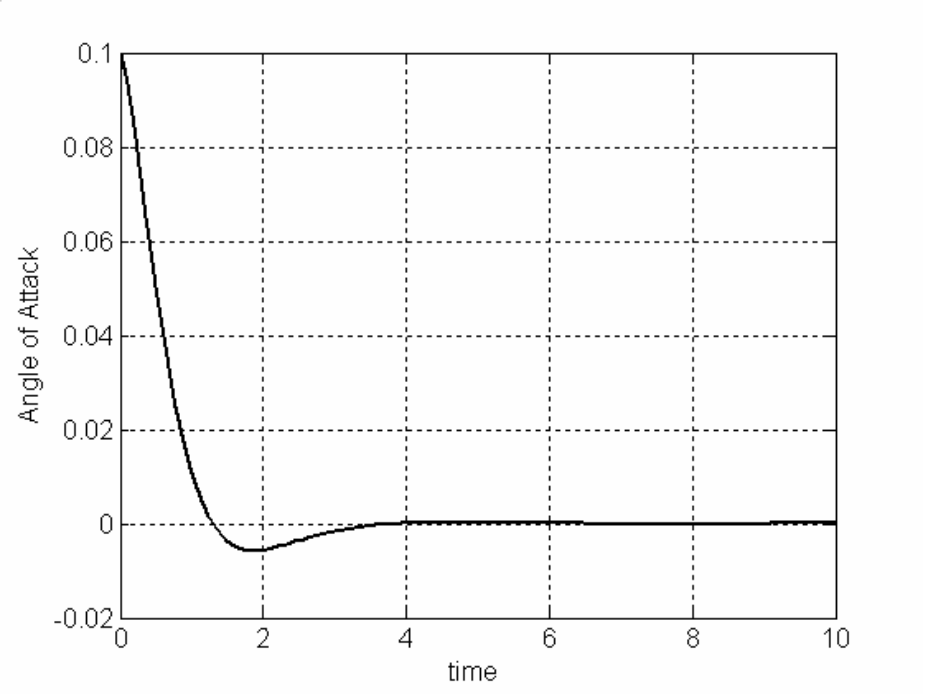

Figure 4.2 Angle of Attack

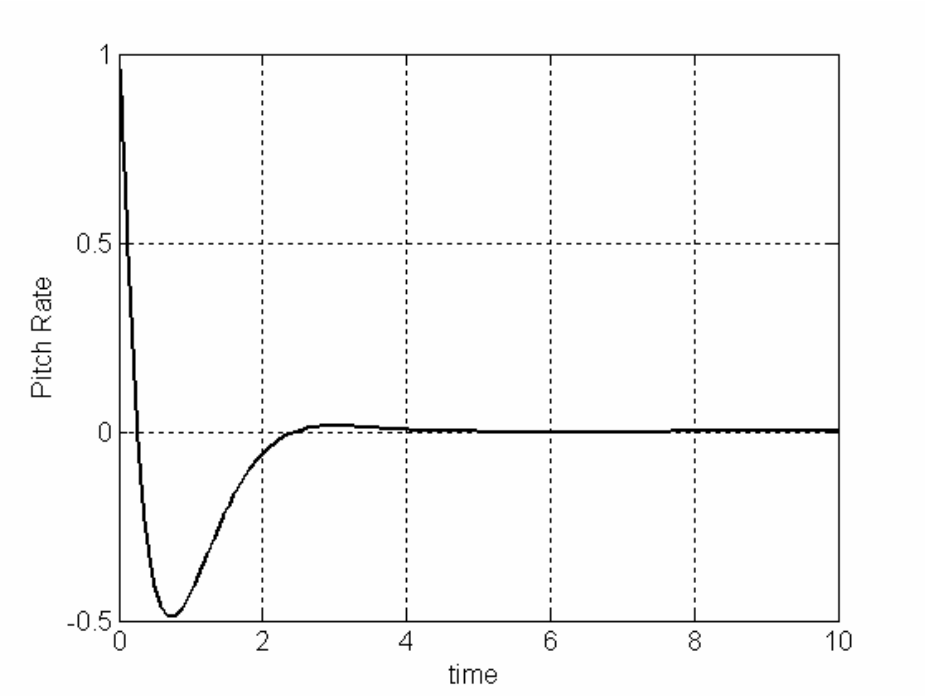

Figure 4.3 Pitch Rate

Note on selecting γ:

The gain parameter γ defines the L_2 bound for a given disturbance. One can quickly perform the design using the above algorithm for a prescribed value of γ in a few seconds using MATLAB. If the algorithm converges, the parameter γ may be reduced. If γ is taken too small, the algorithm will not converge since the ARE has no PD solution. This provides an efficient and fast trial-and-error method for determining the smallest allowable γ, for given Q and R design matrices which solves the H-Infinity problem. For this example, the H-Infinity value of γ is found to be equal to 0.2, for which the above results were obtained.

4.3 Solution Algorithm II

In this section we present another algorithm to solve H-Infinity Output Feedback. Assuming Conditions defined in theorem 2.1, closed form coupled equations can be written as

$$K * C = R^{-1}(B^T P + L) \tag{4.4}$$

$$PA_c + A_c{}^T P + Q + \frac{1}{\gamma^2} PDD^T P + C^T K^T RKC = 0 \tag{4.5}$$

This OPFB H-Infinity design algorithm solves Equation (4.4) and (4.5) and is an extension of Klienman's algorithm which was originally proposed for state-variable feedback control without disturbance (Klienman, 1968) . At this point it is important to state that unlike the algorithms of (Moerder and Calise, 1985), (Jen Te-Yu 2004), it uses a Riccati equation solution, not a Lyapunov equation, at each step to solve for the H-Infinity design for a given admissible disturbance attenuation.

Algorithm:

1. Initialization: $L_0 = 0$, $K_0 =$ Initial stabilizing gain.

2. Solve for P

$$P_n(A - BK_nC) + (A - BK_nC)^T P_n + \frac{1}{\gamma^2} P_n DD^T P_n + Q + C^T K_n{}^T RK_nC = 0 \quad (4.6)$$

3. Update K

$$K_{n+1} = R^{-1}(B^T P_n + L_n)C^+ . \quad (4.7)$$

Where $C^+ = C^T(CC^T)^{-1}$ is defined as the right inverse of C.

4. Update L

$$L_{n+1} = RK_{n+1}C - B^T P_n . \quad (4.8)$$

Check for convergence $\|P_n - P_{n-1}\| < \varepsilon$, at convergence define K_∞=K, go to 1 if not converged.

Lemma 4.2 : If this algorithm converges, it provides the solution to Equations (4.4) and (4.5).

Proof: Clearly at convergence Equation (4.5) holds for P_n. Note that substitution of Equation (4.7) into Equation (4.8) yields.

$$L_{n+1} = R[R^{-1}(B^T P_n + L_n)C^+]C - B^T P_n$$

At convergence $L_{n+1} = L_n \equiv L$, $P_n \equiv P$ so that

$$L = (B^T P + L)C^+ C - B^T P, \text{ or}$$

$$B^T P + L = (B^T P + L)C^+ C \quad (4.9)$$

This guarantees that there exists a solution K^* to (4.4) given by $K = R^{-1}(B^T P + L)C^+$.

4.4 Aircraft Flight Tracking Controller Design using H-Infinity Static Output-Feedback Algorithm II

This example aims to analyze the effects by combining aircraft control design techniques for tracking with H-Infinity output-feedback design, algorithm 2 is used. It is shown that for the F-16 Aircraft model H-Infinity OPFB performs better than Optimal OPFB if disturbance exists.

4.4.1 Structure of Aircraft Tracking System

In aircraft control design, experience is often utilized to make the decisions about the compensator, Figure 4.4 describes an approach to the design of tracking control system which is very useful in aircraft control application; this approach will allow one to design a servo control system that has any structure desired.

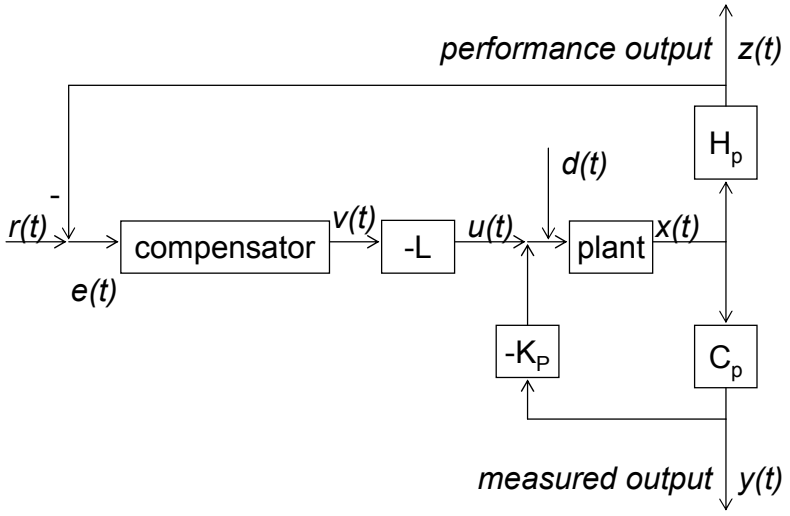

Figure 4.4 Plant with Compensator of Desired Structure under Disturbance

By defining the state, the output and the matrix variable to stream line the notations we see that the augmented dynamics that contain the aircraft, compensator and the disturbance are of the form described by Equation 4.10.

$$\begin{aligned} \dot{x} &= Ax + Bu + Gr + Dd \\ y &= Cx + Fr \\ \zeta &= Hx \end{aligned} \tag{4.10}$$

The modifying procedure is illustrated in the example. The admissible controls are proportional output feedback of the form

$$u = -Ky = -KCx - KFr \tag{4.11}$$

Using these equations the closed-loop system is found to be of the form as in Equation 4.12, and illustrated in Figure 4.5.

$$\dot{x} = A_c x + B_c r + Dd \tag{4.12}$$

with $A_c \equiv (A - BKC), B_c \equiv (G - BKF)r$.

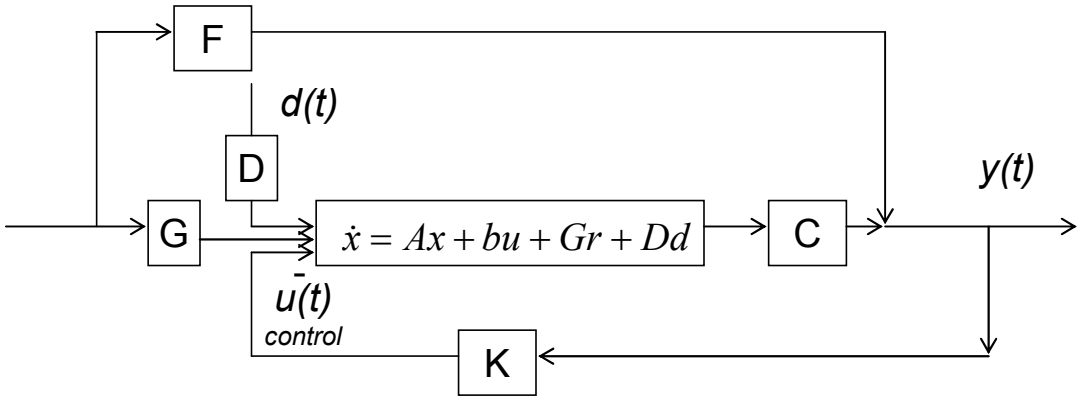

Figure 4.5 Plant/Feedback Structure with Disturbance

It is well known that if the compensator is required to have a specific structure, the selection of control gains is an output feedback problem. Even if state-variable feedback might be able to guarantee stability, the resulting compensator has no structure and is unsuitable. Another important issue is that disturbances can affect the system performance even if stability is guaranteed. Therefore one is motivated to consider H-Infinity OPFB design.

Design of this tracking system can be converted to a regulator design problem (Stevens and Lewis, 2003). Having designed a suitable regulator using H-Infinity technique, the structure in Figure 4.4, which includes a unity gain outer tracking loop, then guarantees good tracking performance.

Disturbance $d_\delta(t)$ is affecting the elevator actuation and *n(t)* is affecting the filtered measurement, so that $d(t) = \begin{bmatrix} d_\delta(t) & n(t) \end{bmatrix}^T$.

The optimal output feedback gain K_2 for the Q and R shown below is given in (Stevens and Lewis, 2003). It is

$$K_2 = \begin{bmatrix} -1.629 & -1.316 & 18.56 & 77.6 \end{bmatrix}.$$

$$Q = \begin{bmatrix} 264 & 16 & 1 & 0 & 0 \\ 16 & 60 & 0 & 0 & 0 \\ 1 & 0 & 0 & 0 & 0 \\ 0 & 0 & 0 & 0 & 0 \\ 0 & 0 & 0 & 0 & 100 \end{bmatrix}, \quad R = [0.01]$$

Using these Q and R which yields the H-Infinity output feedback matrix K_∞ and resulting closed loop poles

$$K_\infty = \begin{bmatrix} 0 & -0.5171 & 30.9091 & 100.0003 \end{bmatrix}.$$

$s = -42.9359,\ -1.6099 \pm 1.1082i,\ -6.4347,\ -10.$

The resulting gains are applied to the system, and step disturbances *d(t)* with varying magnitude is introduced in simulations to verify robustness of the design. The resulting time responses shown in Figures 4.6 and 4. 7 are very good. The structure of the H- Infinity static OPFB controller with the prescribed loops guarantees good tracking when disturbance is introduced. In Figure 4.7 one sees the effect of disturbance on the transient response; in Figure 4.8 the increased disturbances of magnitude 10 times higher than unit step will make the response of the optimal output-feedback worse.

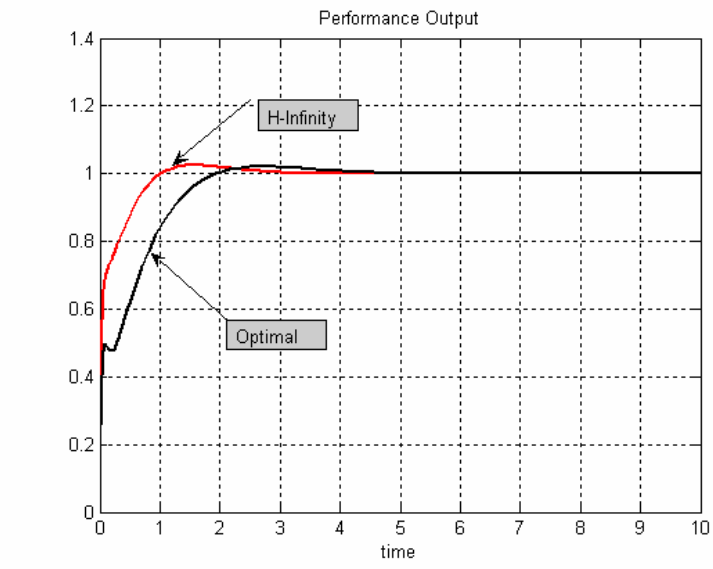

Figure 4.6 Response without Disturbance

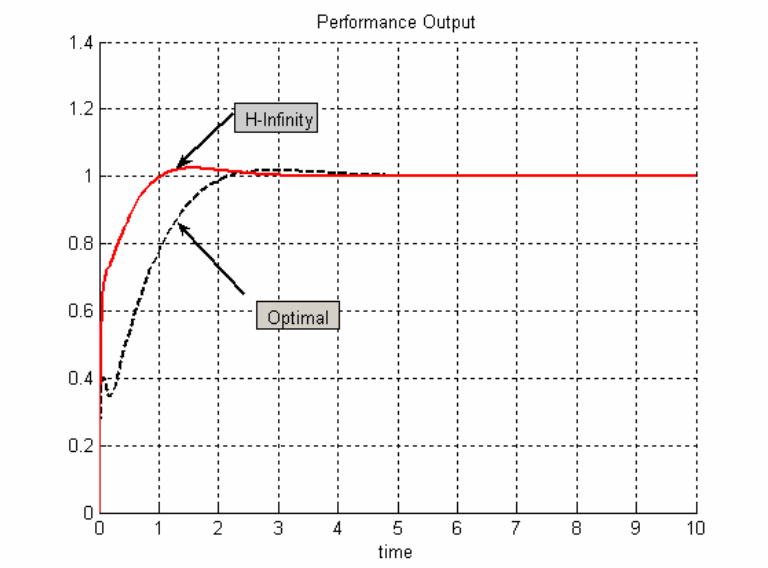

Figure 4.7 Response with unit step Disturbance

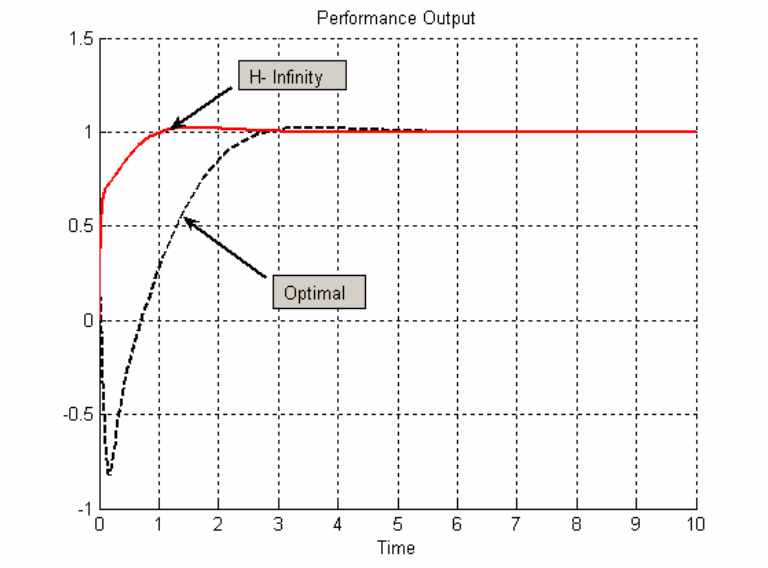

Figure 4.8 Response with increased Disturbance

4.5 Solution Algorithm III

This section presents an algorithm to solve the two coupled design equations in Corollaries 3.1 and 3.2. The algorithm starts with a stabilizing SVFB gain, which can

easily be found using standard computational tools (e.g. LQR). It is shown that the algorithm, if it converges, solves the output feedback problem.

Since C has full row rank, the right inverse is defined as $C^+ \equiv C^T (CC^T)^{-1}$, which is best computed using the SVD

$$C = USV^T = U\begin{bmatrix} S_0 & 0 \end{bmatrix}\begin{bmatrix} V_1^T \\ V_2^T \end{bmatrix}. \tag{4.10}$$

Then $CV = C[V_1 \quad V_2] = [C_1 \quad 0]$, so that $CV_1 = C_1$, and $CV_2 = 0$. Note that $I = V_1 V_1^T + V_2 V_2^T$. Therefore,

i. $C^+ = VS^+U^T = V_1 (S_0)^{-1} U^T$.

ii. $V_1 V_1^T = I - V_2 V_2^T = C^+ C$ is the projection onto nullspace perpendicular of C.

iii. $V_2 V_2^T = I - V_1 V_1^T = I - C^+ C$ is the projection onto the nullspace of C.

The equation $KC = R^{-1}(B^T P + L)$ has an exact solution K if and only if

$$0 = (B^T P + L)(I - C^+ C) = (B^T P + L) V_2 V_2^T.$$

Then the solution is given by

$$K = R^{-1}(B^T P + L) C^+ = R^{-1}(B^T P + L) V_1 (S_0)^{-1} U^T.$$

The following algorithm is based on Yu (2004), where, however, three coupled equations must be solved. It solves for a state feedback at each iteration, and then projects that SVFB onto nullspace perpendicular of *C*.

OPFB Design Algorithm

1. Initialize: Fix $\gamma \geq \gamma^*$. Set $n = 0$, $L_0 = 0$. Solve a standard (e.g. LQR) Riccati equation for given Q and R and obtain a stabilizing SVFB gain as initial gain $K_{s(0)}$. Define closed-loop matrix $\widetilde{A}_0 = A - BK_{s(0)}$.

2. n-th iteration:

   Solve ARE for P

$$P_n(\widetilde{A}_n) + (\widetilde{A}_n)^T P_n + Q + K_{sn}{}^T R K_{sn} + \frac{1}{\gamma^2} P_n D D^T P_n = 0, \qquad (4.11)$$

   update *K*, project onto nullspace perpendicular of *C*

$$K_{s(n+1)} = R^{-1}(B^T P_n + L_n)(I - V_2 V_2{}^T), \qquad (4.12)$$

   update *L*

$$L_{n+1} = R K_{s(n)} - B^T P_n, \qquad (4.13)$$

   update closed-loop system matrix

$$\widetilde{A}_{n+1} = A - B K_{s(n+1)}, \qquad (4.14)$$

3. Check convergence. If converged, go to step 4 otherwise set $n = n + 1$ go to step 2.

4. End. Set $K_s = K_{s(n+1)}$ and compute OPFB gain $K = K_s V_1 (S_0)^{-1} U^T$.

The convergence can be checked using the norm of $P_{n+1} - P_n$.

This algorithm has converged on all examples tried. The next result shows the correctness of the algorithm, namely, that if it converges, it provides the H-Infinity OPFB gain.

Lemma 4.3

If this algorithm converges, it provides the H_∞ OPFB gain.

Proof: Clearly, at convergence (3.7) holds for $P_{n+1} = P_n \equiv P$. Substitution of Equation (4.12) into Equation (4.13) yields.

$$L_{n+1} = RR^{-1}(B^T P_n + L_n)(I - V_2 V_2{}^T) - B^T P_n$$

At convergence $L_{n+1} = L_n \equiv L$, so that

$L = (B^T P + L)(I - V_2 V_2{}^T) - B^T P$, therefore

$$B^T P + L = (B^T P + L)C^+ C \tag{4.15}$$

This guarantees that there exists a solution F to (3.12) given by $K = K_s C^+ = R^{-1}(B^T P + L)C^+ = K_s V_1 (S_0)^{-1} U^T$.

4.6 Design Example using Solution Algorithm III

In this example we demonstrate the effectiveness of the proposed static H-Infinity OPFB design technique on a more complex design example. It is desired to design a lateral-directional (e.g., roll damper/yaw damper) command augmentation system (CAS) for the F-16 dynamics from Stevens and Lewis (2003) linearized at the nominal flight condition in Table 3.6-3 (Stevens and Lewis, 2003) ($V_T = 502$ ft/s, 300psf dynamic pressure, cg at $0.35\,\bar{c}$). This CAS has two input channels, and includes actuators and a washout filter. The design requires the selection of 8 control gains. The structured nature of the CAS means that OPFB, not SVFB, must be used.

The lateral states are sideslip β, bank angle ϕ, roll p, and yaw rate r. Additional states δ_a and δ_r are introduced by the aileron and rudder actuators

$$\delta_a = \frac{20.2}{s+20.2} u_a \,,\ \delta_r = \frac{20.2}{s+20.2} u_r \,.$$

A washout filter

$$r_w = \frac{s}{s+1} r$$

is used, with r the yaw rate and r_w the washed out yaw rate. The washout filter state is denoted x_w. The entire state vector is

$$x = [\beta \quad \phi \quad p \quad r \quad \delta_a \quad \delta_r \quad x_w]^T \,.$$

The control inputs are the rudder and aileron servo inputs so that

$$u = \begin{bmatrix} u_a \\ u_r \end{bmatrix}.$$

The disturbance is given by $d(t) = [d_a(t) \quad d_r(t) \quad n(t)]^T$, where $d_a(t)$ affects the aileron actuation, $d_r(t)$ the rudder actuation, and $n(t)$ the washout filter state.

The full state variable model of the aircraft plus actuators, washout filter, disturbance, and control dynamics has matrices.

$$A = \begin{bmatrix} -0.3220 & 0.0640 & 0.0364 & -0.9917 & 0.003 & 0.0008 & 0 \\ 0 & 0 & 1 & 0.0037 & 0 & 0 & 0 \\ -30.6492 & 0 & -3.6784 & 0.6646 & -0.7333 & 0.1315 & 0 \\ 8.5396 & 0 & -0.0254 & -0.4764 & -0.0319 & -0.0620 & 0 \\ 0 & 0 & 0 & 0 & -20.2 & 0 & 0 \\ 0 & 0 & 0 & 0 & 0 & -20.2 & 0 \\ 0 & 0 & 0 & 57.2958 & 0 & 0 & -1 \end{bmatrix}$$

$$B = \begin{bmatrix} 0 & 0 \\ 0 & 0 \\ 0 & 0 \\ 0 & 0 \\ 20.2 & 0 \\ 0 & 20.2 \\ 0 & 0 \end{bmatrix}$$

$$D = \begin{bmatrix} 0 & 0 & 0 & 0 & 1 & 0 & 0 \\ 0 & 0 & 0 & 0 & 0 & 1 & 0 \\ 0 & 0 & 0 & 0 & 0 & 0 & 1 \end{bmatrix}^T$$

The output is

$$y = \begin{bmatrix} r_w \\ p \\ \beta \\ \phi \end{bmatrix},$$

and $y = Cx$ with

$$C = \begin{bmatrix} 0 & 0 & 0 & 57.2958 & 0 & 0 & -1 \\ 0 & 0 & 57.2958 & 0 & 0 & 0 & 0 \\ 57.2958 & 0 & 0 & 0 & 0 & 0 & 0 \\ 0 & 57.2958 & 0 & 0 & 0 & 0 & 0 \end{bmatrix}$$

The factor of 57.2958 is added to convert angles from radians to degrees. The feedback control is output feedback of the form $u = Fy$, so that the F is a 2×4 matrix. That is, eight feedback gains must be selected.

For the computation of the H-Infinity output feedback gain F it is necessary to select Q, R, and γ. The proposed algorithm makes it very easy and fast to perform the design for different values of Q, R, γ. We selected $Q = C^T C$ and $R = I$. If the resulting gain F is not suitable in terms of time responses and closed-loop poles, the

elements of Q and R can be changed and the design repeated. These values were found suitable in this example.

After some design repetitions, which were performed very quickly using the algorithm, we found the smallest value of the gain to be $\gamma^* = 1.499$. The results for that gain are

$$K_s = \begin{bmatrix} 95.1780 & -56.0021 & -47.1518 & -17.6280 & 0 & 0 & 0.3077 \\ -19.7080 & 10.1009 & 9.3495 & -50.5608 & 0 & 0 & 0.8825 \end{bmatrix}$$

$$K = \begin{bmatrix} -0.3077 & -0.8230 & 1.6612 & -0.9774 \\ -0.8825 & 0.1632 & -0.3440 & 0.1763 \end{bmatrix}.$$

The resulting closed-loop poles are at

$$s = -11.3762 \pm 25.4311i, -15.1711, \ -4.1338, -1.3423 \pm 1.0468i, -1.1350 .$$

The resulting gains are applied to the system, and step disturbances *d(t)* are introduced in simulations to verify robustness of the design. The resulting time responses shown in Figures 4.9 and 4.10 are very good. The design procedure based on solving two coupled equations is significantly easier than methods based on solving three coupled equations, e.g. as described in Lewis and Syrmos (1995) and Moerder and Calise (1985). Moreover, the H-Infinity static OPFB controller generally outperforms the H_2 optimal OPFB controller when disturbances are introduced.

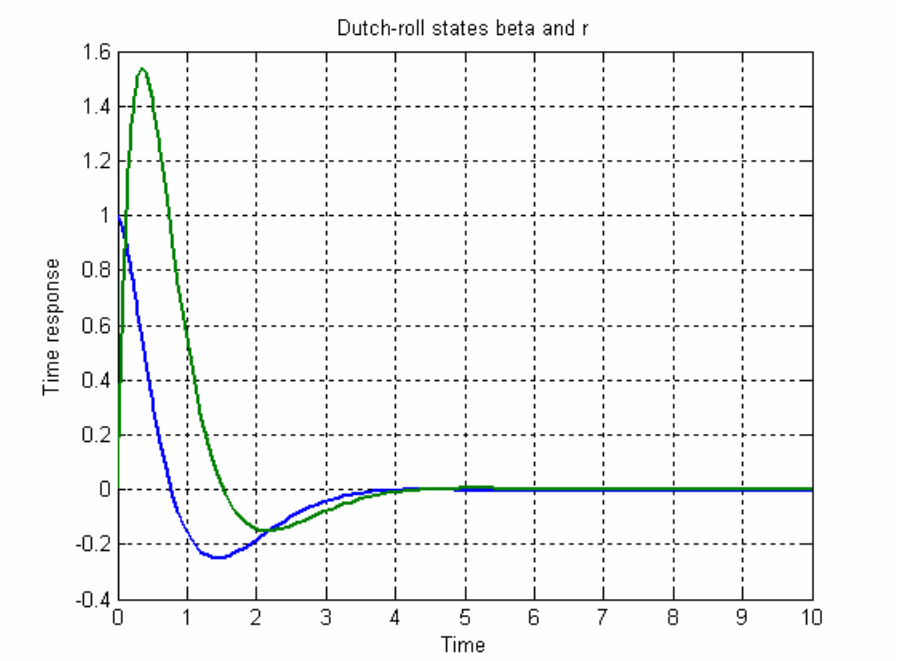

Figure 4.9 Closed loop response dutch roll states

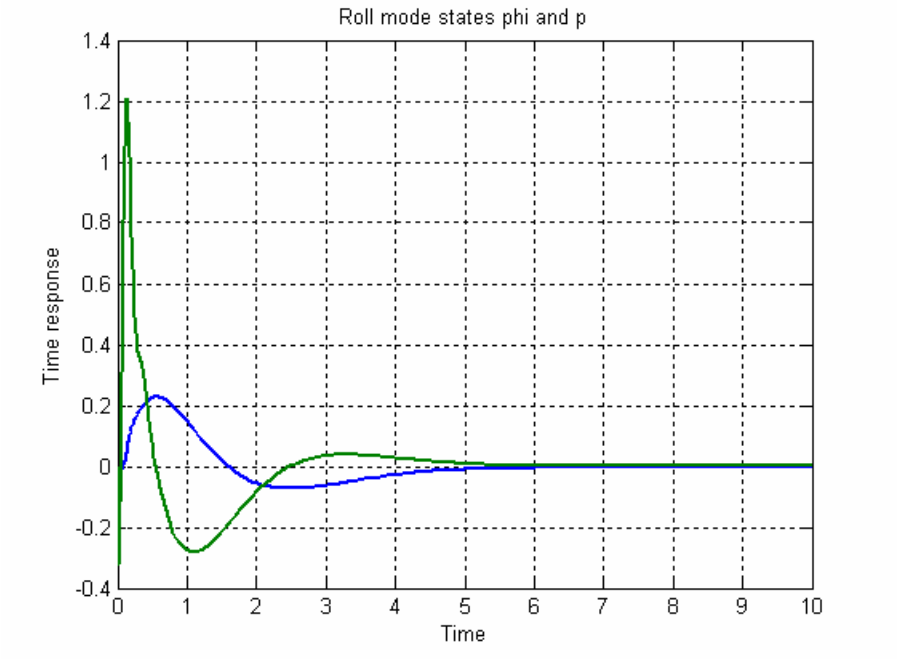

Figure 4.10 Closed loop response roll mode states

CHAPTER 5

UNMANNED AERIAL VEHICLE CONTROL

5.1 Helicopter Dynamics

There is a growing interest in developing control strategies for unmanned autonomous helicopters, in particular a small scale one. From a strictly aerodynamic point of view, these rotary-wing aircrafts may be defined as configurations which derive their forces directly from open airscrews. The dynamics of rotorcrafts are significantly more complex than those of fixed wing aircrafts. A rotorcraft is an inherently unstable, high order, cross coupled and challenging to model dynamic system. Low weight modern instrumentation and new theoretical contributions in systems theory is resulting in important breakthroughs. This work in section 5.1 is not claimed to be an original work of the dissertation, this introductory work is given for completeness and continuity. This section is organized as follows- Section 5.1.1 derives 12th order rigid body dynamics (Friedland, 1986), trim conditions are discussed in Section 5.1.2. A reduced order helicopter model is derived in section 5.1.3.

5.1.1 Rigid Body Dynamics

The motion of a single rigid body has six dynamic degrees of freedom: three of those define the location of a reference point (usually the center of gravity) in the body, and three define the orientation (attitude) of the body. Each of the six degrees of

freedom takes two state variables (one position and one velocity) a total of 12 first-order differential equations are required to completely describe the motion of the body. The motion of a rigid body is governed by the familiar Newtonian laws of motion

$$\frac{d\vec{p}}{dt} = \vec{f} \tag{5.1}$$

$$\frac{d\vec{h}}{dt} = \vec{\tau} \tag{5.2}$$

Where $\vec{p} = \begin{bmatrix} p_x \\ p_y \\ p_z \end{bmatrix}$ is the linear momentum of the body, $\vec{h} = \begin{bmatrix} h_x \\ h_y \\ h_z \end{bmatrix}$ is the angular momentum of the body, $\vec{f} = \begin{bmatrix} f_x \\ f_y \\ f_z \end{bmatrix}$ is the force acting on the body, $\vec{\tau} = \begin{bmatrix} \tau_x \\ \tau_y \\ \tau_z \end{bmatrix}$ is the torque acting on the body.

It is important to understand that (5.1) and (5.2) are valid only when the axes along with the motion is resolved are an inertial frame of reference, i.e., they are neither rotating or accelerating. If the axes are accelerating linearly or rotating then (5.1) and (5.2) must be modified to account for the motion of the reference axes.

The rotational dynamics of a rigid body are more complicated than the translational dynamics for several reasons: the mass *M* of a rigid body is a scalar, but for the moment of Inertia *J* is a 3×3 matrix. If the body axes are chosen to coincide with the principal axis, the moment of inertia matrix is diagonal; otherwise the matrix J has off diagonal terms. However the main complication is in the description of the attitude

or orientation of the body in space. To define the orientation of the body in space, we can define three axes $(x_B, \quad y_B, \quad z_B)$ fixed in the body, as shown in Figure 5.1

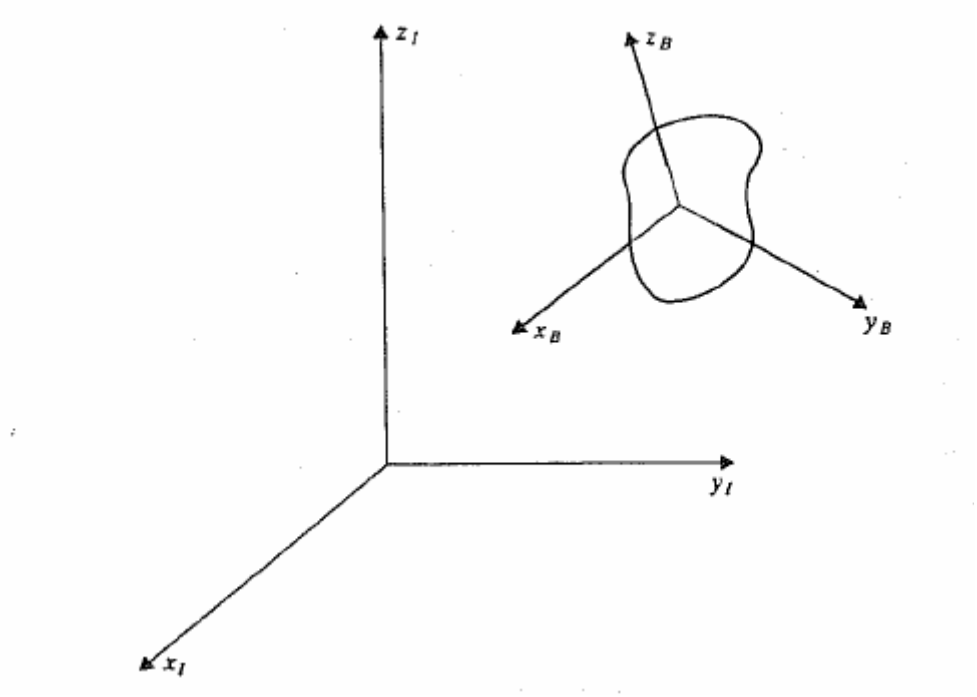

Figure 5.1 Inertial and body-fixed axes

One way of defining the attitude of the body is the define the angles between the body axes and the inertial reference axes $(x_{I,} \quad y_{I,} \quad z_I)$. In aircraft and space mechanics it is now customary to define the orientation of a set of orthogonal axes in the body (body axes) with respect to the inertial reference.

Suppose the body axes are initially aligned with the inertial reference axes. Then the following sequences of rotations are made to bring the body axes into general position:

1. First, a rotation ψ (yaw) about the z axis
2. Second, a rotation θ (pitch) about the resulting y axis

3. Third, a rotation ϕ (roll) about the resulting x axis

It can be shown that

$$\begin{bmatrix} x_{B1} \\ y_{B1} \\ z_{B1} \end{bmatrix} = \begin{bmatrix} \cos\psi & \sin\psi & 0 \\ -\sin\psi & \cos\psi & 0 \\ 0 & 0 & 1 \end{bmatrix} \begin{bmatrix} x_I \\ y_I \\ z_I \end{bmatrix} \tag{5.3}$$

$$\begin{bmatrix} x_{B2} \\ y_{B2} \\ z_{B2} \end{bmatrix} = \begin{bmatrix} \cos\theta & 0 & -\sin\theta \\ 0 & 1 & 0 \\ \sin\theta & 0 & \cos\theta \end{bmatrix} \begin{bmatrix} x_{B1} \\ y_{B1} \\ z_{B1} \end{bmatrix} \tag{5.4}$$

$$\begin{bmatrix} x_B \\ y_B \\ z_B \end{bmatrix} = \begin{bmatrix} x_{B3} \\ y_{B3} \\ z_{B3} \end{bmatrix} = \begin{bmatrix} 1 & 0 & 0 \\ 0 & \cos\phi & \sin\phi \\ 0 & -\sin\phi & \cos\phi \end{bmatrix} \begin{bmatrix} x_{B2} \\ y_{B2} \\ z_{B2} \end{bmatrix} \tag{5.6}$$

Thus we see that

$$\begin{bmatrix} x_B \\ y_B \\ z_B \end{bmatrix} = T_{BI} \begin{bmatrix} x_I \\ y_I \\ z_I \end{bmatrix} \tag{5.7}$$

Where T_{BI} is the matrix that rotates the body axes from reference position, and is the product of three matrices

$$T_{BI} = \begin{bmatrix} 1 & 0 & 0 \\ 0 & \cos\phi & \sin\phi \\ 0 & -\sin\phi & \cos\phi \end{bmatrix} \begin{bmatrix} \cos\theta & 0 & -\sin\theta \\ 0 & 1 & 0 \\ \sin\theta & 0 & \cos\theta \end{bmatrix} \begin{bmatrix} \cos\psi & \sin\psi & 0 \\ -\sin\psi & \cos\psi & 0 \\ 0 & 0 & 1 \end{bmatrix} \tag{5.8}$$

Each factor of T_{BI} is orthogonal matrix and hence T_{BI} is orthogonal, i.e.,

$$T_{IB} = \left(T_{BI}\right)^{-1} = \left(T_{BI}\right)^{T} \tag{5.9}$$

Note that $T_{IB} = \left(T_{BI}\right)^{-1}$ is the matrix that returns the body axes from the general position to the reference position.

Since any vector in space can be resolved into its components in body axes or in inertial axes, we can use the transformation T_{BI} to obtain the components of a vector in one set of axes, given its component in the other. In particular suppose $\vec{a}$ is any vector in space. When it is resolved into components along an inertial reference we attach the subscript *I* ; when it is resolved in body axes, we attach the subscript *B*.

$$\vec{a}_I = \begin{bmatrix} a_{xI} \\ a_{yI} \\ a_{zI} \end{bmatrix} \vec{a}_B = \begin{bmatrix} a_{xB} \\ a_{yB} \\ a_{zB} \end{bmatrix}$$

Using (5.7) we obtain

$$\vec{a}_B = T_{BI}\vec{a}_I \tag{5.10}$$

This relationship can be applied to newtonial law of motion $\frac{d\vec{h}}{dt} = \vec{\tau}$ for the angular motion of a rigid body and, for describing the motion of a rotorcraft along rotating body axes. In the case of a rigid body, the angular momentum vector is

$$\vec{h} = J\vec{\omega} \tag{5.11}$$

Where J is the moment of inertia matrix and $\vec{\omega}$ is the angular velocity vector. If the axes along which angular momentum vector of the body $\vec{h}$ is resolved are defined to be coincident with the physical principal axes of the body, then J is a diagonal matrix. Thus when $\vec{h}$ is resolved along principal body axes we get

$$\vec{h}_B = \begin{bmatrix} J_x & 0 & 0 \\ 0 & J_y & 0 \\ 0 & 0 & J_z \end{bmatrix} \begin{bmatrix} \omega_x \\ \omega_y \\ \omega_y \end{bmatrix} \tag{5.12}$$

Because of the fact that newtonian law of motion $\frac{d\vec{h}}{dt} = \vec{\tau}$ holds only when the body angular momentum vector $\vec{h}$ is measured with to an inertial reference, one can write

$$\frac{d\vec{h}_I}{dt} = \frac{d}{dt}\left(T_{IB}\vec{h}_B\right) = \vec{\tau}_I \tag{5.13}$$

The transformation T_{IB}, however, is not constant. Hence (2.12) can be written as

$$T_{IB}\dot{\vec{h}}_B + \dot{T}_{IB}\vec{h}_B = \vec{\tau}_I$$

$$\dot{\vec{h}}_B + T_{BI}\dot{T}_{IB}\vec{h}_B = T_{BI}\vec{\tau}_I$$

$$\dot{\vec{h}}_B + T_{BI}\dot{T}_{IB}\vec{h}_B = \vec{\tau}_B \tag{5.14}$$

Which in component form can be written as

$$\begin{bmatrix} J_x\dot{\omega}_{xB} \\ J_y\dot{\omega}_{yB} \\ J_z\dot{\omega}_{zB} \end{bmatrix} + T_{BI}\dot{T}_{IB}\begin{bmatrix} J_x\omega_{xB} \\ J_y\omega_{yB} \\ J_z\omega_{zB} \end{bmatrix} = \begin{bmatrix} \tau_{xB} \\ \tau_{yB} \\ \tau_{zB} \end{bmatrix} \tag{5.15}$$

These differential equations relate the components of the angular velocity vector, $\vec{\omega}$ projected onto rotating body axes

$$\vec{\omega}_B = \begin{bmatrix} \omega_{xB} \\ \omega_{yB} \\ \omega_{zB} \end{bmatrix}$$

to the torque vector also projected along body axes. To complete (5.15) we need the matrix $T_{BI}\dot{T}_{IB}$. It can be shown that

$$\dot{T}_{IB} = T_{IB}\begin{bmatrix} 0 & -\omega_{zB} & \omega_{yB} \\ \omega_{zB} & 0 & -\omega_{xB} \\ -\omega_{yB} & \omega_{xB} & 0 \end{bmatrix} \tag{5.16}$$

So that

$$T_{BI}\dot{T}_{IB} = \begin{bmatrix} 0 & -\omega_{zB} & \omega_{yB} \\ \omega_{zB} & 0 & -\omega_{xB} \\ -\omega_{yB} & \omega_{xB} & 0 \end{bmatrix} \tag{5.17}$$

Hence one can write

$$\begin{bmatrix} J_x\dot{\omega}_{xB} \\ J_y\dot{\omega}_{yB} \\ J_z\dot{\omega}_{zB} \end{bmatrix} + \begin{bmatrix} 0 & -\omega_{zB} & \omega_{yB} \\ \omega_{zB} & 0 & -\omega_{xB} \\ -\omega_{yB} & \omega_{xB} & 0 \end{bmatrix} \begin{bmatrix} J_x\omega_{xB} \\ J_y\omega_{yB} \\ J_z\omega_{zB} \end{bmatrix} = \begin{bmatrix} \tau_{xB} \\ \tau_{yB} \\ \tau_{zB} \end{bmatrix}$$

$$\begin{bmatrix} J_x\dot{\omega}_{xB} \\ J_y\dot{\omega}_{yB} \\ J_z\dot{\omega}_{zB} \end{bmatrix} + \begin{bmatrix} (J_z - J_y)\omega_{yB}\omega_{zB} \\ (J_x - J_z)\omega_{xB}\omega_{zB} \\ (J_y - J_x)\omega_{xB}\omega_{yB} \end{bmatrix} = \begin{bmatrix} \tau_{xB} \\ \tau_{yB} \\ \tau_{zB} \end{bmatrix} \tag{5.18}$$

These are the famous Euler equations that describe how the body-axis components of the angular velocity evolve in time, in response to torque components in body axes. In order to completely define the attitude (orientation), we need to relate the rotation angles ϕ, θ, and ψ to the angular velocity components

$$\begin{aligned} \dot{\phi} &= \omega_x + (\omega_y \sin\phi + \omega_z \cos\phi)\tan\theta \\ \dot{\theta} &= \omega_y \cos\phi - \omega_z \sin\phi \\ \dot{\psi} &= (\omega_x \sin\phi + \omega_y \cos\phi)/\cos\theta \end{aligned} \tag{5.19}$$

The rotation motion of a general rigid body has been given in (5.15). In aircraft terminology the projections of the angular velocity vector on the body *x*, *y*, and *z* axes have standard symbols.

$$\begin{aligned} \omega_x &= p \text{ (roll rate)} \\ \omega_y &= q \text{ (pitch rate)} \end{aligned} \tag{5.20}$$

$$\omega_z = r \text{ (yaw rate)}$$

Thus assuming the body axes are the principal axes of the aircraft, the rotational dynamics can be expressed as

$$\begin{aligned} \dot{p} &= \frac{L}{J_x} - \frac{J_z - J_y}{J_x} qr \\ \dot{q} &= \frac{M}{J_y} - \frac{J_x - J_z}{J_y} pr \\ \dot{r} &= \frac{N}{J_z} - \frac{J_y - J_x}{J_z} pq \end{aligned} \tag{5.21}$$

Where L is the rolling moment, M is the pitching moment, and N is the yawing moment. To define the translational motion of an rotorcraft it is customary to project the velocity vector onto body fixed axes.

$$\vec{v}_B = \begin{bmatrix} u \\ v \\ w \end{bmatrix} \tag{5.22}$$

Where u, v, and w are the projections of the vehicle velocity vector onto the body x, y, and z axes. The linear momentum of the body, in an inertial frame is

$$\vec{p} = m\vec{v}_I = mT_{IB}\vec{v}_B$$

Hence , the dynamic equations for translation are

$$\frac{d}{dt}\left(mT_{IB}\vec{v}_B\right) = m\left(T_{IB}\frac{d\vec{v}_B}{dt} + \dot{T}_{IB}\vec{v}_B\right) = \vec{f}_I \tag{5.23}$$

where $\vec{f}_I$ are the external forces acting on the aircraft referred to an inertial frame. Proceeding as before, we can find that

$$\frac{d\vec{v}_B}{dt} = -T_{BI}\dot{T}_{IB}\vec{v}_B + \frac{1}{m}\vec{f}_B \tag{5.24}$$

also

$$T_{BI}\dot{T}_{IB} = \begin{bmatrix} 0 & -r & q \\ r & 0 & -p \\ -q & p & 0 \end{bmatrix} \tag{5.25}$$

In component form (5.24) becomes

$$\begin{aligned} \dot{u} &= rv - qw + \frac{1}{m} f_{xB} \\ \dot{v} &= -ru + pw + \frac{1}{m} f_{yB} \\ \dot{w} &= qu - pv + \frac{1}{m} f_{zB} \end{aligned} \tag{5.26}$$

Where f_{xB}, $f_{yB,}$ and f_{zB} are the total forces acting on the body. The equations for the vehicle position are

$$\begin{bmatrix} \dot{x} \\ \dot{y} \\ \dot{z} \end{bmatrix} = T_{IB} \begin{bmatrix} u \\ v \\ w \end{bmatrix} \tag{5.27}$$

Complete dynamic equations of the vehicle is given in (5.28), this system of 12 first order differential equations, with the moments and forces constitute the complete six-degrees-of-freedom description of a rotorcraft behavior.

$$
\begin{aligned}
\dot{p} &= \frac{L}{J_x} - \frac{J_z - J_y}{J_x} qr \\
\dot{q} &= \frac{M}{J_y} - \frac{J_x - J_z}{J_y} pr \\
\dot{r} &= \frac{N}{J_z} - \frac{J_y - J_x}{J_z} pq \\
\dot{u} &= rv - qw + \frac{1}{m} f_{xB} \\
\dot{v} &= -ru + pw + \frac{1}{m} f_{yB} \\
\dot{w} &= qu - pv + \frac{1}{m} f_{zB} \\
\dot{\phi} &= \omega_x + (\omega_y \sin\phi + \omega_z \cos\phi)\tan\theta \\
\dot{\theta} &= \omega_y \cos\phi - \omega_z \sin\phi \\
\dot{\psi} &= (\omega_x \sin\phi + \omega_y \cos\phi)/\cos\theta \\
\begin{bmatrix} \dot{x} \\ \dot{y} \\ \dot{z} \end{bmatrix} &= T_{IB} \begin{bmatrix} u \\ v \\ w \end{bmatrix}
\end{aligned}
\tag{5.28}
$$

5.1.2 Helicopter Flight Dynamics: Trim, Stability, and Response

In most applications, not all of the 12 states variables derived in the previous section are of interest, and not all the differential equations are needed. A mathematical description or simulation of helicopter's flight dynamics needs to embody the important aerodynamic, structural and other internal dynamic effects (e.g. engine, actuation) that combine to influence the response of the aircrafts to controls. The problem is highly complex and the dynamic behavior of the helicopter is often limited by local effects that rapidly grow in their influence to inhibit larger or faster motion.

The behavior of a helicopter in flight can be modeled as the combination of a large number of interacting sub-systems. Figure 5.2 highlights the main rotor elements, the fuselage, power plant, and the resulting forces and moments.

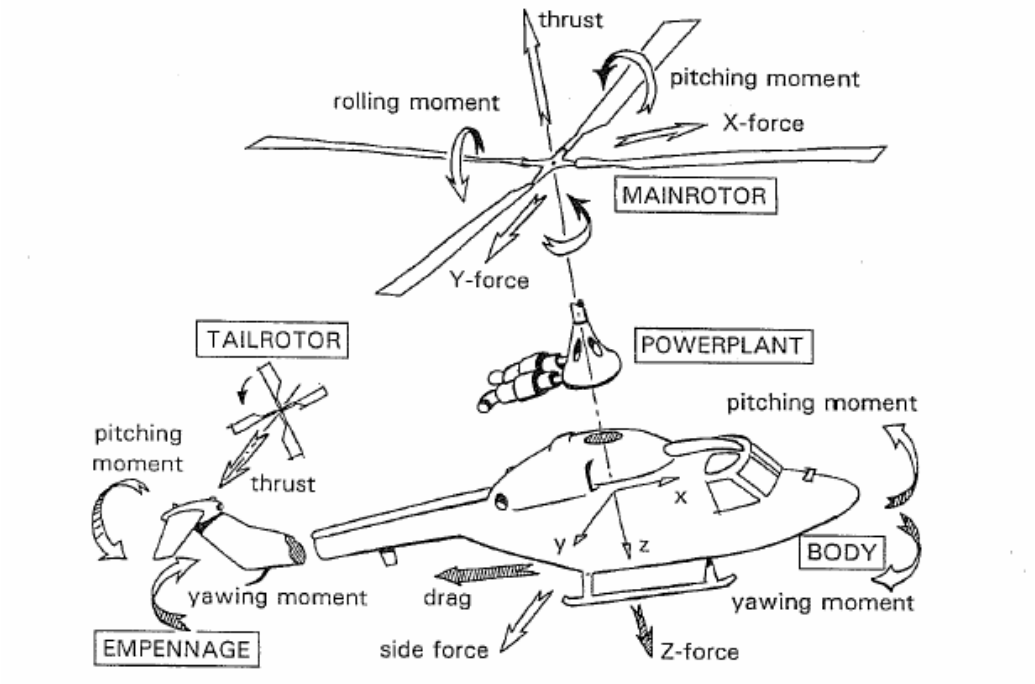

Figure 5.2 The modeling components of a helicopter

Helicopter states in body frame coordinate system are shown in simplified form in Figure 5.3. Strictly speaking, the center of gravity will move as the rotor blades flap, but we shall assume that the center of gravity is located at the mean position, relative to a particular trim state.

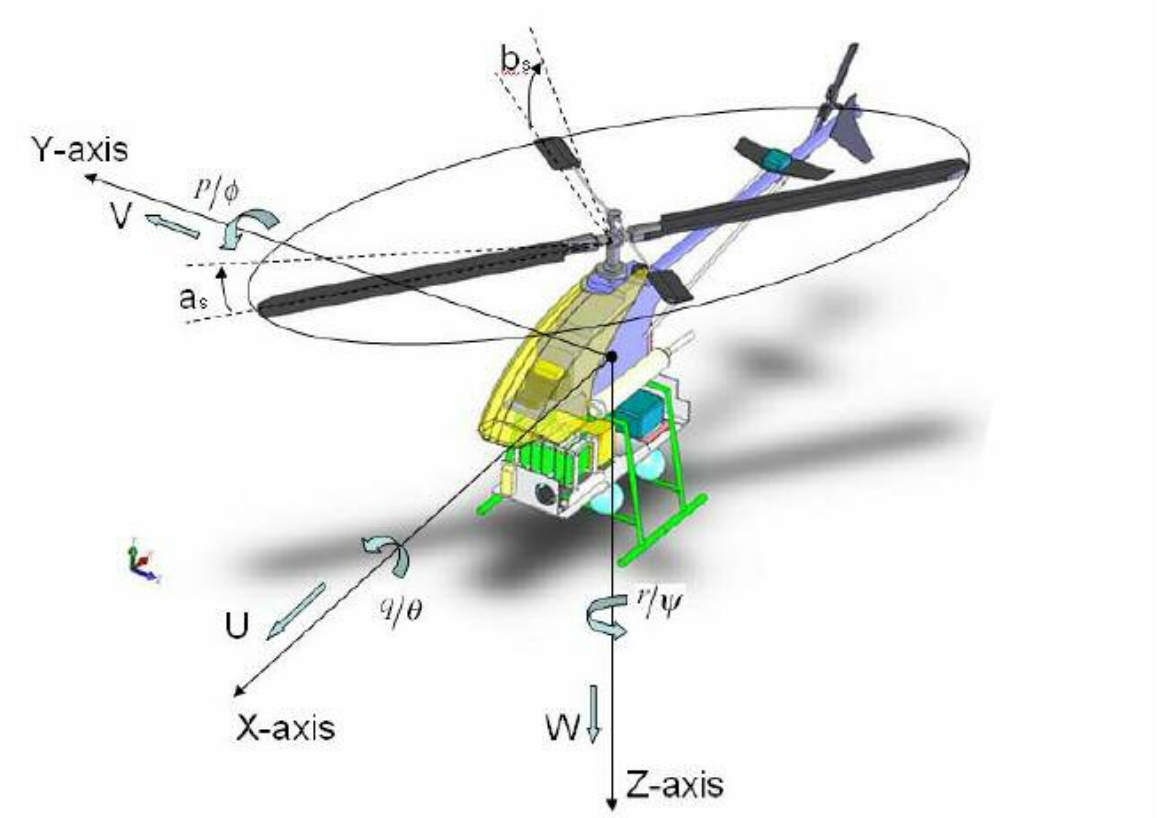

Figure 5.3 Helicopter states in body frame coordinate system

The equations governing the behavior of these interactions are developed from the application of the physical laws, e.g., conservation of energy, Newton's law of motion, to the individual components, and commonly take the form of nonlinear differential equations written in the first order vector form

$$\frac{dx}{dt} = f(x,u,t) \tag{5.29}$$

with initial conditions $x(0)=x_0$

$x(t)$ is the column vector of state variables; $u(t)$ is the vector of control variables and f is a nonlinear function of the aircraft motion, control inputs and external disturbances.

For the special case where only six rigid body degrees of freedom are considered, the state vector x, comprises the three translational velocity components $u, v, \text{and } w$, the three rotational velocity components $p, q, \text{and } r$ and the Euler angles $\phi, \theta, \text{and } \psi$. The three Euler attitude angles augment the equations of motion through the kinematic relationship between the fuselage rates $p, q, \text{and } r$ and the rate of change of euler angles $\dot{\phi}, \dot{\theta}, \text{and } \dot{\psi}$. The velocities are referred to an axes system fixed at the center of gravity as shown in the Figure 5.3 and the Euler angles define the orientation of the fuselage with respect to an earth fixes axes system.

The degrees of freedom can be arranged in the state vector as longitudinal and lateral motion subsets, as

$$x = [u \quad w \quad q \quad \theta \quad v \quad p \quad \phi \quad r \quad \psi]^T \tag{5.30}$$

The function f then contains the applied forces and moments, again referred to the aircraft centre of gravity, from aerodynamic, structural, gravitational, and inertial sources. Strictly speaking, the inertial and gravitational forces are not applied but it is conventional to label them so and place them on the right-hand side of the describing equation. The derivation of these equations from Newton's laws of motion is carried out in appendix.

It is important to note that this six degrees-of-freedom model, while itself complex and widely used is still an approximation to the aircraft behavior. This process of approximation is a common feature of flight dynamics, in the search for simplicity to enhance physical understanding and ease the computational burden.

Solution to the three fundamental problems of flight dynamics can be cab be formulated using Trim, Stability and the Response notions.

Trim is generally defined as a condition in which none of the state variables change with time (that is, all of the state variable rates are zero) and the resultant of applied forces and moments is zero. This does not, however, preclude accelerating conditions; the velocities must remain fixed in body axes, but will change direction in an inertial reference frame if the helicopter rotates. In a trimmed maneuver, the helicopter will be accelerating under the action of a non-zero resultant aerodynamic and gravitational forces and moments, but these will then be balanced by effects such as centrifugal and gyroscopic inertial forces and moments. The trim solution is represented by zeros of a nonlinear algebraic function, where the control u_e required holding a defined state x_e in equilibrium. With four controls, only four states can be prescribed in trim, the remaining set forming into the additional unknowns in Equation (3.1).

$$f(x_e, u_e) = 0 \tag{5.31}$$

The solution of the stability problem is found by linearizing the equations about a particular trim condition and computing the eigen values of the aircraft system matrix written in Equation (5.32) as the partial derivative of the forcing vector with respect to the system states. The stability thus found refers to small motions about the trim point, for larger motions, nonlinearities can alter the behavior.

$$\det\left[\lambda I - \left(\frac{\partial f}{\partial x}\right)_{x_e}\right] = 0 \tag{5.32}$$

The response solution is found from the time integral of the forcing function and allows the evolution of the aircraft states, forces and moments to be computed following disturbed initial conditions *x(0)*, and/or prescribed control inputs and atmospheric disturbances. In simulations, the nonlinear equations are usually solved numerically; analytical solutions generally do not exist.

$$x(t) = x(0) + \int_0^t f(x(\tau), u(\tau), \tau) d\tau \tag{5.33}$$

Helicopter as a six-degrees-of freedom rigid body model can be augmented with servo/rotor dynamics, and artificial yaw damping dynamics.

5.1.3 Helicopter Reduced Order Modeling

To initialize the design process reduced order model can be derived from a full order model. Full order state dynamics is shown in equations (5.34) to (5.44).

$$\dot{U} = X_U U - g\theta + X_{a_s} a_s \tag{5.34}$$

$$\dot{V} = Y_V V + g\phi + Y_{b_s} b_s \tag{5.35}$$

$$\dot{p} = L_U U + L_V V + L_{a_s} a_s + L_{b_s} b_s \tag{5.36}$$

$$\dot{q} = M_U U + M_V V + M_{a_s} a_s + M_{b_s} b_s \tag{5.37}$$

$$\dot{\phi} = p \tag{5.38}$$

$$\dot{\theta} = q \tag{5.39}$$

$$\dot{a}_s = -q - \frac{1}{\tau_f} a_s + A_{b_s} b_s + A_{lati}\delta_{lati} + A_{longi}\delta_{longi} \tag{5.40}$$

$$\dot{b}_s = -p + B_{a_s} a_s - \frac{1}{\tau_f} b_s + B_{lati}\delta_{lati} + B_{longi}\delta_{longi} \tag{5.41}$$

$$\dot{W} = Z_{as} a_s + Z_{b_s} b_s + Z_w w + Z_r r + Z_{col} \delta_{col} \tag{5.42}$$

$$\dot{r} = N_p p + N_w W + N_r r - N_{ped} r_{fb} + N_{col} \delta_{col} + N_{ped} \delta_{ped} \tag{5.43}$$

$$\dot{r}_{fb} = K_r r - K_{r_{fb}} r_{fb} \tag{5.44}$$

For small scale rotorcrafts, lateral & longitudinal blade flapping angles, and yaw rate feedback can be neglected as the first stage of control design process

Neglecting yaw rate feedback i.e Equation (5.44)

Equation (5.43) can be written as

$$\dot{r} = N_p p + N_w W + N_r r + N_{col} \delta_{col} + N_{ped} \delta_{ped} \tag{5.45}$$

One has to take care of the coupling of the dynamics (intended to be neglected) with Equations (5.34), (5.35), (5.36), (5.37) and (5.43).

To neglect the dynamics involved with a_s and b_s, we assume no change with respect to time, i.e. $\dot{a}_s = 0, \dot{b}_s = 0$.

$$\dot{a}_s = -q - \frac{1}{\tau_f} a_s + A_{b_s} b_s + A_{lati} \delta_{lati} + A_{longi} \delta_{longi} = 0 \tag{5.46}$$

$$\dot{b}_s = -p + B_{a_s} a_s - \frac{1}{\tau_f} b_s + B_{lati} \delta_{lati} + B_{longi} \delta_{longi} = 0 \tag{5.47}$$

Working with Equations (5.46) and (5.47) will lead to (5.48) and (5.49)

$$a_s = \tau_f (-q + A_{b_s} b_s + A_{lati} \delta_{lati} + A_{longi} \delta_{longi}) \tag{5.48}$$

$$b_s = \tau_f (-p + B_{a_s} a_s + B_{lati} \delta_{lati} + B_{longi} \delta_{longi}) \tag{5.49}$$

Substituting (5.49) into (5.48)

$$a_s = \tau_f \left[-q + A_{b_s} \left\{ \begin{matrix} \tau_f (-p + B_{a_s} a_s \\ + B_{lati} \delta_{lati} + B_{longi} \delta_{longi}) \end{matrix} \right\} + A_{lati} \delta_{lati} + A_{longi} \delta_{longi} \right] \tag{5.50}$$

$$a_s = \left[-\tau_f q + \tau_f \begin{Bmatrix} A_{b_s}\tau_f(-p + B_{a_s}a_s + \\ B_{lati}\delta_{lati} + B_{longi}\delta_{longi}) \end{Bmatrix} + \tau_f A_{lati}\delta_{lati} + \tau_f A_{longi}\delta_{longi} \right]$$

$$a_s = \left[-\tau_f q + \begin{Bmatrix} A_{b_s}\tau_f{}^2(-p + B_{a_s}a_s + \\ B_{lati}\delta_{lati} + B_{longi}\delta_{longi}) \end{Bmatrix} + \tau_f A_{lati}\delta_{lati} + \tau_f A_{longi}\delta_{longi} \right]$$

$$a_s(1 - A_{b_s}\tau_f{}^2 B_{a_s}) = -A_{b_s}\tau_f{}^2 p - \tau_f q + (\tau_f A_{lati} + A_{b_s}\tau_f{}^2 B_{lati})\delta_{lati} + (\tau_f A_{longi} + A_{b_s}\tau_f{}^2 B_{longi})\delta_{longi}$$

$$\begin{aligned} a_s &= -\frac{A_{b_s}\tau_f{}^2}{(1 - A_{b_s}\tau_f{}^2 B_{a_s})} p - \frac{\tau_f}{(1 - A_{b_s}\tau_f{}^2 B_{a_s})} q \\ &+ \frac{(\tau_f A_{lati} + A_{b_s}\tau_f{}^2 B_{lati})}{(1 - A_{b_s}\tau_f{}^2 B_{a_s})}\delta_{lati} + \frac{(\tau_f A_{longi} + A_{b_s}\tau_f{}^2 B_{longi})}{(1 - A_{b_s}\tau_f{}^2 B_{a_s})}\delta_{longi} \end{aligned} \qquad (5.51)$$

Substituting (5.48) into (5.49)

$$b_s = \tau_f[-p + B_{a_s}\{\tau_f(-q + A_{b_s}b_s + A_{lati}\delta_{lati} + A_{longi}\delta_{longi}\} + B_{lati}\delta_{lati} + B_{longi}\delta_{longi}]$$

$$b_s(1 - B_{a_s}\tau_f{}^2 A_{b_s}) = -\tau_f p - B_{a_s}\tau_f{}^2 q + (B_{a_s}\tau_f{}^2 A_{lati} + \tau_f B_{lati})\delta_{lati} + (B_{a_s}\tau_f{}^2 A_{longi} + \tau_f B_{longi})\delta_{longi}$$

Finally

$$\begin{aligned} b_s &= -\frac{\tau_f}{(1 - B_{a_s}\tau_f{}^2 A_{b_s})} p - \frac{B_{a_s}\tau_f{}^2}{(1 - B_{a_s}\tau_f{}^2 A_{b_s})} q \\ &+ \frac{(B_{a_s}\tau_f{}^2 A_{lati} + \tau_f B_{lati})}{(1 - B_{a_s}\tau_f{}^2 A_{b_s})}\delta_{lati} + \frac{(B_{a_s}\tau_f{}^2 A_{longi} + \tau_f B_{longi})}{(1 - B_{a_s}\tau_f{}^2 A_{b_s})}\delta_{longi} \end{aligned} \qquad (5.52)$$

Substituting (5.51) into Equation (5.34)

$$\dot{U} = X_U U - g\theta + X_{a_s}\left[\begin{aligned} &-\frac{A_{b_s}\tau_f{}^2}{(1 - A_{b_s}\tau_f{}^2 B_{a_s})} p - \frac{\tau_f}{(1 - A_{b_s}\tau_f{}^2 B_{a_s})} q \\ &+ \frac{(\tau_f A_{lati} + A_{b_s}\tau_f{}^2 B_{lati})}{(1 - A_{b_s}\tau_f{}^2 B_{a_s})}\delta_{lati} + \frac{(\tau_f A_{longi} + A_{b_s}\tau_f{}^2 B_{longi})}{(1 - A_{b_s}\tau_f{}^2 B_{a_s})}\delta_{longi} \end{aligned} \right]$$

Modified dynamics for body frame x axis velocity is now

$$\dot{U} = X_U U - g\theta - \left[\frac{X_{a_s} A_{b_s} \tau_f{}^2}{(1 - A_{b_s} \tau_f{}^2 B_{a_s})}\right] p - \left[\frac{X_{a_s} \tau_f}{(1 - A_{b_s} \tau_f{}^2 B_{a_s})}\right] q + \left[\frac{X_{a_s} (\tau_f A_{lati} + A_{b_s} \tau_f{}^2 B_{lati})}{(1 - A_{b_s} \tau_f{}^2 B_{a_s})}\right] \delta_{lati} + \left[\frac{X_{a_s} (\tau_f A_{longi} + A_{b_s} \tau_f{}^2 B_{longi})}{(1 - A_{b_s} \tau_f{}^2 B_{a_s})}\right] \delta_{longi} \tag{5.53}$$

Similarly

$$\dot{V} = Y_V V + g\phi + Y_{b_s} \left[\begin{array}{l} -\frac{\tau_f}{(1 - B_{a_s} \tau_f{}^2 A_{b_s})} p - \frac{B_{a_s} \tau_f{}^2}{(1 - B_{a_s} \tau_f{}^2 A_{b_s})} q \\ + \frac{(B_{a_s} \tau_f{}^2 A_{lati} + \tau_f B_{lati})}{(1 - B_{a_s} \tau_f{}^2 A_{b_s})} \delta_{lati} + \frac{(B_{a_s} \tau_f{}^2 A_{longi} + \tau_f B_{longi})}{(1 - B_{a_s} \tau_f{}^2 A_{b_s})} \delta_{longi} \end{array} \right]$$

$$\dot{V} = Y_V V + g\phi - \left[\frac{Y_{b_s} \tau_f}{(1 - B_{a_s} \tau_f{}^2 A_{b_s})}\right] p - \left[\frac{Y_{b_s} B_{a_s} \tau_f{}^2}{(1 - B_{a_s} \tau_f{}^2 A_{b_s})}\right] q + \left[\frac{Y_{b_s} (B_{a_s} \tau_f{}^2 A_{lati} + \tau_f B_{lati})}{(1 - B_{a_s} \tau_f{}^2 A_{b_s})}\right] \delta_{lati} + \left[\frac{Y_{b_s} (B_{a_s} \tau_f{}^2 A_{longi} + \tau_f B_{longi})}{(1 - B_{a_s} \tau_f{}^2 A_{b_s})}\right] \delta_{longi} \tag{5.54}$$

Working with Equation (5.36)

$$\dot{p} = L_U U + L_V V + L_{a_s} a_s + L_{b_s} b_s$$

$$\dot{p} = L_U U + L_V V$$
$$+ L_{a_s} \begin{bmatrix} -\dfrac{A_{b_s}\tau_f{}^2}{(1 - A_{b_s}\tau_f{}^2 B_{a_s})} p - \dfrac{\tau_f}{(1 - A_{b_s}\tau_f{}^2 B_{a_s})} q \\ + \dfrac{(\tau_f A_{lati} + A_{b_s}\tau_f{}^2 B_{lati})}{(1 - A_{b_s}\tau_f{}^2 B_{a_s})} \delta_{lati} + \dfrac{(\tau_f A_{longi} + A_{b_s}\tau_f{}^2 B_{longi})}{(1 - A_{b_s}\tau_f{}^2 B_{a_s})} \delta_{longi} \end{bmatrix}$$
$$+ L_{b_s} \begin{bmatrix} -\dfrac{\tau_f}{(1 - B_{a_s}\tau_f{}^2 A_{b_s})} p - \dfrac{B_{a_s}\tau_f{}^2}{(1 - B_{a_s}\tau_f{}^2 A_{b_s})} q \\ + \dfrac{(B_{a_s}\tau_f{}^2 A_{lati} + \tau_f B_{lati})}{(1 - B_{a_s}\tau_f{}^2 A_{b_s})} \delta_{lati} + \dfrac{(B_{a_s}\tau_f{}^2 A_{longi} + \tau_f B_{longi})}{(1 - B_{a_s}\tau_f{}^2 A_{b_s})} \delta_{longi} \end{bmatrix}$$

$$\dot{p} =$$
$$L_U U + L_V V + \begin{bmatrix} -\dfrac{L_{a_s} A_{b_s}\tau_f{}^2}{(1 - A_{b_s}\tau_f{}^2 B_{a_s})} \\ -\dfrac{L_{b_s}\tau_f}{(1 - B_{a_s}\tau_f{}^2 A_{b_s})} \end{bmatrix} p$$
$$+ \begin{bmatrix} -\dfrac{L_{a_s}\tau_f}{(1 - A_{b_s}\tau_f{}^2 B_{a_s})} \\ -\dfrac{L_{b_s} B_{a_s}\tau_f{}^2}{(1 - B_{a_s}\tau_f{}^2 A_{b_s})} \end{bmatrix} q$$
$$+ \begin{bmatrix} \dfrac{L_{a_s}(\tau_f A_{lati} + A_{b_s}\tau_f{}^2 B_{lati})}{(1 - A_{b_s}\tau_f{}^2 B_{a_s})} \\ + \dfrac{L_{b_s}(B_{a_s}\tau_f{}^2 A_{lati} + \tau_f B_{lati})}{(1 - B_{a_s}\tau_f{}^2 A_{b_s})} \end{bmatrix} \delta_{lati}$$
$$+ \begin{bmatrix} \dfrac{L_{a_s}(\tau_f A_{longi} + A_{b_s}\tau_f{}^2 B_{longi})}{(1 - A_{b_s}\tau_f{}^2 B_{a_s})} \\ + \dfrac{L_{b_s}(B_{a_s}\tau_f{}^2 A_{longi} + \tau_f B_{longi})}{(1 - B_{a_s}\tau_f{}^2 A_{b_s})} \end{bmatrix} \delta_{longi} \qquad (5.55)$$

Working with Equation (5.37)

$$\dot{q} = M_U U + M_V V$$

$$+ M_{a_s}\left[\begin{array}{l} -\dfrac{A_{b_s}\tau_f{}^2}{(1-A_{b_s}\tau_f{}^2 B_{a_s})}p - \dfrac{\tau_f}{(1-A_{b_s}\tau_f{}^2 B_{a_s})}q \\ +\dfrac{(\tau_f A_{lati} + A_{b_s}\tau_f{}^2 B_{lati})}{(1-A_{b_s}\tau_f{}^2 B_{a_s})}\delta_{lati} + \dfrac{(\tau_f A_{longi} + A_{b_s}\tau_f{}^2 B_{longi})}{(1-A_{b_s}\tau_f{}^2 B_{a_s})}\delta_{longi} \end{array}\right]$$

$$+ M_{b_s}\left[\begin{array}{l} -\dfrac{\tau_f}{(1-B_{a_s}\tau_f{}^2 A_{b_s})}p - \dfrac{B_{a_s}\tau_f{}^2}{(1-B_{a_s}\tau_f{}^2 A_{b_s})}q \\ +\dfrac{(B_{a_s}\tau_f{}^2 A_{lati} + \tau_f B_{lati})}{(1-B_{a_s}\tau_f{}^2 A_{b_s})}\delta_{lati} + \dfrac{(B_{a_s}\tau_f{}^2 A_{longi} + \tau_f B_{longi})}{(1-B_{a_s}\tau_f{}^2 A_{b_s})}\delta_{longi} \end{array}\right]$$

$$\begin{aligned} &\dot{q} \\ &= M_U U + M_V V + \left[-\frac{M_{a_s} A_{b_s}\tau_f{}^2}{(1-A_{b_s}\tau_f{}^2 B_{a_s})} - \frac{M_{b_s}\tau_f}{(1-B_{a_s}\tau_f{}^2 A_{b_s})}\right]p \\ &+ \left[-\frac{M_{a_s}\tau_f}{(1-A_{b_s}\tau_f{}^2 B_{a_s})} - \frac{M_{b_s} B_{a_s}\tau_f{}^2}{(1-B_{a_s}\tau_f{}^2 A_{b_s})}\right]q \\ &+ \left[\frac{M_{a_s}(\tau_f A_{lati} + A_{b_s}\tau_f{}^2 B_{lati})}{(1-A_{b_s}\tau_f{}^2 B_{a_s})} + \frac{M_{b_s}(B_{a_s}\tau_f{}^2 A_{lati} + \tau_f B_{lati})}{(1-B_{a_s}\tau_f{}^2 A_{b_s})}\right]\delta_{lati} \\ &+ \left[\frac{M_{a_s}(\tau_f A_{longi} + A_{b_s}\tau_f{}^2 B_{longi})}{(1-A_{b_s}\tau_f{}^2 B_{a_s})} + \frac{M_{b_s}(B_{a_s}\tau_f{}^2 A_{longi} + \tau_f B_{longi})}{(1-B_{a_s}\tau_f{}^2 A_{b_s})}\right]\delta_{longi} \end{aligned} \tag{5.56}$$

Working with Equation (5.42)

$$\dot{W} = Z_{as}\left[\begin{array}{l} -\dfrac{A_{b_s}\tau_f{}^2}{(1-A_{b_s}\tau_f{}^2 B_{a_s})}p - \dfrac{\tau_f}{(1-A_{b_s}\tau_f{}^2 B_{a_s})}q \\ +\dfrac{(\tau_f A_{lati} + A_{b_s}\tau_f{}^2 B_{lati})}{(1-A_{b_s}\tau_f{}^2 B_{a_s})}\delta_{lati} + \dfrac{(\tau_f A_{longi} + A_{b_s}\tau_f{}^2 B_{longi})}{(1-A_{b_s}\tau_f{}^2 B_{a_s})}\delta_{longi} \end{array}\right]$$

$$+ Z_{b_s}\left[\begin{array}{l} -\dfrac{\tau_f}{(1-B_{a_s}\tau_f{}^2 A_{b_s})}p - \dfrac{B_{a_s}\tau_f{}^2}{(1-B_{a_s}\tau_f{}^2 A_{b_s})}q \\ +\dfrac{(B_{a_s}\tau_f{}^2 A_{lati} + \tau_f B_{lati})}{(1-B_{a_s}\tau_f{}^2 A_{b_s})}\delta_{lati} + \dfrac{(B_{a_s}\tau_f{}^2 A_{longi} + \tau_f B_{longi})}{(1-B_{a_s}\tau_f{}^2 A_{b_s})}\delta_{longi} \end{array}\right]$$

$$+ Z_w w + Z_r r + Z_{col}\delta_{col}$$

$$\dot{W} = \left[-\frac{Z_{as} A_{b_s} \tau_f{}^2}{(1 - A_{b_s} \tau_f{}^2 B_{a_s})} - -\frac{Z_{b_s} \tau_f}{(1 - B_{a_s} \tau_f{}^2 A_{b_s})} \right] p$$
$$+ \left[-\frac{Z_{as} \tau_f}{(1 - A_{b_s} \tau_f{}^2 B_{a_s})} - \frac{Z_{b_s} B_{a_s} \tau_f{}^2}{(1 - B_{a_s} \tau_f{}^2 A_{b_s})} \right] q + Z_w W + Z_r r$$
$$+ \left[\frac{Z_{as} (\tau_f A_{lati} + A_{b_s} \tau_f{}^2 B_{lati})}{(1 - A_{b_s} \tau_f{}^2 B_{a_s})} + \frac{Z_{b_s} (B_{a_s} \tau_f{}^2 A_{lati} + \tau_f B_{lati})}{(1 - B_{a_s} \tau_f{}^2 A_{b_s})} \right] \delta_{lati}$$
$$+ \left[\frac{Z_{as} (\tau_f A_{longi} + A_{b_s} \tau_f{}^2 B_{longi})}{(1 - A_{b_s} \tau_f{}^2 B_{a_s})} + \frac{Z_{b_s} (B_{a_s} \tau_f{}^2 A_{longi} + \tau_f B_{longi})}{(1 - B_{a_s} \tau_f{}^2 A_{b_s})} \right] \delta_{longi} + Z_{col} \delta_{col} \tag{5.57}$$

The reduced order model will become

for

$$x\_m = \begin{bmatrix} U & V & p & q & \phi & \theta & W & r \end{bmatrix}^T$$

$$A = \begin{bmatrix}
X_U & 0 & -\left[\frac{X_{a_s} A_{b_s} \tau_f{}^2}{(1 - A_{b_s} \tau_f{}^2 B_{a_s})}\right] & -\left[\frac{X_{a_s} \tau_f}{(1 - A_{b_s} \tau_f{}^2 B_{a_s})}\right] & 0 & -g & 0 & 0 \\
0 & Y_V & -\left[\frac{Y_{b_s} \tau_f}{(1 - B_{a_s} \tau_f{}^2 A_{b_s})}\right] & -\left[\frac{Y_{b_s} B_{a_s} \tau_f{}^2}{(1 - B_{a_s} \tau_f{}^2 A_{b_s})}\right] & g & 0 & 0 & 0 \\
L_U & L_V & \left[-\frac{L_{a_s} A_{b_s} \tau_f{}^2}{(1 - A_{b_s} \tau_f{}^2 B_{a_s})} - \frac{L_{b_s} \tau_f}{(1 - B_{a_s} \tau_f{}^2 A_{b_s})}\right] & \left[-\frac{L_{a_s} \tau_f}{(1 - A_{b_s} \tau_f{}^2 B_{a_s})} - \frac{L_{b_s} B_{a_s} \tau_f{}^2}{(1 - B_{a_s} \tau_f{}^2 A_{b_s})}\right] & 0 & 0 & 0 & 0 \\
M_U & M_V & \left[-\frac{M_{a_s} A_{b_s} \tau_f{}^2}{(1 - A_{b_s} \tau_f{}^2 B_{a_s})} - \frac{M_{b_s} \tau_f}{(1 - B_{a_s} \tau_f{}^2 A_{b_s})}\right] & \left[-\frac{M_{a_s} \tau_f}{(1 - A_{b_s} \tau_f{}^2 B_{a_s})} - \frac{M_{b_s} B_{a_s} \tau_f{}^2}{(1 - B_{a_s} \tau_f{}^2 A_{b_s})}\right] & 0 & 0 & 0 & 0 \\
0 & 0 & 1 & 0 & 0 & 0 & 0 & 0 \\
0 & 0 & 0 & 1 & 0 & 0 & 0 & 0 \\
0 & 0 & \left[-\frac{Z_{as} A_{b_s} \tau_f{}^2}{(1 - A_{b_s} \tau_f{}^2 B_{a_s})} - -\frac{Z_{b_s} \tau_f}{(1 - B_{a_s} \tau_f{}^2 A_{b_s})}\right] & \left[-\frac{Z_{as} \tau_f}{(1 - A_{b_s} \tau_f{}^2 B_{a_s})} - \frac{Z_{b_s} B_{a_s} \tau_f{}^2}{(1 - B_{a_s} \tau_f{}^2 A_{b_s})}\right] & 0 & 0 & Z_w & Z_r \\
0 & 0 & N_p & 0 & 0 & 0 & N_w & N_r
\end{bmatrix}$$

and $u = \begin{bmatrix} \delta_{lati} & \delta_{longi} & \delta_{col} & \delta_{ped} \end{bmatrix}^T$,

$B = \begin{bmatrix} B_1 & B_2 & B_3 & B_4 \end{bmatrix}$ such that

$$B_1 = \begin{bmatrix}
\left[\frac{X_{a_s}(\tau_f A_{lati} + A_{b_s} \tau_f{}^2 B_{lati})}{(1 - A_{b_s} \tau_f{}^2 B_{a_s})}\right] \\
\left[\frac{Y_{b_s}(B_{a_s} \tau_f{}^2 A_{lati} + \tau_f B_{lati})}{(1 - B_{a_s} \tau_f{}^2 A_{b_s})}\right] \\
\left[\frac{L_{a_s}(\tau_f A_{lati} + A_{b_s} \tau_f{}^2 B_{lati})}{(1 - A_{b_s} \tau_f{}^2 B_{a_s})} + \frac{L_{b_s}(B_{a_s} \tau_f{}^2 A_{lati} + \tau_f B_{lati})}{(1 - B_{a_s} \tau_f{}^2 A_{b_s})}\right] \\
\left[\frac{M_{a_s}(\tau_f A_{lati} + A_{b_s} \tau_f{}^2 B_{lati})}{(1 - A_{b_s} \tau_f{}^2 B_{a_s})} + \frac{M_{b_s}(B_{a_s} \tau_f{}^2 A_{lati} + \tau_f B_{lati})}{(1 - B_{a_s} \tau_f{}^2 A_{b_s})}\right] \\
0 \\
0 \\
\left[\frac{Z_{as}(\tau_f A_{lati} + A_{b_s} \tau_f{}^2 B_{lati})}{(1 - A_{b_s} \tau_f{}^2 B_{a_s})} + \frac{Z_{b_s}(B_{a_s} \tau_f{}^2 A_{lati} + \tau_f B_{lati})}{(1 - B_{a_s} \tau_f{}^2 A_{b_s})}\right] \\
0
\end{bmatrix},$$

$$B_2 = \begin{bmatrix} \left[\frac{X_{a_s}(\tau_f A_{longi} + A_{b_s}\tau_f{}^2 B_{longi})}{(1 - A_{b_s}\tau_f{}^2 B_{a_s})}\right] \\ \left[\frac{Y_{b_s}(B_{a_s}\tau_f{}^2 A_{longi} + \tau_f B_{longi})}{(1 - B_{a_s}\tau_f{}^2 A_{b_s})}\right] \\ \left[\frac{L_{a_s}(\tau_f A_{longi} + A_{b_s}\tau_f{}^2 B_{longi})}{(1 - A_{b_s}\tau_f{}^2 B_{a_s})} + \frac{L_{b_s}(B_{a_s}\tau_f{}^2 A_{longi} + \tau_f B_{longi})}{(1 - B_{a_s}\tau_f{}^2 A_{b_s})}\right] \\ \left[\frac{M_{a_s}(\tau_f A_{longi} + A_{b_s}\tau_f{}^2 B_{longi})}{(1 - A_{b_s}\tau_f{}^2 B_{a_s})} + \frac{M_{b_s}(B_{a_s}\tau_f{}^2 A_{longi} + \tau_f B_{longi})}{(1 - B_{a_s}\tau_f{}^2 A_{b_s})}\right] \\ 0 \\ 0 \\ \left[\frac{Z_{as}(\tau_f A_{longi} + A_{b_s}\tau_f{}^2 B_{longi})}{(1 - A_{b_s}\tau_f{}^2 B_{a_s})} + \frac{Z_{b_s}(B_{a_s}\tau_f{}^2 A_{longi} + \tau_f B_{longi})}{(1 - B_{a_s}\tau_f{}^2 A_{b_s})}\right] \\ 0 \end{bmatrix},$$

$$B_3 = \begin{bmatrix} 0 \\ 0 \\ 0 \\ 0 \\ 0 \\ 0 \\ Z_{col} \\ N_{col} \end{bmatrix}, \text{ and } B_4 = \begin{bmatrix} 0 \\ 0 \\ 0 \\ 0 \\ 0 \\ 0 \\ 0 \\ N_{ped} \end{bmatrix}$$

5.2 Attitude Control Loop Design Example

The controller design is based on an 11-state linear model of a "Raptor-90" helicopter shown in Figure 5.4.

Figure 5.4 Raptor-90 helicopter

The results are based on the model derived at National University of Singapore. A linearized model for hover operating point has been established. The model currently used is a state-space model which represents the helicopter as 6-degree-of-freedom (DOF) rigid body augmented with servo/rotor dynamics and artificial yaw damping dynamics(Chen, 2004). The state vector physically shown in Figure 5.3 (repeated here) contains eleven states and can be expressed as $x = [U \quad V \quad p \quad q \quad \phi \quad \theta \quad a_s \quad b_s \quad W \quad r \quad r_{fb}]^T$.

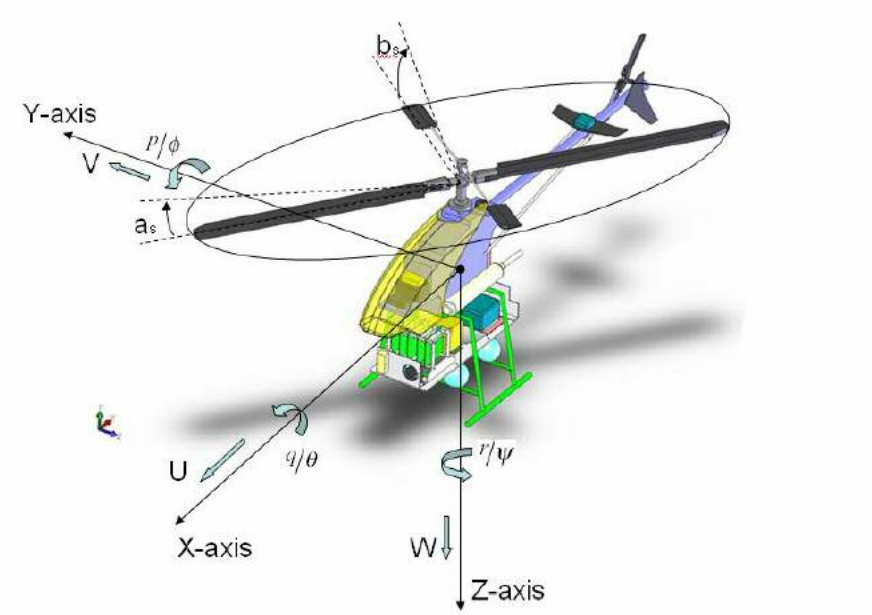

Figure 5.3 Helicopter states in body frame coordinate system

The input vector can be written as $u = [\delta_{lati} \quad \delta_{longi} \quad \delta_{ped}]^T$. Where δ_{lati} is the lateral channel input and affects roll motion, δ_{longi} is longitudinal channel input and affects pitch, δ_{ped} is pedal channel input of remote controller and affects yaw motion. In helicopters there is a high degree of coupling between lateral and longitudinal dynamics. In this paper collective channel, the fourth actuator which produces lift, is left to be controlled manually.

The primary variables to be controlled are the pitch angle and roll angle. Two extra rate gyros measuring pitch angular rate and roll angular rate will also be used for feedback purposes. Five system states constitute the output vector $y = [\phi \quad \theta \quad r \quad p \quad q]^T$. The rotorcraft equations mentioned were trimmed in a hover configuration to obtain the reference trim condition. The nonlinear equations then

linearized for the hover configuration based on the reference values obtained[5]. The plant linear matrices are as below

$$A = \begin{bmatrix} -0.1778 & 0 & 0 & 0 & 0 & -9.7807 & -9.7807 & 0 & 0 & 0 & 0 \\ 0 & -0.3104 & 0 & 0 & 9.7807 & 0 & 0 & 9.7807 & 0 & 0 & 0 \\ -0.3326 & -0.5353 & 0 & 0 & 0 & 0 & 75.7640 & 343.8600 & 0 & 0 & 0 \\ 0.1903 & -0.2940 & 0 & 0 & 0 & 0 & 172.6200 & -59.9580 & 0 & 0 & 0 \\ 0 & 0 & 1 & 0 & 0 & 0 & 0 & 0 & 0 & 0 & 0 \\ 0 & 0 & 0 & 1 & 0 & 0 & 0 & 0 & 0 & 0 & 0 \\ 0 & 0 & 0 & -1 & 0 & 0 & -8.1222 & 4.6535 & 0 & 0 & 0 \\ 0 & 0 & -1 & 0 & 0 & 0 & -0.0921 & -8.1222 & 0 & 0 & 0 \\ 0 & 0 & 0 & 0 & 0 & 0 & 17.1680 & 7.1018 & -0.6821 & -0.1070 & 0 \\ 0 & 0 & -0.2834 & 0 & 0 & 0 & 0 & 0 & -0.1446 & -5.5561 & -36.6740 \\ 0 & 0 & 0 & 0 & 0 & 0 & 0 & 0 & 0 & 2.7492 & -11.1120 \end{bmatrix}$$

$$B = \begin{bmatrix} 0 & 0 & 0 \\ 0 & 0 & 0 \\ 0 & 0 & 0 \\ 0 & 0 & 0 \\ 0 & 0 & 0 \\ 0 & 0 & 0 \\ 0.0632 & 3.3390 & 0 \\ 3.1739 & 0.2216 & 0 \\ 0 & 0 & 0 \\ 0 & 0 & -74.3640 \\ 0 & 0 & 0 \end{bmatrix}$$

5.2.1 Wind Turbulence Model

The disturbance vector d given in (5.58) has wind components along the $[x \quad y]^T$ fuselage axes, disturbance input matrix D defines dynamics involved with body frame x, and y velocities. For this example D is a 11×2 matrix and is constituted from first two columns of the plant matrix A.

$$d = [d_U \quad d_V]^T \tag{5.58}$$

In Hall and Bryson(1973) the wind components along the fuselage axes are modeled by independently excited correlated Gauss-Markov processes

$$\begin{bmatrix} \dot{d}_U \\ \dot{d}_V \end{bmatrix} = \begin{bmatrix} -1/\tau_c & 0 \\ 0 & -1/\tau_c \end{bmatrix} \begin{bmatrix} d_U \\ d_V \end{bmatrix} + \rho * B_w \begin{bmatrix} q_U \\ q_V \end{bmatrix} \tag{5.59}$$

Equation (5.59) is called a "shaping filter" for the wind, where q_U, and q_V are independent with zero mean, $\tau_c = 3.2\,\text{sec}$ is the correlation time of the wind, $\sigma_{q_U}, \sigma_{q_V} = 20\,ft/s$, B_w is the turbulence input identity matrix, and $\rho = 1/2$ is the scalar weighting factor.

5.2.2 Controller Structure

The control structure shown in Figure 5.5 is basically an attitude control loop; each input channel is augmented with a compensator. Precompensators $G_{lat}(s)$, $G_{long}(s)$, and $G_{ped}(s)$ shape the plant prior to closing the loop. Loop shaping procedure is explained in the next section.

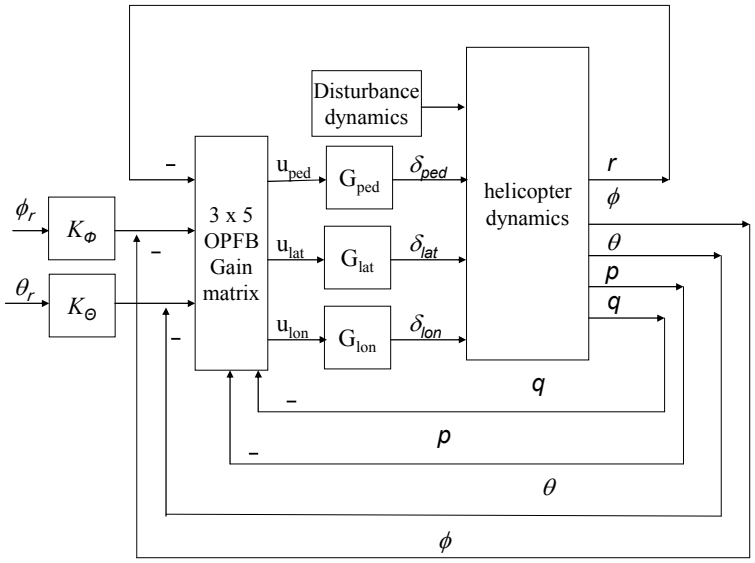

Figure 5.5 Controller Structure

5.2.3 H-Infinity Loop Shaping Design Procedure

We will now formally state the design procedure. The objective of this approach is to balance the tradeoff between performance and robustness in loop shaping. The procedure couples loop shaping design with H-Infinity output-feedback control techniques.

Using a precompensator W_1 and a postcompensator W_2, the singular values of the nominal plant are shaped to achieve a desired open-loop shape. The nominal plant G and the compensators are combined to form the shaped plant G_s. Let (A, B, C, D_{sys}) be a realization of G_s.

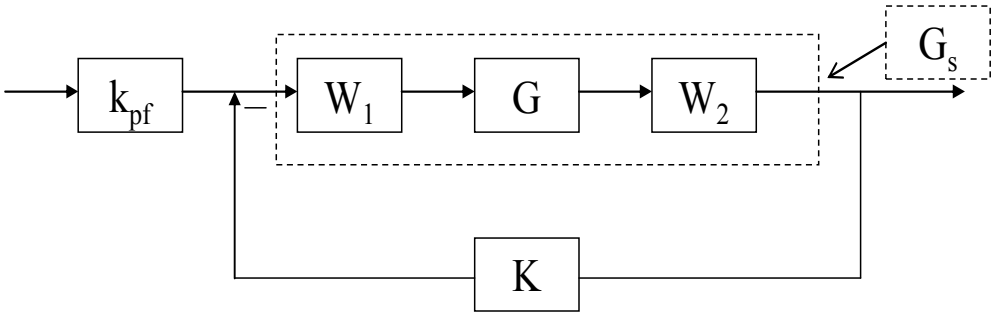

Figure 5.6 Loop shaped plant with controller

- Choose weighing matrices Q and R for G_s.
- Use H-Infinity static output feedback algorithm to find the static output-feedback gain. The algorithm is described in Chapter 3.
- Find prefilter gain K_{pf} for unity steady state gain between input and output pairs.

In this example precompensators $G_{lat}(s), G_{lon}(s), \text{and } G_{ped}(s)$ all are chosen as $G_{precomp}(s) = 2\left(\frac{s+0.5}{s(s+5)}\right)$ to shape the open loop plant. Additional dynamics in the Pre-Compensators is included to pull the cut-off to within the 2-5 rad/sec region, which is typical with aircraft and rotorcraft controllers. The design was effective using only the Pre-Compensators, so no Post-Compensators were chosen, i.e., the Post-Compensator weights was set to the identity matrix. The singular value plots of the original loop-gain and the shaped loop-gain are shown in Figure 5.7. Also shown is the wind gust spectrum.

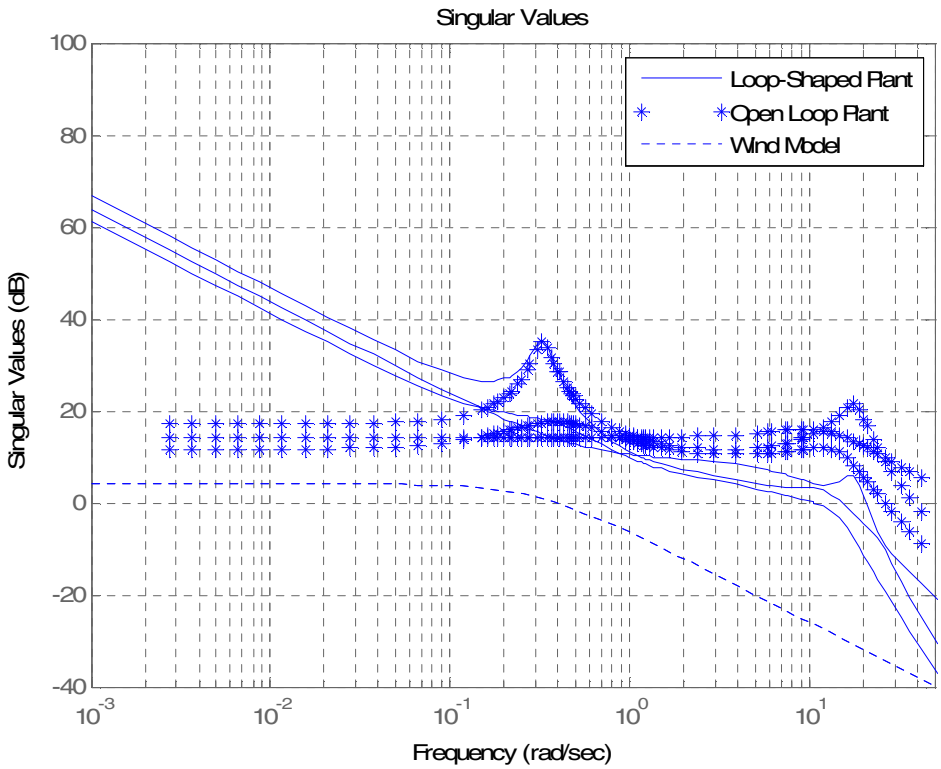

Figure 5.7 Loop-gain singular value plots

Weighting Matrices

In this example the weighting matrices are taken as

$$Q = \text{diag}\begin{bmatrix} 0.25 & 0.25 & 0.01 & 0.01 & 100 & 100 & 1E\text{-}4 & 1E\text{-}4 & 0.25 & 0.01 & 0.01 & 0 & 0 & 0 & 0 & 0 & 0 \end{bmatrix}$$

$$R = \text{diag}\begin{bmatrix} 169 & 169 & 0.78 \end{bmatrix}.$$

The selection of Q and R is further discussed in the next subsection.

5.2.4 Simulation Results with Disturbance Effects

The static output feedback solution derived in Chapter 2 is applied to obtain an output feedback controller to stabilize the loop-shaped plant. The controller is then simulated subject to the wind disturbances to evaluate the efficacy of the proposed control law. The closed-loop system is shown in Figure 5.8, where the exogenous disturbance input *d(t)* is a random variable, shown in Figure 5.9, generated in the time domain to match statistical properties of the turbulence model, as discussed in Section B.

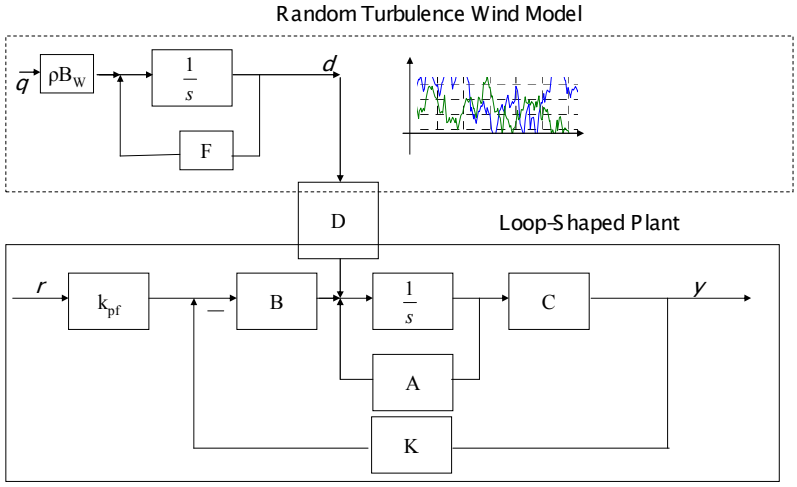

Figure 5.8 Simulation with turbulence model

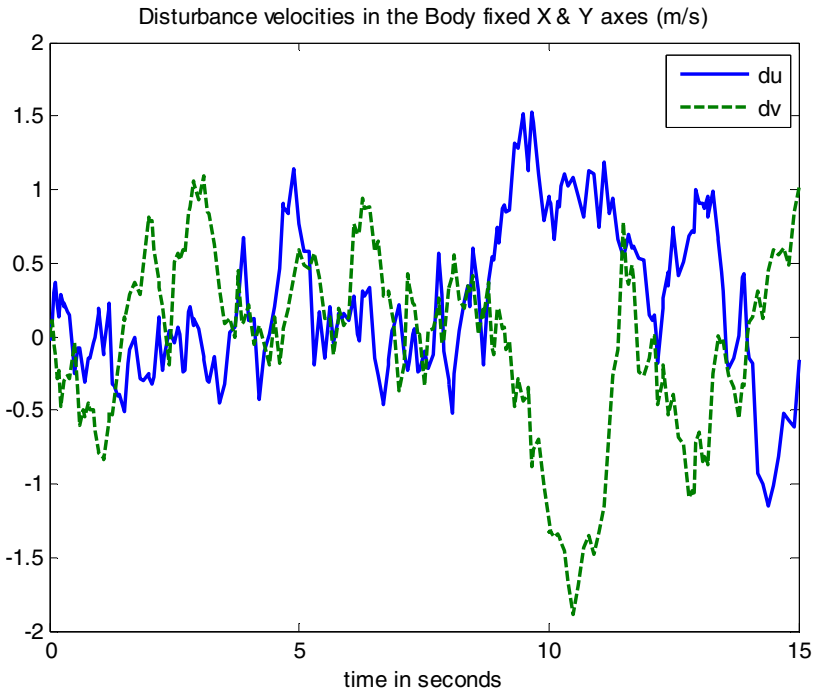

Figure 5.9 Random velocity disturbance vector

For the computation of the output-feedback gain K it is necessary to select weighting matrices Q and R. A diagonal structure is used for Q and R. The diagonal entries are tuned iteratively. That is, for a given selection of Q and R, our algorithm was run to find the OPFB gain K. Then, the closed-loop system was simulated. If the results are not satisfactory, Q and R were modified and the procedure was repeated. Our algorithm makes it very fast and easy to perform this procedure., To avoid the excitation of un-modeled high frequency dynamics, the control input and velocity states are heavily penalized.

The gain parameter γ defines the desired L_2 gain bound. For the initial design, a fairly large γ is selected. If the algorithm converges, the parameter γ may be

reduced. If γ is taken too small the algorithm will not converge since the Algebraic Riccati Equation has no positive semidefinite solution. After some design repetitions, which were performed very quickly using the algorithm; we found the smallest value of the gain to be 0.62.

Two particular cases were simulated to evaluate the closed loop system performance, namely bank angle command tracking i.e. $\phi_{command}$ and a pitch angle command tracking i.e. $\theta_{command}$

Bank angle command tracking ($\phi_{command}$): The step responses of the lateral-directional states for a unit bank angle command (equivalent of 1 radian) are shown in Figure 5.10. The inner loop simulation is begun at a hover configuration at an altitude of 50 m and was subjected to a turbulent wind disturbance with peak amplitude of 4.0 m/s. Considering, that the helicopter is initially in the hover configuration, this is a significant perturbation. It is seen that the bank angle settles to less than 5% of the steady state value within 5 seconds. The overshoot is 18.5%. The roll rate does not peak beyond 1 rad/s, which is within acceptable limits. We also note that the yaw rate activity is consistent with the build up in the lateral velocity. It is to be mentioned that throughout this inner loop control design, the collective pitch is not utilized. The consequence of this is a velocity build-up that causes the helicopter to drift from its current position. It was seen that without the collective pitch being active, the helicopter loses altitude very rapidly as the main rotor thrust vector is no longer aligned along the inertial Z-axis. The only way to increase the component of the thrust along the inertial Z-axis to balance the weight of the helicopter is to use the collective pitch.

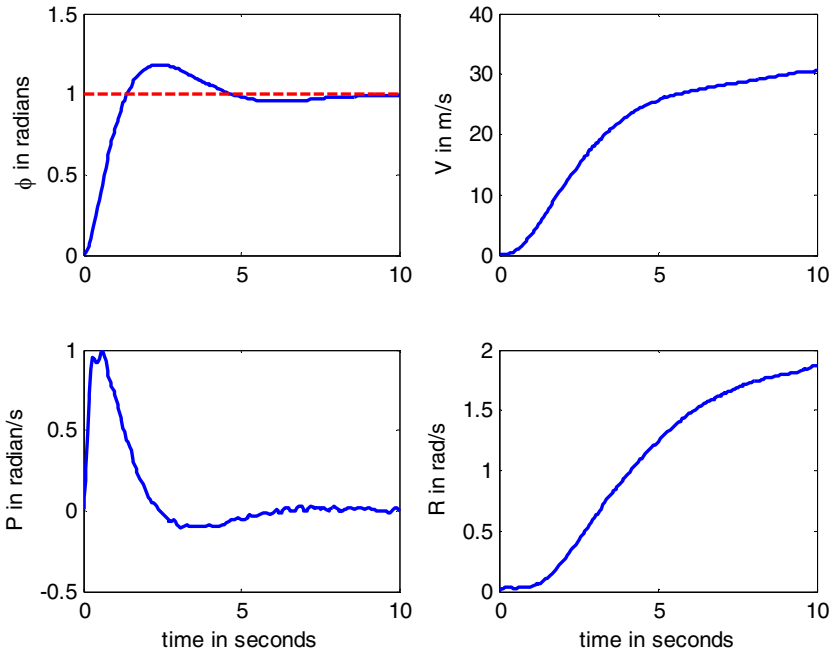

Figure 5.10 Closed loop lateral-directional state responses to a unity bank angle step command

Figure 5.11 shows the longitudinal state responses for this case. It is seen that the states are all within acceptable limits. Note, the slight build up in the body axes U and W components of the velocities is attributed to the loss in lift due to the vectoring of the main rotor thrust to achieve the desired bank angle as well as the coupling between the longitudinal and lateral-directional dynamics. In addition, there is a velocity disturbance along the body X-axis due to turbulent wind.

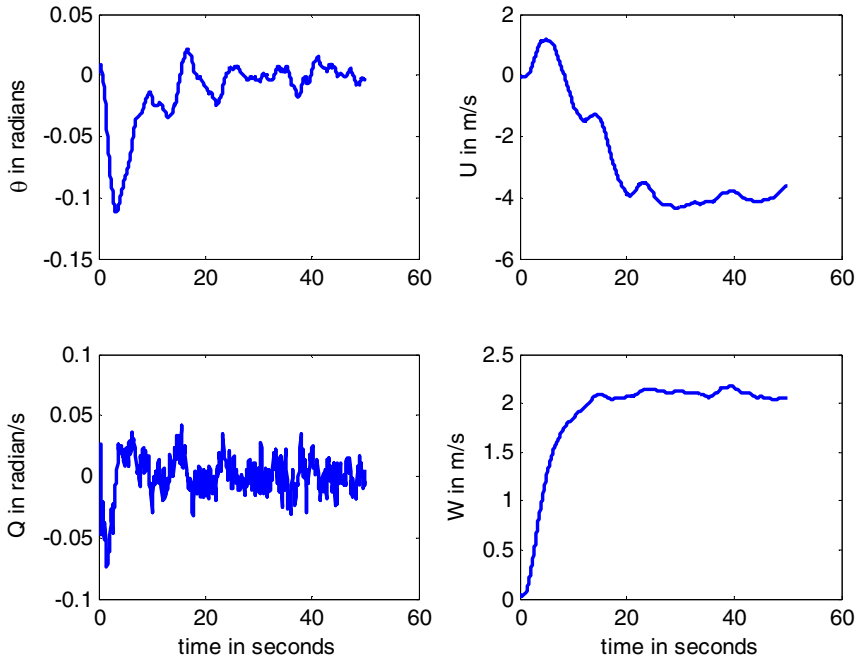

Figure 5.11 Closed loop longitudinal state responses to a unity bank angle step command

Figure 5.12 shows the cyclic-pitch activity in the lateral as well as the longitudinal axes and the rudder pedal activity. As expected the activity in the rudder is minimal. The longitudinal cyclic-pitch responds to arrest the build up in the longitudinal states (pitch angle and pitch rate).

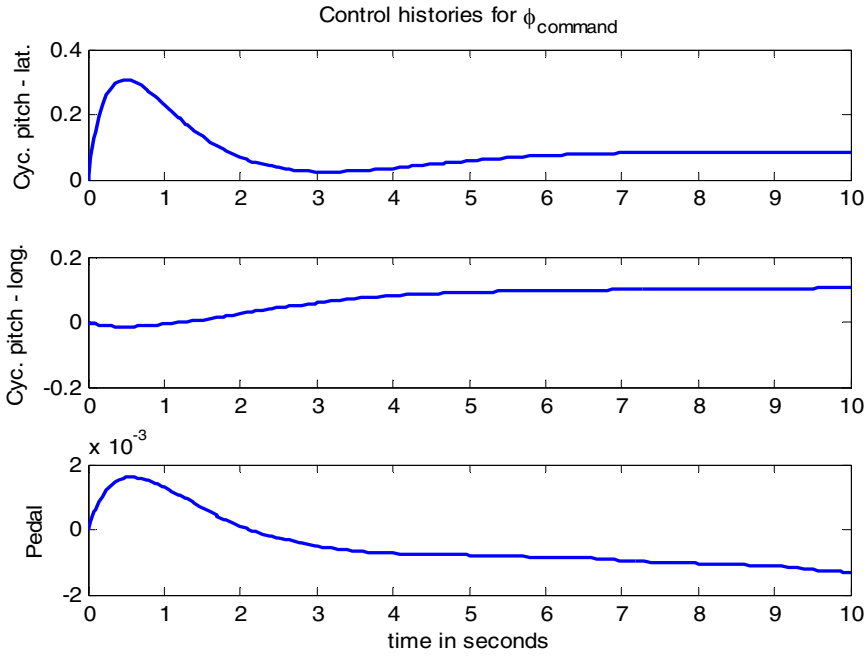

Figure 5.12 Control history for unity bank angle step demand

Pitch angle command tracking ($\theta_{command}$): The step responses of the longitudinal states for a unit pitch angle command (equivalent of 1 radian) are shown in Figure 5.13. The helicopter configuration is identical to the earlier case, i.e. there is no collective pitch activity and similar turbulent wind disturbances are injected into the system. It is seen that the pitch angle settles to less than 6% of the steady state value within 5 seconds. The overshoot is < 18.5%. The slight oscillations within the 5% settling band are due to the external state disturbance (due to turbulent wind). The pitch rate does not peak beyond 1.5 rad/s, which is within acceptable limits (< 90 deg/s). While there is a significant change in the horizontal velocity there isn't as much change in the vertical velocity. The pitch angle demand is very aggressive, almost 60 degrees whose primary effect is to drastically slow down the helicopter. In the hover configuration, this would

mean that the helicopter moves backwards while losing altitude. There is also a lateral shift in the inertial position due to the external disturbance activity and the weak coupling inherent in the vehicle dynamics. One way to arrest the build up in the translational velocities is to include an inner-loop for the translational dynamics (velocity loops) and use collective pitch.

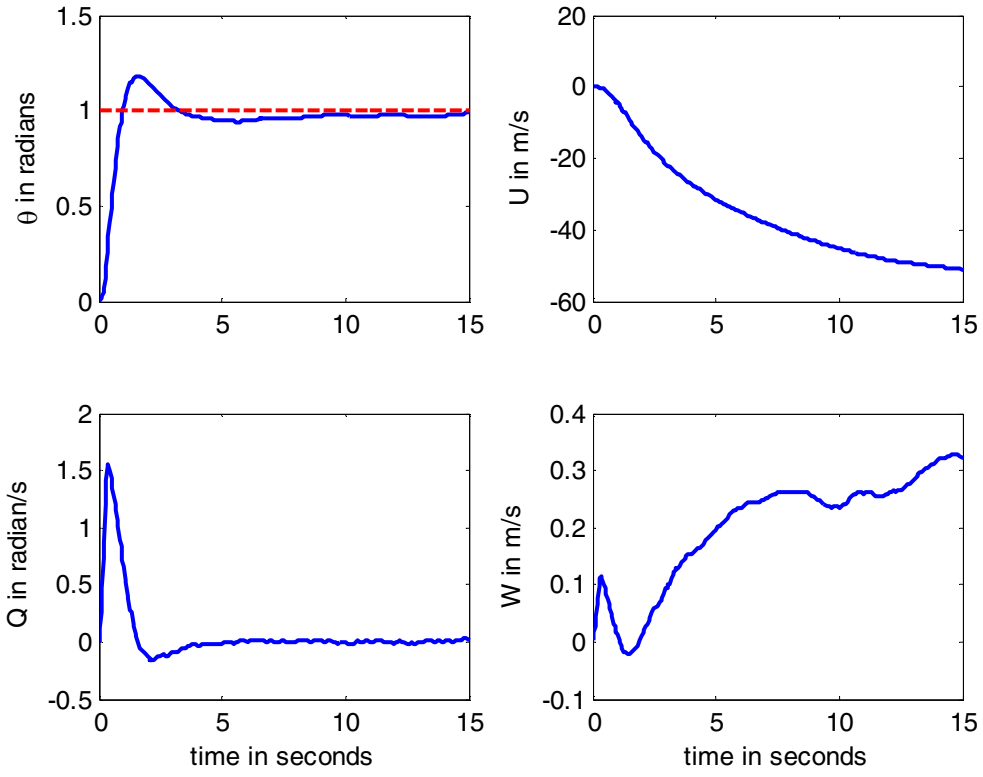

Figure 5.13 Closed loop longitudinal state responses to a unity pitch angle step command

Figures 5.14 and 5.15 show the lateral-directional responses and the control activity for this maneuver (pitch angle command). As it is seen from the plots, the lateral-directional responses are within acceptable limits and the control histories are as expected.

We note from the plots for both the maneuvers the cross coupling between the longitudinal and lateral-directional modes is minimal. Additionally the roll rate and the pitch rate have low peaks for the respective maneuvers (< 90 deg/s). Our objective was to reduce these rate peaks as much as possible and also obtain good step responses in the attitude variables.

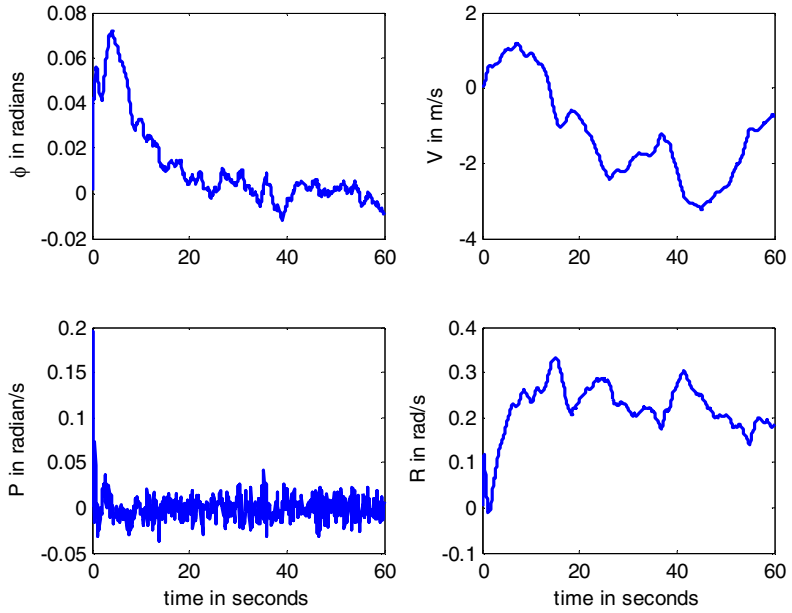

Figure 5.14 Closed loop lateral-directional state responses to a unity pitch angle step command

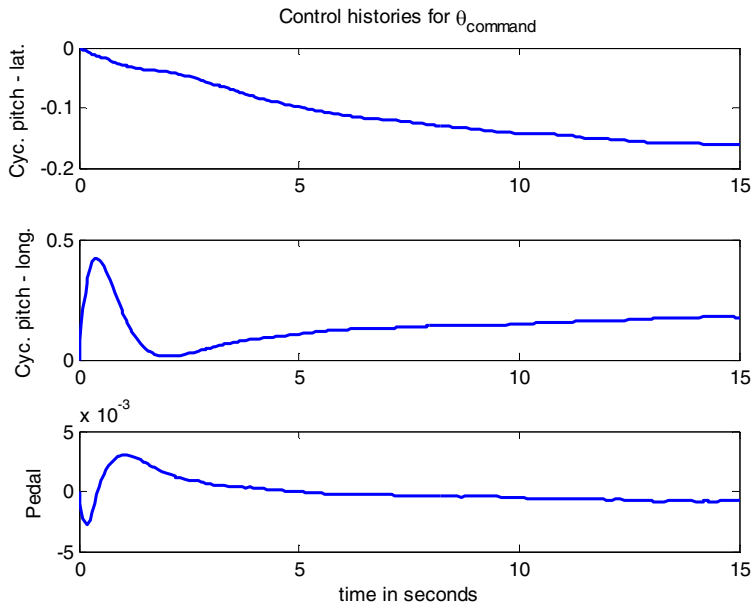

Figure 5.15 Control history for unity pitch angle step demand

5.3 Position Control Design

The ability to hold position and to hover over a particular point in a three dimensional space is a requirement common to rotary-wing Unmanned Aerial Vehicles (UAVs). Position tracking control system design for a UAV is challenging because of the nonlinear dynamics, and strong coupling present in the rotorcraft. The aim of this paper is to design a helicopter position control system with guaranteed performance that allows tracking control of Unmanned Aerial Vehicle positions - *x, y, z*, and yaw while preserving a structure that is generally accepted in the helicopter control community. The paper presents an approach for designing compensators for shaping the closed-loop inertial positions and yaw step response using H-Infinity output-feedback design techniques. The current paper is giving an inner loop design where all three attitudes

rates along with attitudes yaw and roll are controlled. We specifically focus on the problem of control in a hover configuration which in general is an unstable configuration. Further, in the presence of disturbances, the helicopter exhibits deviations in the dynamical states which complicate the control problem as the helicopter dynamical states are very tightly coupled. For example, in hover, pitch motion almost always is accompanied by forward and vertical motion and all three states need to be controlled simultaneously.

5.3.1 Controller Structure (Inner Loop)

The input vector can be written as $u = [\delta_{lati} \quad \delta_{longi} \quad \delta_{col} \quad \delta_{ped}]^T$. Where δ_{lati} is the lateral channel input and affects roll motion, δ_{longi} is longitudinal channel input and affects pitch, δ_{ped} is pedal channel input of remote controller and affects yaw motion, δ_{col} is collective channel, the fourth actuator which produces lift. Note that we are using all of the control channels to do the position control.

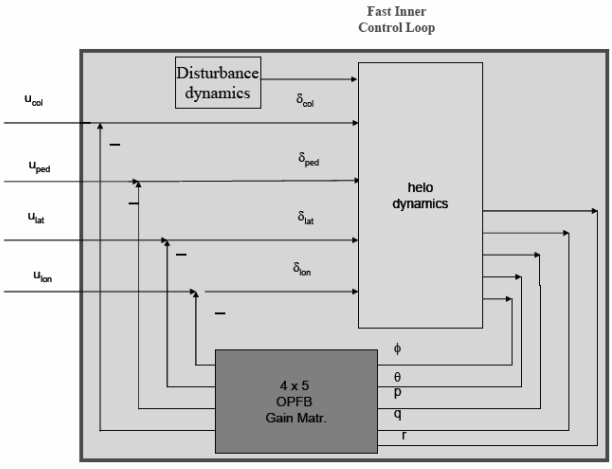

Figure 5.16 Controller structure

The control structure shown in Figure 5.16 is basically a stabilization control loop. Inner loop controls the attitude states roll, pitch and attitude rates.

The closed loop responses in roll and pitch are given in Figure 5.17. It can be observed that roll and pitch angles converge very quickly so to facilitate a fast inner loop.

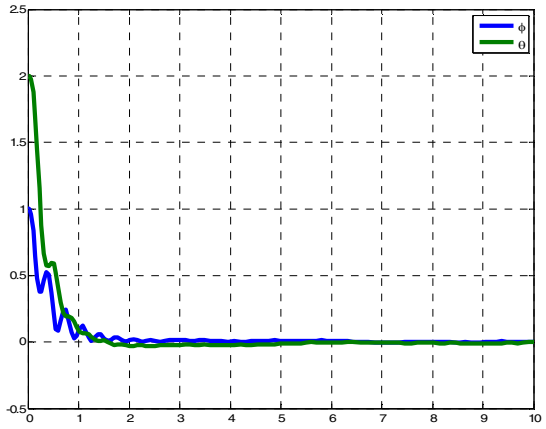

Figure 5.17 Closed-loop time response

It is important to mention that although inner loop has a good control on the attitude states it can not hold position of the UAV in hover. Position tracking in hover is addressed in the next section.

5.3.2 Controller Structure (Outer Loop)

In order to meet the objective to maintain the station position it is imperative to add an outer tracking loop *i.e.* the primary variables to be controlled in the outer loop are the positions x, y, and z, body rates u, v, w, and yaw angle, seven system states constitute the outer loop output vector $y_o = [x \quad y \quad z \quad u \quad v \quad w \quad \psi]^T$. Figure 5.18 explains the structure

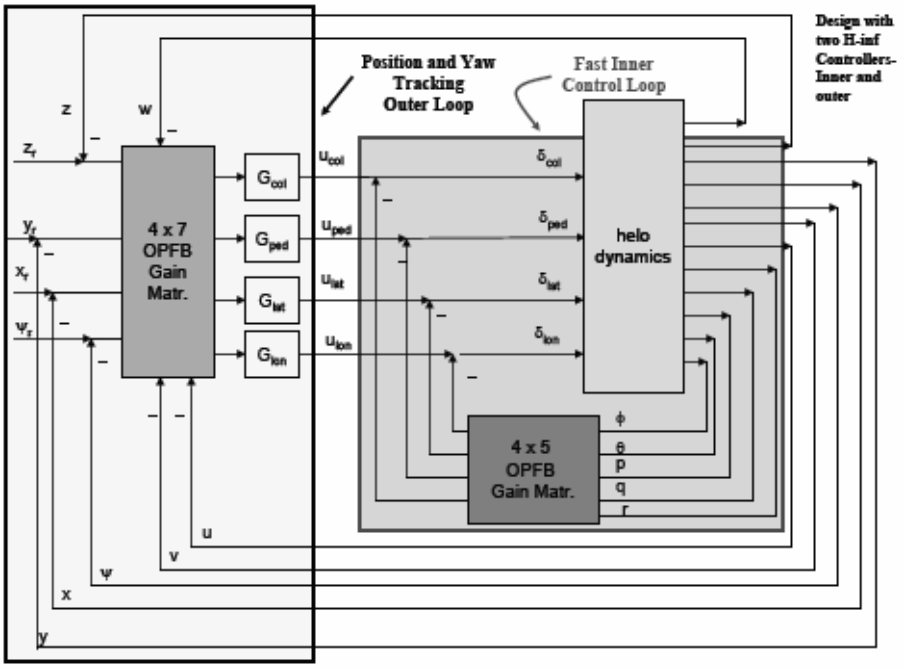

Figure 5.18 Outer and Inner loop Controller structure

Precompensators $G_{lat}(s)$, $G_{long}(s)$, $G_{col}(s)$, and $G_{ped}(s)$ shape the plant prior to closing the loop. Loop shaping procedure is explained in the next section.

Disturbance Effects in the Outer Loop: In the inner loop we have used the model of the wind components as disturbance. To further see the efficacy of the design disturbance can be formulated as the noise getting in to the helicopter control channels in the outer tracking loop. In this example disturbance is modeled as an external wind gust affecting Lateral control input channel. A band limited white noise source is used to simulate disturbance input signal.

5.3.3 Simulation Results with Disturbance Effects

Inner closed loop plant is given as

$$\begin{aligned} \dot{x} &= A_{in}x + Bu \\ y_{in} &= [\phi \quad \theta \quad r \quad p \quad q]^T = C_{in}x \end{aligned} \tag{5.60}$$

where $A_{in} = A - BK_{in}C_{in}$ is the inner closed loop system matrix. An inertial measurement unit can be used to measure the position (Ben Chen, 2005). For a fast inner loop it is equivalent of introducing integrators. Equation (5.61) is used to calculate the outer loop H-Infinity Output feedback gain

$$\begin{bmatrix} \dot{x}_{in} \\ x \\ y \\ z \\ \psi \end{bmatrix} = \begin{bmatrix} A_{in} & 0 \\ A_I & 0 \end{bmatrix} \begin{bmatrix} x_{in} \\ u \\ v \\ w \\ r \end{bmatrix} + Bu = A_0 x_o + Bu \tag{5.61}$$

$$y_o = [x \quad y \quad z \quad u \quad v \quad w \quad \psi]^T = C_o x_o \tag{5.62}$$

Loop shaping for outer loop is not required for station keeping because of the addition of the effective integrators. In simulations body to inertial transformation is used to generate outer loop outputs which recreate a real life situation.

Figures below shows the effectiveness of the design, configuration 1 in Figure 5.19 shows the plots for an altitude command i.e. UAV is commanded from initial position vector (x_1, y_1, z_1) to (x_1, y_1, z_2). Configuration 2 shows the convergence properties of the closed loop system i.e. how UAV converges to the station position from a different initial position vector i.e from $(x + \Delta x, y + \Delta y, z + \Delta z)$ to (x, y, z). One can see also that the yaw angle is maintained at the commanded position. Next configuration,

configuration 3 shown in Figure 5.21 is an illustration of successful following of a yaw step command while maintaining the position. Last configuration show in Figure 5.22 simulates the effects of disturbance in the lateral channel of the control input.

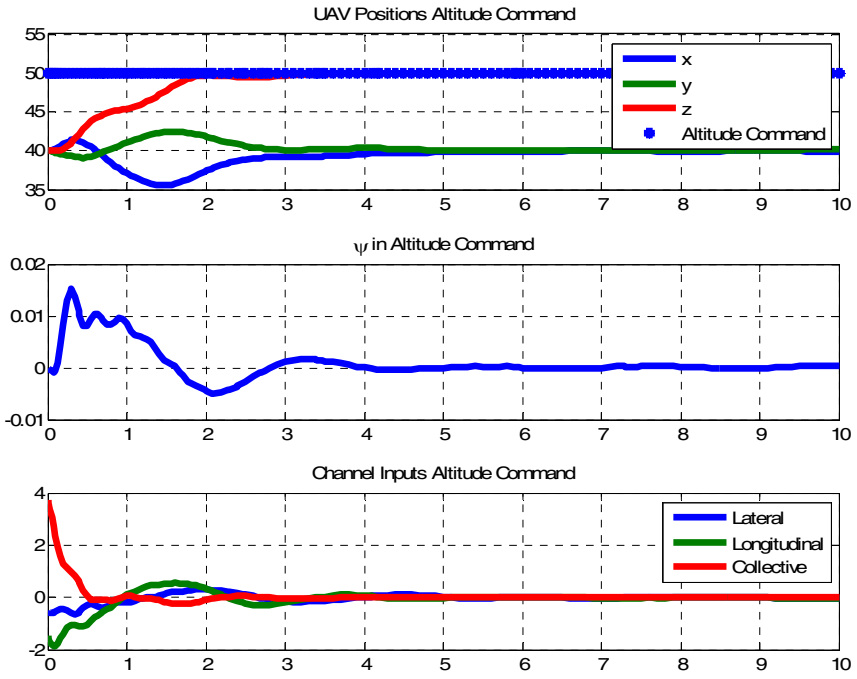

Figure 5.19 Configuration 1: Altitude Command

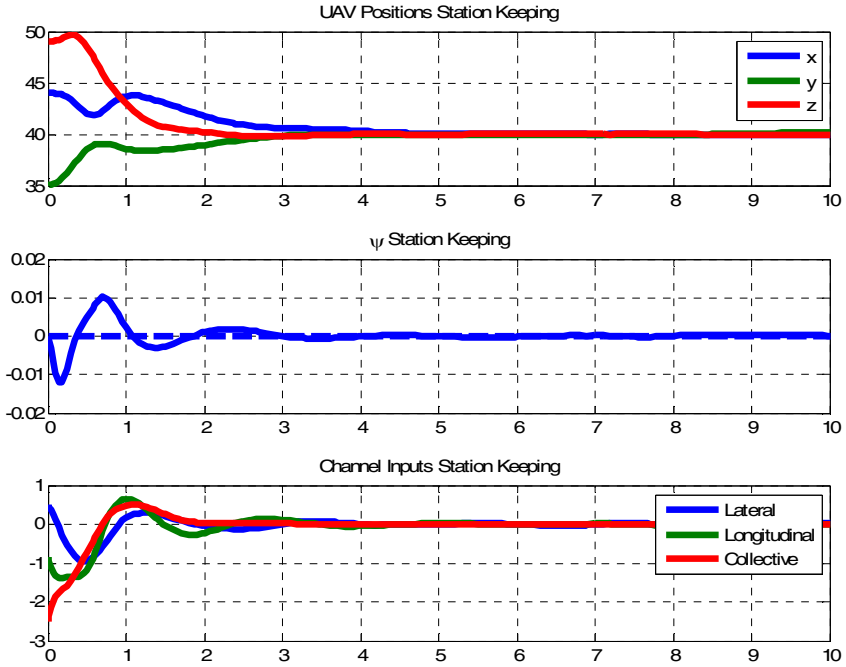

Figure 5.20 Configuration 2:Station Keeping

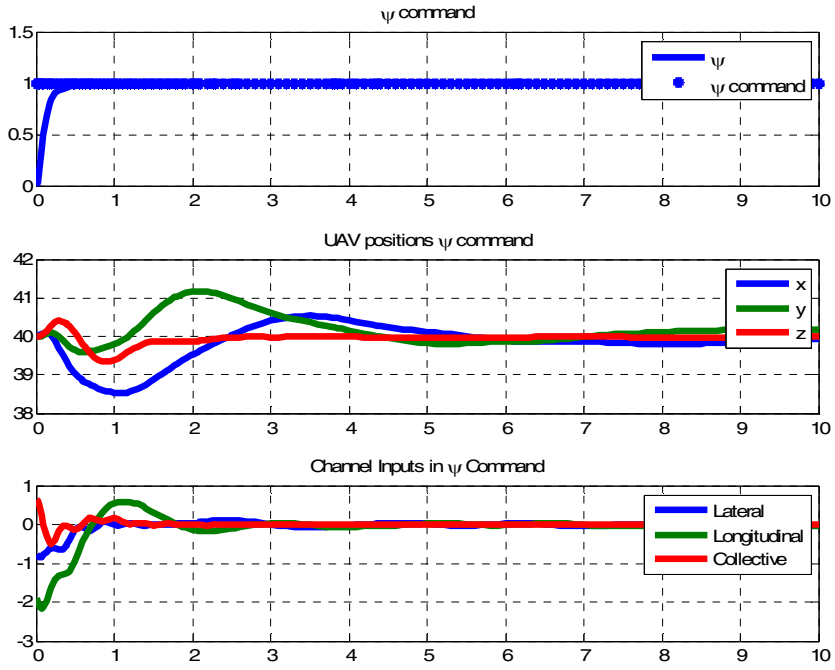

Figure 5.21 Configuration 3: Yaw Tracking while maintaining position

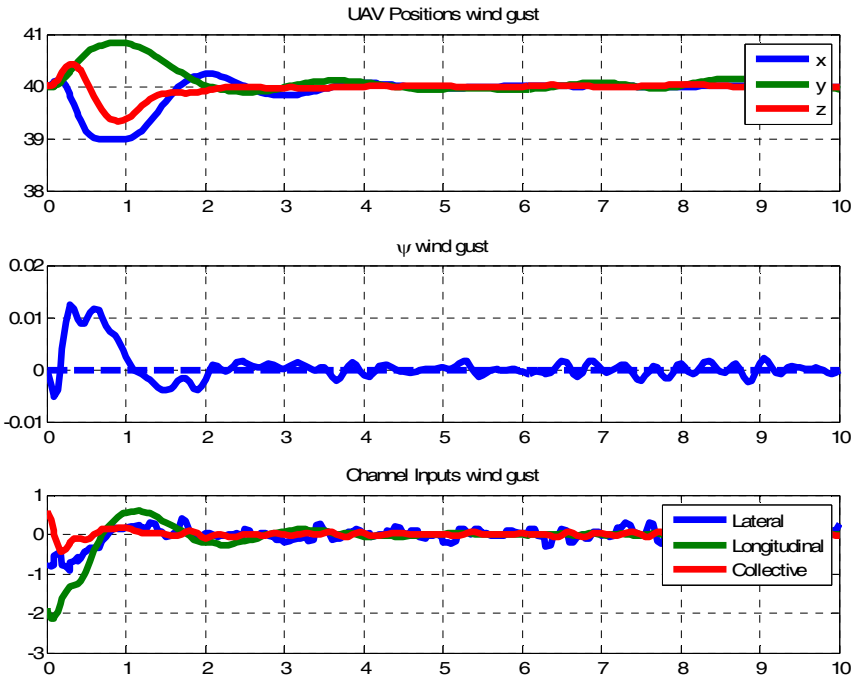

Figure 5.22 Configuration 4: Lateral Wind Gust

CHAPTER 6

ELECTROMECHANICAL IMPLEMENTATION

6.1 Introduction

For electro-mechanical systems, static OPFB controllers are less expensive to implement than full state variable feedback (SVFB). In a real situation, it is often not possible to measure the whole state vector for the feedback. Moreover, static OPFB preserves the desirable structure of the control system (Stevens and Lewis, 2003). Static OPFB controllers can also be employed as back-up controllers, *i.e.* as controllers which are not active during the regular operation, but which are used in the case of faults. For this reason back-up controllers have to be as simple as possible (Astolfi *et al.*, 2005). Issues of importance to the design of practical static OPFB controllers include (i) on-line computational simplicity, (ii) ability to operate solely with available measurable quantities, and (iii) design and implementability in a short time. However, implementation experiences and results on industry-like test beds are rarely published in the research literature. In this chapter we offer a design procedure which addresses the above issues. The proposed procedure is different than existing approaches such as classical control, optimal SVFB, or optimal OPFB. The procedure described in this paper allows one to achieve disturbance attenuation and control with prescribed performance at the same time.

Today's industrial systems have complex & possibly unknown dynamics, unknown disturbances, and nonlinear effects such as friction & deadzone. Such systems include but are not limited to VLSI, manufacturing positioning systems, hard disk drives, high speed robotic assembly systems, and CNC machine tools. In eletro-mechanical systems it is expensive and sometimes difficult to achieve and implement full state-feedback. Uncertainties in the electromechanical systems and the disturbances affect the performance of the optimal controller. Controllers may require prescribed desirable structures as well. Implementation experiences on electromechanical system are addressed at many forums. Kuljaca *et al.* (2003) implemented a novel neural network backstepping controller for application to an industrial motor drive system with a fairly complex real time computational platform. A robust tracking Servo System considering force disturbance is implemented on the optical disk recording system in(Ohishi *et al.*, 2006). Recent work (Wai *et al.*, 2006) addresses uncertainties in practical applications with a Neural-Fuzzy-Network Controller; implementation is done on a Robot Manipulator which includes actuator dynamics. A multistage Position/Force Control for constrained Robotic systems with friction is presented in Khayati *et al.* (2006) with an LMI formulation. Hammoto *et al.* (2000) presented a two degrees-of-freedom controller for two-mass spring system based on an iterative feedback tuning approach. However, simplified procedures using a practical implementation platform are rarely addressed.

6.2 Plant Description

We implemented H-Infinity OPFB control algorithm on a spring mass damper system shown in Figure 6.1. This platform is representative of realistic industrial and automotive systems with flexibility and vibration effects.

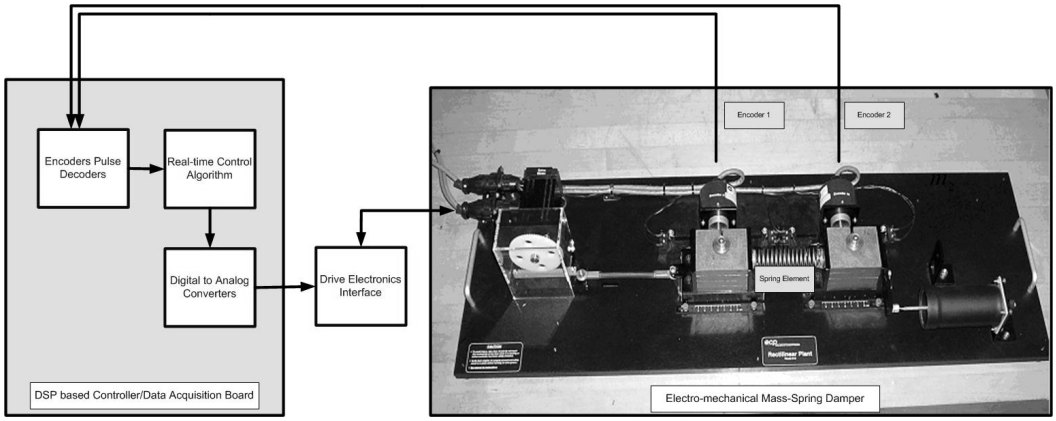

Figure 6.1 Spring Mass System

The schematic of the system is shown in Figure 6.2

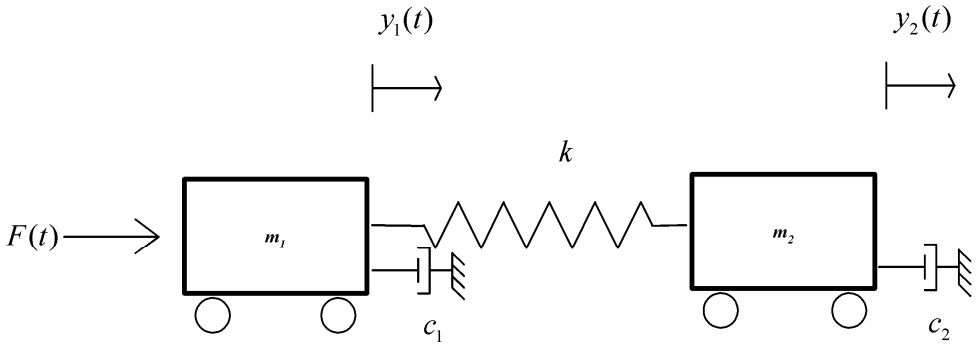

Figure 6.2 Two Degrees of Freedom Spring Mass System

The dynamics are

$$\begin{aligned} m_1\ddot{y}_1(t) + c_1\dot{y}_1(t) + k(y_1(t) - y_2(t)) &= F(t) \\ m_2\ddot{y}_2(t) + c_2\dot{y}_2(t) + k(y_2(t) - y_1(t)) &= 0 \end{aligned} \tag{6.1}$$

The states and output are assigned as $x = [y_1 \quad \dot{y}_1 \quad y_2 \quad \dot{y}_2]^T$, $y = [y_1 \quad y_2]^T$ respectively. The state-space description is

$$\dot{x} = \begin{bmatrix} 0 & 1 & 0 & 0 \\ -\frac{k}{m_1} & -\frac{c_1}{m_1} & \frac{k}{m_1} & 0 \\ 0 & 0 & 0 & 1 \\ \frac{k}{m_2} & 0 & -\frac{k}{m_2} & -\frac{c_2}{m_2} \end{bmatrix} x + \begin{bmatrix} 0 \\ \frac{k_{hw}}{m_1} \\ 0 \\ 0 \end{bmatrix} u, \quad y = \begin{bmatrix} 1 & 0 & 0 & 0 \\ 0 & 0 & 1 & 0 \end{bmatrix} x, \quad (6.2)$$

where the hardware gain $k_{hw} = 12478.20102\,\text{N/m}$ translates force units into the servo voltage actuation signal. The parameter values for the case dealt with are: $m_1 = 2.77\,\text{kg}$, $m_2 = 2.59\,\text{kg}$, $c_1 = 2.1\,\text{N/ (m/s)}$, $c_2 = 1.2\,\text{N/ (m/s)}$, $k = 830\,\text{N/m}$. The details of the identification process to determine these parameters are given in Bhilegaonkar (2005). The electrical drive motor dynamics were neglected since they are much faster than the actual dynamics of the mechanical system (Parks, 2005).

In addition

$$\zeta = Hx = y_2 \quad (6.3)$$

is the tracking output which must track the step reference input *r*(*t*).

6.3 Problem Description

Our objective is to do the performance analysis with disturbances present in the system. A damper attached to mass 2 is used to introduce the disturbance into the system. The disturbance dynamics are given by

$$D = \begin{bmatrix} 0 & 0 & 0 & \delta_d \end{bmatrix}^T \quad (6.4)$$

where $\delta_d = -\frac{c_d}{m_2}$, and c_d represents unmeasured disturbance component. In this paper we are focusing on the exogenous disturbance formulation presented in Section III.

6.4 Controller Structure

Algorithm 1 was used to calculate the bounded L2 gain OPFB. It is emphasized that Algorithm 1 requires no initial stabilizing OPFB gain. Figure 6.3 describes the closed-loop structure.

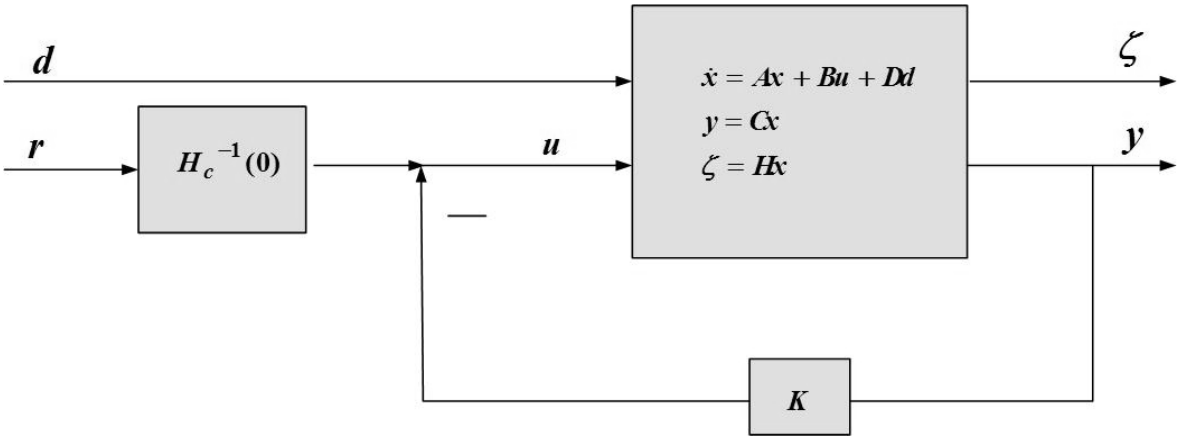

Figure 6.3 Closed loop Controller Structure

Figure 6.4 summarizes the static OPFB controller structure. To ensure good tracking of the reference trajectory, the servo control signal u(t) is equal to the H∞ regulator feedback control $-Ky$ plus a feed forward term involving the inverse of the dc gain of the closed loop system. The loop is closed using the available measurement outputs *y(t)* so that the output variable $\zeta(t)$ tracks the reference command r(t) (Lewis, 1992).The tracking output variable $\zeta(t)$, (6.3) dictates the formulation of the feedforward term $H_c^{-1}(0)$.

	STATE FEEDBACK	OUTPUT-FEEDBACK
Controller Gains	$K_s = [k_{11} \quad k_{12} \quad k_{13} \quad k_{14}]$	$K = [f_{11} \quad f_{12}]$
Closed-loop transfer function	$H_{cs}(s) = H\{sI - (A - BK)\}^{-1} B$	$H_c(s) = H\{sI - (A - BKC)\}^{-1} B$
Control signal	$u = -K_s x + H_{cs}^{-1}(0) r$	$u = -Ky + H_c^{-1}(0) r$
Closed loop description	$\dot{x} = (A - BK)x + BH_{cs}^{-1}(0) r + Dd$	$\dot{x} = (A - BKC)x + BH_c^{-1}(0) r + Dd$

Figure 6.4 Bounded L2 gain Output-feedback Controller

The closed-loop system description with OPFB and SVFB is respectively

$$\dot{x} = \begin{bmatrix} 0 & 1 & 0 & 0 \\ -\frac{k}{m_1} - f_{11}\frac{k_{hw}}{m_1} & -\frac{c_1}{m_1} & \frac{k}{m_1} - f_{12}\frac{k_{hw}}{m_1} & 0 \\ 0 & 0 & 0 & 1 \\ \frac{k}{m_2} & 0 & \frac{-k}{m_2} & \frac{-c_2}{m_2} \end{bmatrix} x + \begin{bmatrix} 0 \\ \frac{k_{hw}}{m_1}(f_{11} + f_{12}) \\ 0 \\ 0 \end{bmatrix} r + Dd, \tag{6.5}$$

$$\dot{x} = \begin{bmatrix} 0 & 1 & 0 & 0 \\ \frac{k}{m_1} - k_{11}\frac{k_{hw}}{m_1} & c_1 - k_{12}\frac{k_{hw}}{m_1} & \frac{k}{m_1} - k_{13}\frac{k_{hw}}{m_1} & -k_{14}\frac{k_{hw}}{m_1} \\ 0 & 0 & 0 & 1 \\ \frac{k}{m_2} & 0 & \frac{-k}{m_2} & \frac{-c_2}{m_2} \end{bmatrix} x + \begin{bmatrix} 0 \\ \frac{k_{hw}}{m_1}(k_{11} + k_{13}) \\ 0 \\ 0 \end{bmatrix} r + Dd, \tag{6.6}$$

For the computation of bounded L_2 gain output feedback K it is necessary to select Q and R. The H_∞ static output feedback controller gains are obtained with $\gamma = 10$. Using the algorithms described in earlier section for the given γ, Q and R, the control signal K can be found easily using MATLAB in a few seconds. If the time response and closed loop poles are not satisfactory, the elements of Q and R can be changed and the design repeated. After repeating the design several times we selected the design parameters as

$$Q = C_s{}^T C_s = \begin{bmatrix} 0 & 0 & 0 & 0 \\ 0 & 0.004 & 0.02 & 2\times10^{-5} \\ 0 & .02 & 1 & 0.001 \\ 0 & 2\times10^{-5} & 0.001 & 1\times10^{-6} \end{bmatrix}, \; R = 100000 .$$

Where $C_s = [0 \quad .02 \quad 1 \quad .001]$ specifies the desired state performance in terms of heavy weighting on y_2, and reduced weighting on velocities $\dot{y}_1$, and $\dot{y}_2$. Note that the tracking output variable state x_3 is weighted heavier than other elements in matrix Q. This design shows that the feedback output $y = Cx$ and the performance output can be different. See(Lewis, 1992). For optimal OPFB gain calculation, initial stabilizing gain was taken as $K_0 = [1 \quad 0.1]$. We have assumed that initial states are uniformly distributed on unit sphere, such that $X = I$ (Knobloch, 1993).

6.5 Implementation Results

The resulting time simulation responses shown compare bounded L_2 gain OPFB, optimal OPFB, and optimal state feedback control. In the simulations all three controllers have commensurate settling times, State-feedback has better transient response characteristics than both bounded L_2 gain output feedback and optimal Output feedback. However, bounded L_2 gain output feedback is superior for practical applications since the actual system has unmodelled dynamics and disturbances that are better controlled by H-Infinity Control than by optimal design techniques. Infact, Figure 6.7 shows the implementation results. This Figure clearly shows that in the actual system L_2 gain OPFB outperforms both the other methods.

Figures 6.5 and 6.6 show the implementation results for a step reference trajectory. Figure 6.5 shows that the implemented controller has good transient tracking response characteristics. Figure 6.6 is the error response plot that shows practically achieved good steady state results using the available encoder measurements. It is to be emphasized that numerical quantization occurs by necessity in all control systems that contain inexpensive measurement elements such as incremental encoders (Parks, 2005). It can be concluded here that bounded L_2 gain output feedback gives good results.

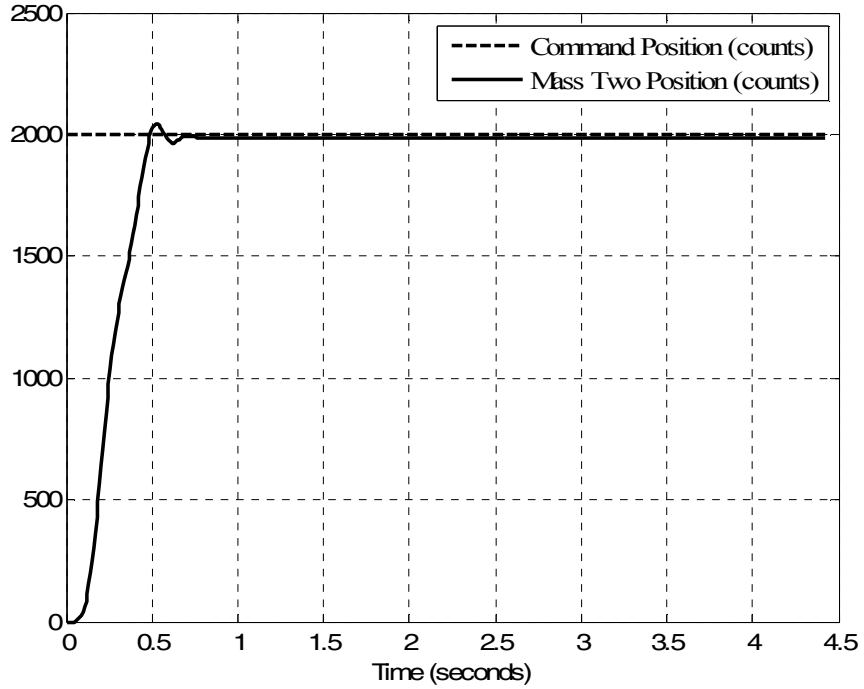

Figure 6.5 Implementation Results (Step Response)

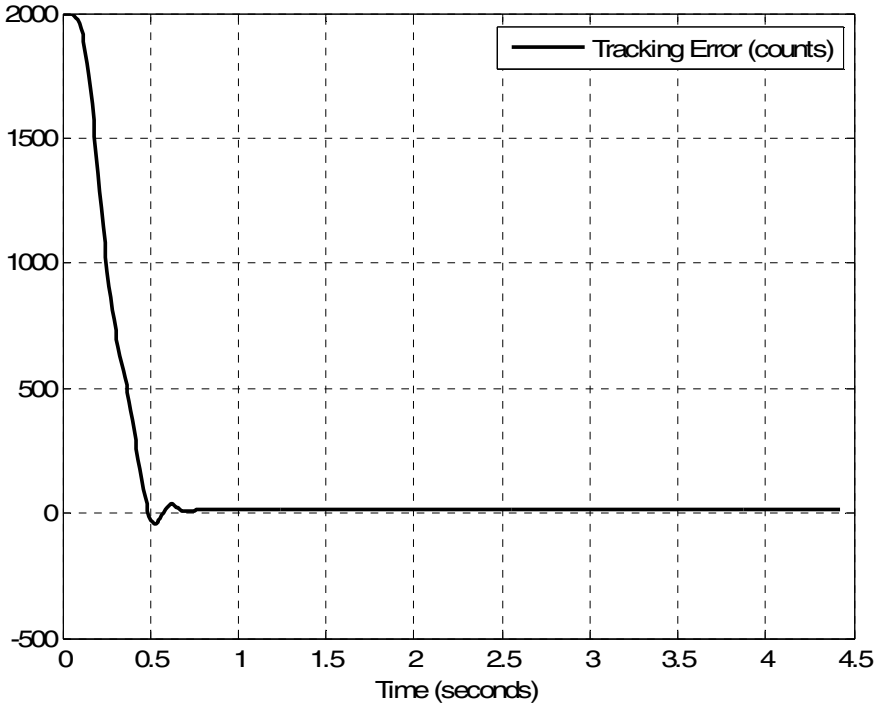

Figure 6.6 Implementation Results (Tracking error)

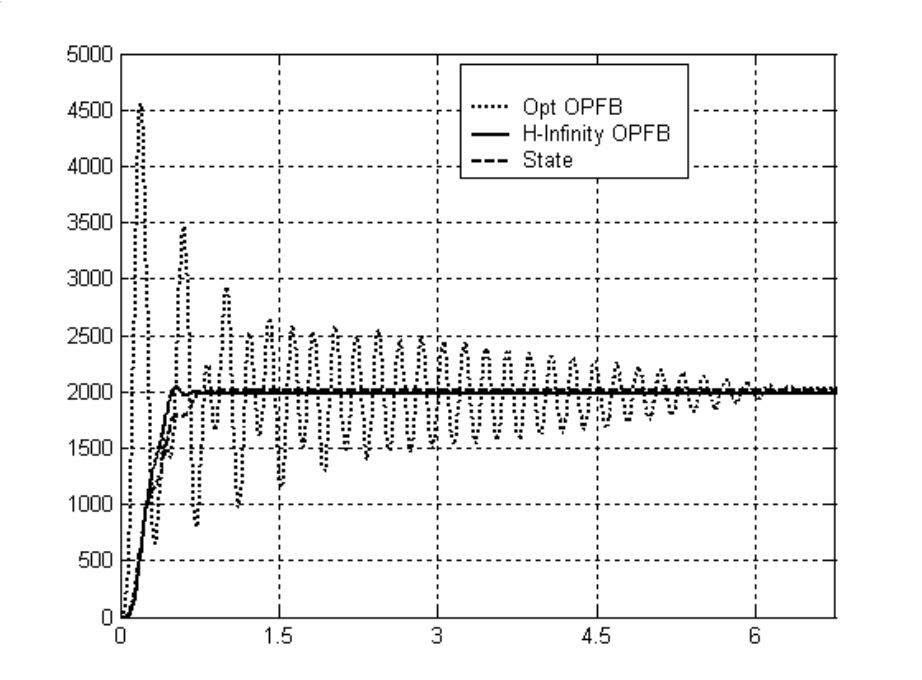

Figure 6.7 Comparison Plots

CHAPTER 7

FUTURE APPLICATIONS: MEASUREMENT AND CONTROL IN WIRELESS NETWORKS

Over the years a lot of rigorous mathematical analysis has been done by systems and controls community for optimization of multivariable systems with a mathematically rigorous systems theoretic approach. In parallel, wireless telecommunication industry was working on performance measurement analysis tools and achieved demonstrable optimization. This chapter will elaborate on the need for finding common grounds between optimization of telecommunication networks and optimal control theory; some existing measurement tools will be presented.

Decision on measurement tools for designing optimal, reliable telecommunications networks implies tradeoffs between reliability, capacity, and the economics of meeting present and future customer demands. The creation of efficient wireless networks is an everyday challenge in front of service providers. In this chapter there are first identified the parameters which can and should be measured to facilitate the optimization for performance of telecommunication networks. Secondly, there are given available resources on measurements tools for these parameters together with a comparative analysis. Finally, the hardware setup for the some of these measurements will be explained. This work extends, elaborates, and concocts wealth of knowledge

with available open source tools, and the documentation available in the popular literature.

7.1 Introduction

In the recent past, there have been many technological developments in telecommunication networks and the optimization (Hoesel, 2005). Data applications are expected to be the primary drivers for deployment of third generation (3G) wireless systems. Performance of Data applications over a CDMA air interface is given in (Khan *et. al. 2000)*. TCP/IP has been widely used in computer networks for many years. It has also been recommended as a major protocol suit for async data and data and fax communications. Performance evaluation of TCP/RLP protocol stack over CDMA wireless link is discussed (Bao, 1996). The popularity of network-based control systems is continuously growing, to a large extent the actual quality of control in such systems depends on network timing such as delay and delay jitter. In a seminal work Soucek and Sauter (2004) discussed quality of service concerns in IP based Control Systems. Wireless control systems can have a huge impact in future development of integrated control systems in decentralized plants, such as refineries, chemical foundries, and hydro power plants. Replacing the wired connections with wireless systems would immensely simplify the amount of work and material involved in maintenance, and, providing that network functions properly, may also enhance the control performance.

It is clear that the evaluating the performance of a networked system is very important and that necessitates the need for choosing a good testing and measurement tool. Also there are huge benefits in correlating performance optimization of networked

systems to the optimal control developed by systems and controls community. This chapter aims at bringing both together.

This chapter is organized as follows. Section 7.2 elaborates on optimization of multi-input multi-output systems with a system theoretic approach. Performance index and the mathematical description of the system are given for both discrete time and continuous time systems. In section 7.3 a description of Quality of Service in Telecommunication networks is given delay and jitter measurements for an IP based network is explained along with the hardware setup description. Power control is an important factor to achieve higher communication link quality and better system capacity. Section 7.4 poses CDMA power control within a system theoretic H-Infinity framework.

7.2 Optimization with a System Theoretic Approach

There has been a lot of work done in systems and controls community to achieve optimization in multi-input multi-output systems. The objective of optimal control theory is to determine the control signals that will cause a process to satisfy the physical constraints and at the same time minimize (or maximize) some performance criterion (Lewis and Syrmos, 1995). We shall briefly visit the problem formulation and some mathematically rigorous approaches here.

7.2.1 Problem Formulation

The formulation of an optimal control problem requires a mathematical description or the model of the system, a statement of the physical constraints, and specification of the performance criterion. Mathematical model is the starting point and

it has to be in the state variable form. Below are presented continuous and discrete time optimal control problem formulations.

Optimal Control: Discrete Time Systems: Suppose the plant is described by the very general nonlinear discrete time dynamical equation

$$x_{k+1} = f^k(x_k, u_k) \tag{7.1}$$

with initial condition x_0. Let the state x_k be an *n* vector and the control input u_k be an m vector. Since (7.1) determines the state at the time $k+1$ given the control and the state at time *k*, (1) is our constraint relation. Clearly, $f \in R^n$. Suppose there is an associated scalar performance index given in the general form

$$J_i = \phi(N, x_N) + \sum_{k=i}^{N-1} L^k(x_k, u_k). \tag{7.2}$$

where $[i, \quad N]$ is the time interval over which we are interested in the behavior of the system. $\phi(N, x_N)$ is a function of the final time *N* and the state at the final time, and $L^k(x_k, u_k)$ is an in-general time varying function of the state and control input at each intermediate time k in $[i, \quad N]$. The optimal control problem is to find the control u^*_k on the interval $[i, \quad N]$ that drives the system (7.1) along a trajectory x^*_k such that the performance index is minimized. The optimal controller solution involves state equation, costate equation, stationarity condition and boundary conditions that given in (Lewis and Syrmos, 1995), where also are given fixed final state and final state free solutions.

7.3 Performance of Wireless Networks

Quality of services is a major issue for telecom providers. There is a conflict of interest in what customer desires and what he/she is willing to pay. Growing competition within telecommunication operators and the increase in the expectations of the customers necessitate the operators to keep improvising the network. Also, the demand for the calls and bandwidth capacity is time variant. So the installed capacity is to have a guaranteed availability probability, the Quality of Service

Below we are explaining which parameters are relevant to most systems in deciding on the performance of the systems.

7.3.1 End to End Delay

End-to-end delay refers to the time taken for a packet to be transmitted across a network from source to destination. It is explained in RFC2326 Real time streaming protocol.

7.3.2 Delay Jitter

The delay jitter (RFC 1889 RTP) is an estimate of the statistical variance of the RTP data packet interarrival time, measured in timestamp units and expressed as an unsigned integer. The interarrival jitter J is defined to be the mean deviation (smoothed absolute value) of the difference *D* in packet spacing at the receiver compared to the sender for a pair of packets. As shown in the Equation (7.3) below, this is equivalent to the difference in the "relative transit time" for the two packets; the relative transit time is the difference between a packet's RTP timestamp and the receiver's clock at the time of arrival, measured in the same units.

Defining S_i as the RTP timestamp from packet *i*. R_i as the time of arrival in RTP timestamp units for packet *i*, then for two packets *i* and *j*, *D* may be expressed as

$$D(i, j) = (R_j - R_i) - (S_j - S_i) = (\mathrm{R_j} - \mathrm{S_j}) - (\mathrm{R_i} - \mathrm{S_i}) \quad (7.3)$$

The interarrival jitter is calculated continuously as each data packet *i* is received from source SSRC_n, using the difference *D* for that packet and the previous packet $i-1$ in order of arrival (not necessarily in sequence), according to the formula

$$J = J + (|D(i-1, i)| - J)/16 \quad (7.4)$$

Whenever a reception report is issued, the current value of J is sampled. The jitter calculation is prescribed in (Cadzow, 1987) allow profile-independent monitors to make valid interpretations of reports coming from different implementations.

Delay Jitter Measurement in an IP based Network System: This section compares two available tools for delay jitter measurement in an IP based network.

IPERF: Iperf is a tool to measure maximum TCP bandwidth, allowing the tuning of various parameters and UDP characteristics. Iperf reports bandwidth, delay jitter, datagram loss. Features include running Iperf in bidirectional mode, removed STDLIB requirement for Iperf , and Client reporting of server side statistics in UDP tests. A hardware setup is explained below in Figure 7.1.

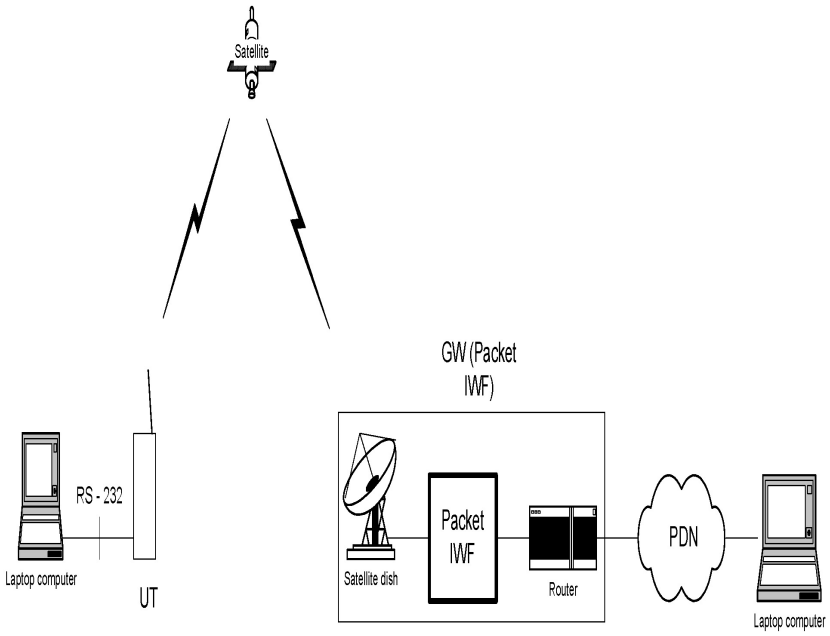

Figure 7.1 System Setup for Delay-Jitter measurement with IPERF

CISCO TOOLS: Delay and jitter can be measured by deploying Cisco routers 17xx or higher with Cisco IOS software code version 12.05T or higher, and configuring the Cisco IOS SAA features. The routers should be placed in the networks next to hosts. This provides statistics for end-to-end connections. Since it is not practical to measure every possible voice path in the network, place the probes in typical host locations providing for a statistical sampling of typical voice paths. Some examples include a local site-to-site path, a local site-to-remote site path via a 384 kbs Frame Relay circuit, a local site-to-remote site via an ATM permanent virtual circuit (PVC). Figure 7.2 below describes the setup.

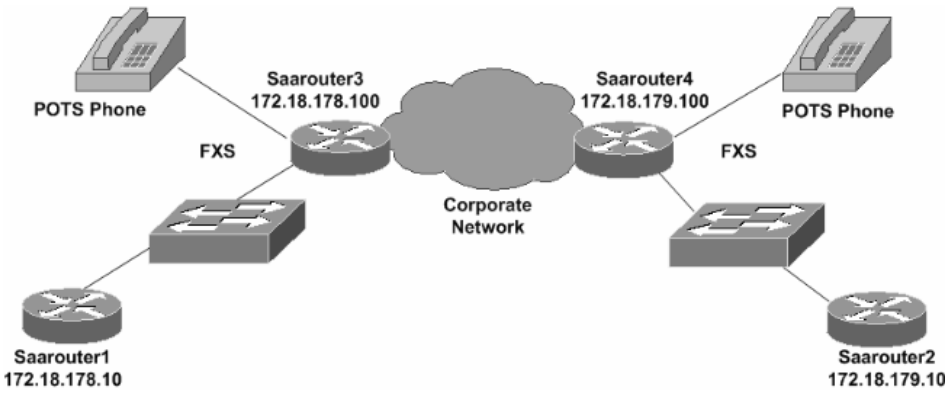

Figure 7.2 Set up with Cisco Tools

7.3.3 Throughput

The throughput defines how many bits per unit time can be transferred over a given network path. In an end-to-end view the delay can be seen as a direct function of the instantaneous throughput. The practical notion of throughput, however, implicitly includes a certain time interval.

The throughput θ can be defined as

$$\theta = \frac{A(t+\Delta t) - A(t)}{\Delta t} \tag{7.5}$$

where $A(t)$ denote the aggregate amount of transferred data up to time *t*.

7.3.4 Power Control

CDMA is interference limited multiple access system. Because all users transmit on the same frequency, internal interference generated by the system is the most significant factor in determining system capacity and call quality. The transmit

power for each user must be reduced to limit interference, however, the power should be enough to maintain the required Eb/No (signal to noise ratio) for a satisfactory call quality. Maximum capacity is achieved when Eb/No of every user is at the minimum level needed for the acceptable channel performance. As the Mobile Station moves around, the RF environment continuously changes due to fast and slow fading, external interference, shadowing, and other factors. The aim of the dynamic power control is to limit transmitted power on both the links while maintaining link quality under all conditions (CDMA Tutorial, Web Link, and unknown Year).

7.4 CDMA Power Control within a System Theoretic H-Infinity Framework

Primary aim of this section is to give an overview of how CDMA power control has been posed with a System Theoretic Optimization framework in the literature (Gadewadikar *et. al.*, submitted 2007).

Spectrum efficiency is one of the biggest positive outcomes of Code Division Multiple Access. It is possible because in this technique, all users operate on the same channel. As described in the section 7.3.2 good power control facilitates higher communication link quality and better system capacity. In order to track the desired signal-to-interference-plus noise ratio (SINR) under round trip delay, multiple access interference, channel fading, and noise, a time delay based state space model described below is developed by Lee *et. al.* (2006), the model represents the tracking error dynamics.

7.4.1 Problem Formulation

Measurement SINR at the base station can be written as

$$y_k = x_k + f_k - w_k \tag{7.6}$$

Here x_k is the transmission power, and f_k is the fading gain. The overall interferences that includes quantization error, Multiple Access Interference, Additive White Gaussian Noise, and nonlinear effect due to transmission power limitation are describes as w_k .

Defining the sum of downlink, uplink, and overall delay respectively as d_1, d_2, and d, such that $d = d_1 + d_2$. Transmission power x_k can be denoted as

$$x_k = x_{k-1} + u_{k-d} \tag{7.7}$$

Here u_k is the power control update command. It is desired to keep the SINR at a set point namely a desired value defined as r_k. Target SINR is specified jointly by the frame error rate (FER) statistics and the SINR error Statistics in the outer loop for power control. Tracking error than can be formulated as

$$e_k = r_k - y_k \tag{7.8}$$

Working with (7.6), (7.7) and in (7.8) will yield

$$e_k = e_{k-1} - u_{k-d} + v_{k-1} \tag{7.9}$$

where $d_{k-1} = w_k - w_{k-1} - f_k + f_{k-1} + r_k - r_{k-1}$ indicates the uncertain interference, fading noise, and nonlinear effects. The State vector X_k can now be defined as

$$X_k = \begin{bmatrix} e_k \\ u_{k-d} \\ . \\ . \\ . \\ . \\ u_{k-2} \\ u_{k-1} \end{bmatrix} \tag{7.10}$$

The past power control update commands u_{k-1} to u_{k-d} are considered in the state vector. Tracking error dynamic equation are expressed as

$$\begin{aligned} X_{k+1} &= Ax_k + Bu_k + Dd_k \\ e_k &= Cx_k \end{aligned} \tag{7.11}$$

where

$$A = \begin{bmatrix} 1 & 0 & -1 & \ldots & \ldots & 0 \\ 0 & 0 & 1 & 0 & \ldots & 0 \\ 0 & 0 & 0 & 1 & \ldots & 0 \\ \ldots & \ldots & \ldots & \ldots & \ldots & \ldots \\ 0 & 0 & 0 & 0 & 0 & 1 \\ 0 & 0 & 0 & 0 & 0 & 0 \end{bmatrix}, \; B = \begin{bmatrix} 0 \\ 0 \\ \ldots \\ \ldots \\ \ldots \\ 1 \end{bmatrix}, \; C = \begin{bmatrix} 1 \\ 0 \\ \ldots \\ \ldots \\ \ldots \\ 0 \end{bmatrix}^T, \; D = \begin{bmatrix} 1 \\ 0 \\ \ldots \\ \ldots \\ \ldots \\ 0 \end{bmatrix}$$

In the tracking error dynamic Equation in (7.11) the power tracking design purpose is to specify control u_k such that e_k is minimum under the influence of the signal d_k. Note that d_k is highly uncertain due to interference, fading, noise and nonlinear effects. For the state space model, the pair (A, B) is controllable.

In the state-space model (7.11), a state feedback controller can be introduced such that

$$u_k = KX_k \tag{7.12}$$

The closed-loop state-space system consisting of (7.11) and (7.12) can be written as

$$\begin{aligned} X_{k+1} &= (A + BK)X_k + Dd_k \\ e_k &= CX_k \end{aligned} \tag{7.13}$$

Now we can solve the H-Infinity tracking problem as

$$\frac{\frac{1}{k_f}\sum_{k=0}^{k_f} e_k{}^T R_1 e_k}{\frac{1}{k_f}\sum_{k=0}^{k_f} d_k{}^T R_2 d_k} < \gamma^2 \tag{7.14}$$

7.4.2 Exploring Bounded Real Lemma

The work by de Souza and Xie (1990) deals with the discrete time bounded real Lemma and its application in the characterization of all static state feedback H-Infinity Controllers for discrete time systems. In this section we are elaborating on the bounded real Lemma with a suggested technique to explore the possibility of parameterizing CDMA H-Infinity Power Controllers. As generalized using Equation (7.11) the results can be given in terms of either the positive semi-definite strong solution, or the positive semi-definite stabilizing solution of a discrete algebraic Riccati equation.

Notations and Definitions: Throughout this section the notation $M \geq N$ ($M > N$) with M and N being symmetric matrices, means that the matrix $M - N$ is positive semi-definite (positive definite). $\|G(z)\|_\infty$ will refers to the infinity norm of a stable discrete-time transfer matrix G(z). $\|G(z)\|_\infty = suo_{0\leq\omega\leq 2\pi}\sigma_{\max}\left[G(e^{j\omega})\right]$, where $\sigma_{\max}(.)$ stands for the maximum singular value of a matrix.

Consider the discrete algebraic Riccati Equation

$$A^T PA - P + (A^T PB + M^T)(R - B^T PB)^{-1}(B^T PA + M) + Q = 0 \qquad (7.15)$$

where A, B, Q, R and M are real matrices of dimensions $n \times n$, $n \times m$, $n \times n$, $m \times m$ and $m \times n$ respectively, and with Q and R being symmetric matrices. A real symmetric matrix P is said to be a stabilizing solution to (7.15) if P satisfies (7.15) and the matrix $\overline{A} = A + (R - B^T PB)^{-1}(B^T PA + M) + Q = 0$ stable. In the case when all of the eigenvalues of $\overline{A}$ lie in the closed unit disk, P is said to be a strong solution to (7.15)

Let G(z) be a $p \times m$ real rational transfer function matrix of a proper linear discrete-time system and consider a state-space realization (A, B, C, D_{sys}) of G(z), i.e. with no feed forward matrix i.e. $D_{sys} = 0$,

$$G(z) = C(zI - A)^{-1} B \qquad (7.16)$$

Note that no a priori assumption on minimality of the realization (A, B, C, D_{sys}) is made. A bound for the H-Infinity norm of G(z) is provided by the following version of the Discrete-time Bounded Real Lemma.

Lemma 1: The following statements are equivelent

(a) A is a stable matrix and $\left\| C(zI - A)^{-1} B \right\|_\infty \le \gamma$.

(b) (C, A) has no observable modes on the inner circle, and there exists a strong positive definite symmetric solution to the riccati equation.

$$\begin{pmatrix} A^T PA \\ -P \end{pmatrix} - \gamma^2 \begin{pmatrix} A^T PB \\ +C^T D \end{pmatrix} \begin{bmatrix} I & \\ & -\gamma^{-2}\left(B^T PB\right) \end{bmatrix}^{-1} \begin{pmatrix} PBA \end{pmatrix} + C^T C = 0 \qquad (7.17)$$

such that $\left[I - \gamma^{-2}\left(B^T PB\right) \right] > 0$.

Lemma 2: The following statements are equivelent

(a) A is a stable matrix and $\left\|C(zI-A)^{-1}B\right\|_{\infty} \le \gamma$.

(b) There exists a matrix $\hat{P} = \hat{P}^T > 0$ satisfying

$$\begin{pmatrix} A^T\hat{P}A \\ -\hat{P} \end{pmatrix} - \gamma^2\left(A^T\hat{P}B\right)\begin{bmatrix} I \\ -\gamma^{-2}\left(B^T\hat{P}B\right) \end{bmatrix}^{-1}\left(B^T\hat{P}A\right) + C^TC < 0 \qquad (7.18)$$

such that $\left[I-\gamma^{-2}\left(B^T\hat{P}B\right)\right] > 0$.

(c) There exists a stabilizing solution $P = P^T > 0$ to the Riccati Equation

$$\begin{pmatrix} A^TPA \\ -P \end{pmatrix} - \gamma^2\left(A^TPB\right)\begin{bmatrix} I \\ -\gamma^{-2}\left(B^TPB\right) \end{bmatrix}^{-1}\left(B^TPA\right) + C^TC = 0$$

such that $\left[I-\gamma^{-2}\left(B^TPB\right)\right] > 0$. Moreover, $P < \hat{P}$.

Main aim of this section was to give an example of a wireless communication problem being posed in a H-Infinity system theoretic framework and hence system theoretic optimal control tools explained in section II can be used. This is an active area of the current research. This chapter is focusing on introducing the problem and finding the common grounds between telecommunication measurements, performance optimization and systems theoretic optimal control.

Telecommunication technology is expected to be the primary driver over the next few decades. With ever increasing demand it is imperative to find common grounds between theoretical achievements in other fields in order to improvise. Test and measurement setups play a big role in improving the performance of a network and the

IP based equipment used by the consumer. This chapter stresses the need for correlating test, measurement, optimization, and performance for telecommunication networks. Along with the presentation of classical optimal control problem this chapter also explains some measurement variables and exemplifies a telecommunication performance problem in a system theoretic framework.

REFERENCES

[1] A. Astolfi, "Parameterization of output feedback controllers that satisfy an H_∞ norm bound" *2nd European Control Conference*, Groningen, The Netherlands, 1993.

[2] A. Astolfi and P. Colaneri, "Static output feedback stabilization of linear and nonlinear systems" Proc. IEEE Conf. Decision and Control, Sydney, 2000, pp 2920-2925.

[3] Astolfi, and P. Colaneri, "Static output feedback stabilization: from linear to nonlinear and back. In *Nonlinear Control in the Year 2000*" A. Isidori, F. Lamnabhi-Lagarrigue and W. Respondek Ed., Springer Verlag, 2000.

[4] A. Astolfi and P. Colaneri, "An algebraic characterization of the static output feedback stabilization problem" *Proc. American Control Conf.*, Arlington VA, 2001, p.p.1408-1412.

[5] W. F. Arnold, and A.J. Laub, "Generalized eigenproblem algorithms and software for algebraic riccati equations" *Proceedings of IEEE*, 72(12), 1746-1754.

[6] T. P. Basar, and P. Bernard, "H_∞ *Optimal Control and Related Minimax Design Problems*" Berlin, Germany, Birkhauser, 1991, pp 4-6, 33-48.

[7] Basar ,T. P, and Oldser, G., *Dynamic Noncooperative Game,* 2nd edition, Soc. for Industrial & Applied Math, New York, 1998, pp. 261-361.

[8] G. Bao, "*Performance evaluation of TCP/RLP protocol stack over CDMA wireless link*", Wireless Networks, 1996, pp 229-237.

[9] Bhilegaonkar, A. "Design and Implementation of Advanced Control Algorithms on an Electromechanical Plant for Trajectory Tracking,". M. S. thesis substitute, Dept. Electrical Engineering., U. T. Arlington, Texas, USA, Spring 2005.

[10] D. U. Campos-Delgado, and K. Zou, "*A parametric optimization approach to H_∞ and H_2 strong stabilization" Automatica*, 39, 2003, 1205-1211.

[11] C.E. de Souza and L. Xie, (1992). On the Discrete-time Bounded Real Lemma with application in the characterization of static state feedback H_∞ controllers. *Systems & Control Letters,*18(1), 61-71

[12] B. Chen,. "*Robust and H_∞ Control*", 2000, Springer, Berlin.

[13] B. Chen, "Fourth Half Yearly Progress Report for the TYIA 2003 Project on Nonlinear Control Methods for Flight Control Systems of Flying Vehicles,DSTA, NUS, and ST AEROSPACE, Nov. 2005.

[14] Y. Cao, Y. Sun, and W. Mao, "A new necessary and sufficient condition for static output feedback stabilizability and comments on " Stabilization via static Output Feedback". *IEEE Transactions on Automatic Control*, 43(2), 1998, p. p. 1110-1112.

[15] Y. Cao, J. Lam, and Y. Sun, "Static Output Feedback Stabilization: An ILMI approach," *IFAC Journal, AUTOMATICA*, Vol. 34, No. 12, 1998, pp. 1641-1645.

[16] P. Colaneri, J. C. Geromel, and A. Locatelli, "*Control theory and design, an RH_2 and RH_∞ viewpoint*" Academic Press Interscience, San Diego, 1997, pp. 87-261.

[17] E. J. Davidson, and I. J.Ferguson, "The design of Controllers for the multivariable Robust servo mechanism Problems Using Parameter Optimization methods" *IEEE Transactions on Automatic Control,* Vol. AC-26, No 1, Feb 1981, 1981, pp. 93-110.

[18] J. H. Doyle, K. Glover, P. Khargonekar, and B. Francis, "State solutions to standard H_2 and H_∞ Control Problems" *IEEE Transactions on Automatic Control*, 34(8),1989, 831-847.

[19] S. Soucek, and T. Sauter, "*Quality of service concerns in IP based control systems*", IEEE transactions on Industrial Electronics, Vol 51, No 6. pp 1249-1258.

[20] C.E. de Souza and L. Xie, "On the Discrete-time Bounded Real Lemma with application in the characterization of static state feedback H_∞ controllers". *Systems & Control Letters,*18(1),1992, 61-71.

[21] B. Francis, "Lecture notes in Mathematics- H-Infinity Control theory" No. 1496, Springer Verlag.

[22] J. Gadewadikar, F. L. Lewis, and M. Abu-Khalaf (to appear), "Necessary and Sufficient Conditions for $\boldsymbol{H}_\infty$ Static Output-Feedback Control" AIAA, *Journal of Guidance Dynamics and Control*.

[23] P. Gahinet, A. Nemirovski, A. Laub, and M. Chilali, "LMI Control Tool box, MATLAB." Mathworks, Inc., Natick, MA, 1995.

[24] J. C. Geromel, and P.L.D. Peres, "Decentralised load frequency control" *IEE Proceedings*, 132(5), 1985, 225-230.

[25] J. C. Geromel, C.C. de Souza and R. E. Skelton, "Static output feedback controllers: stability and convexity" *IEEE Transactions on Automatic Control*, 43(1),1998, 120-125.

[26] J.C. Geromel, A. Yamakami, and V.A. Armentano "Structural constrained controllers for discrete-time linear systems" *J. Optimization Theory and Applications*, 61(1), 1989, 73-94.

[27] L. El Ghaoui, F. Oustry, M. AitRami, "A cone complementarity linearization algorithm for static output-feedback and related problems," *IEEE Transactions on Automatic Control*, Vol. 42, No. 8, 1997, pp. 1171-1176.

[28] G. Gu and P. Misra, "Disturbance Attenuation and H∞ optimization with linear output feedback control" *J. Guidance, Control, and Dynamics*, vol. 17(1), pp. 145-152, 1994.

[29] Hall Jr. W.E., and Bryson Jr. A.E., "The inclusion of rotor dynamics in controller design for helicopters," *J. Aircraft*, Vol 10, No 4.,1973, pp. 200-206.

[30] K. Hammoto, T. Fukuda, and T. Sugie, "Iterative feedback tuning of controllers for a two-mass spring system with friction," *in Proc. 39th IEEE Conference on Decision and Control*, Sydeny, Australia, 3000, pp. 2438-2443.

[31] Henrion, V. Kucera, A. Molina-Cristobal, “Optimizing simultaneously over the numerator and denominator polynomials in the Youla-Kucera Parametrization” *IEEE Transactions on Automatic Control* 50 (2005), 9, 1369-1374.

[32] G. Hewer, “An iterative technique for the computation of the steady state gains for the discrete optimal regulator. *IEEE Transactions on Automatic Control*, 16(4), 1988, 382-384.

[33] S. V. Hoesel, "*Optimization in Telecommunication Networks*". Statistica Neerlandica, Volume 59, Number 2, May 2005, pp. 180-205.

[34] Hol and C. Scherer, “Computing optimal fixed order H_∞-synthesis values by matrix sum of squares relaxations” Proc. IEEE Conf. Decision and Control, Nassau,2004, 3147-3153.

[35] Hotz and R. Skelton, “Covariance control theory” Int. J. Control, 45, 1987, 13-32.

[36] Hua, and P. Lancaster, “Analysis and modification of Newton’s method for algebraic riccati equations” *Mathematics of Computation,*67(223), 1998, 1089-1105.

[37] Isidori and A. Astolfi, “Disturbance attenuation and H_∞-control via measurement feedback in nonlinear systems. IEEE Trans. Automatic Control, 37(9), 1992, 1283-1293.

[38] T. Iwasaki, and R.E. Skelton, “All fixed order H_∞ controllers: observer based structure and covariance bounds” *IEEE Transactions on Automatic Control*, 40(3), ,1995, 512-516.

[39] F. Khan, K. Medepalli, S. Kumar, and S. Nanda, "*Performance of Data Applications over a CDMA Air Interface*" Kluwer Academic Publishers, Multiaccess, mobility and teletraffic for wireless communications: volume 5, pp 353 – 364.

[40] K. Khayati, P. Bigras, L. Dessaint, "A Multistage Position/Force Control for Constrained Robotic Systems With Friction: Joint-Space Decomposition, Linearization, and Multiobjective Observer/Controller Synthesis Using LMI Formalism," *IEEE Transaction on Industrial Electronics* , vol. 53, no. 5, pp. 1698-1712, October 2006.

[41] Y. H. Kim, and F. L. Lewis, *High-Level Feedback Control with Neural Networks*, World Scientific, Singapore, 1998, pp 55-75.

[42] D. Klienman "Stabilizing a discrete, constant, linear system with application to iterative methods for solving the riccati equation" *IEEE Transactions on Automatic Control*, 19(3), 1974, 252-254.

[43] D. L. Klienman, "On an Iterative Technique for Riccati Equations Computations," *IEEE Transactions on Automatic Control*, Vol. 30, No. 1, 1968, pp. 114-115.

[44] H. W. Knobloch, A. Isidori, and D. Flockerzi "Topics in Control Theory" Birkhauser, Berlin, Germany. 1993, pp. 43-49, 58-67,1993, 99-111.

[45] V. Kucera, "Stability of discrete linear feedback systems" Preprints 6th IFAC Congress, vol .1, paper 44.1, Boston 1975.

[46] V. Kucera, “Discrete Linear Control: The Polynomial Equation Approach” Wiley, Chichester, 1979.

[47] V. Kucera, and C. E. De Souza, “A necessary and sufficient condition for output feedback stabilizability,” *IFAC Journal, AUTOMATICA*, Vol. 31, No. 9, 1995, pp. 1357, 1359.

[48] O. Kuljaca, N. Swamy, F. L. Lewis, C. M. Kwan, “Design and Implementation of Industrial Neural Network Controller Using Backstepping,” *IEEE Transaction on Industrial Electronics* , vol. 50, pp. 193-201, 2003.

[49] B. Lee, Y. Chen, B. Chen, “*Robust H-Infinity Power Control for CDMA Cellular Communication Systems*”, IEEE Transactions on Signal Processing, 54(10), pp 3947-3956.

[50] W. S. Levine. and M. Athans, “On the determination of the optimal constant output feedback gains for linear multivariable systems” *IEEE Trans. Automatic Control*. Vol 15,1970, pp 44-48.

[51] F. L. Lewis (1992). Applied Optimal Control, Digital Design and Implementation. Prentice Hall.

[52] F. L. Lewis, V. L. Syrmos, “Optimal Control, 2nd edition” , Wiley-Interscience.New York, 1995.

[53] F. L. Lewis, D. M. Dawson, C. T. Abdallah, “Robot Manipulator Control: Theory and Practice” *Marcel Dekker* 2003.

[54] T. Mita, J. B. Matson, and B. D. O. Anderson, "A complete and simple parametrization of controllers for a non standsrd $\boldsymbol{H}_\infty$ control problem" *Automatica*, 34(3),1998, 369-374.

[55] D. D. Moerder, A. J.Calise, "Convergence of a Numerical Algorithm for calculating Optimal output feedback gains," IEEE Transactions on Automatic Control, Vol. 30, No. 9, 1985, pp. 900, 903.

[56] K. Ohishi, T. Miyazaki, K. Inomata, H. Yanagisawa, D. Koide, and H. Tokumaru "Robust tracking servo system considering force disturbance for the optical disk recording system," *IEEE Transaction on Industrial Electronics* , vol. 53, no. 3, pp. 838-847, June 2006.

[57] T. R. Parks, "Manual for Model 210/210a Rectilinear Control Systems" Educational Control Products, 2005.

[58] E. Prempain, and I. Postlethwaite, "Static H_∞ loop Shaping Control of a Fly-by-wire Helicopter,"*43rd IEEE Conference on Decision and Control*, Atlantis, Paradise Island, Bahmas, 2004, pp. 1188-1195.

[59] U. Shaked, "An LPD approach to robust H_2 and H_∞ static output-feedback design" *IEEE Trans. Automatic Control*, 48(5),2003, 866-872.

[60] R.E. Skelton and T. Iwasaki, Lyapunov and covariance controllers. Int. J. Control, 57, 519-536.

[61] B. L. Stevens, and F. L. Lewis, "Aircraft Control and Simulation" 2nd ed, 2003, Wiley Interscience, New York.

[62] A. Stoorvogel, and A. Weeren, "The discrete time Riccati equation related to the H_∞ control problem" *IEEE Transactions on Automatic Control*, 39(3),1994, 686-691.

[63] V. L. Syrmos, C. Abdallah; P. Dorato, "Static output feedback: a survey," *Proceedings of 33rd IEEE Conference on Decision and Control*, Orlando, FL, 1994, pp. 837-842

[64] V. L. Syrmos, C.T. Abdallah, P. Dorato, and K. Grigoriadis (1997). Static output feedback- a survey. *Automatica*, 33(2),125-137.

[65] A. Trofino-Neto, and V. Kucera, "Stabilization via static output feedback," *IEEE Transactions on Automatic Control*, Vol. 38, No. 5, 1993, pp. 764, 765.

[66] J. Van der schaft "L_2 gain Analysis of Nonlinear Systems and Nonlinear State Feedback H_∞ Control" *IEEE Transactions on Automatic Control*, 37(6), 1992, 770-784.

[67] R. Wai, and P. Chen, "Robust Neural-Fuzzy-Network Control for Robot Manipulator Including Actuator Dynamics," *IEEE Transaction on Industrial Electronics* , vol. 53, no. 4, pp. 1328-1349, August 2006.

[68] W. M. Wonham (1985) Linear Multivariable Control Springer Verlag , Berlin, Germany, 1985.

[69] Yang, C. Kung, K. Huang, and F. Yeh, "Parametrization of nonlinear H_∞ output feedback controllers- an algebraic approach via bounded real lemma" *Proceedings of the 35th Conference on Decision and Control*, Kobe, Japan, 1996.

[70] K. Yang, R. Orsi, and J.B. Moore, "A projective algorithm for static output feedback stabilization" *Symposium on System, Structure and Control,*Oaxaca, 2004, pp 263-268.

[71] K. Yasuda, R. Skelton, and K. Grigoriadis, "Covariance controllers: a new parameterization of the class of all stabilizing controlers" *Automatica,* 29, 1993, 785-788.

[72] D.C. Youla, H. A. Jabr, and I J. Bongiorno, "Modern Wiener-Hopf design of optimal controllers, Part II: The multivariable case" *IEEE Trans. Auto. Control,* vol. AC-21, pp. 319-338, June 1976.

[73] J.-T. Yu, "A convergent algorithm for Computing Stabilizing Static Output-Feedback Gains" *IEEE Transactions on Automatic Control*, 49(12), 2004, 2271-2275.

[74] Yung, and C. Yang, "H_∞ Control for linear time-varying systems: Controller Parameterization" *IEEE Transactions on Automatic Control*, 44(11), 1999, 2058-2062.

[75] G. Zames, "Feedback and optimal sensitivity: Model reference transformations, multiplicative seminorms, and approximate inverses," *IEEE Transactions on Automatic Control*, Vol. 26, No. 2, 1981, pp. 301-320.

[76] M. Zeren, and H. Ozbay, "On the strong stabilization and stable H_∞ controller design problems for MIMO systems" *Automatica*, Vol. 36(x), 2000, 1675-1684.

[77] K. Zhou, "On the parameterization of H_∞ controllers" *IEEE Trans. Automatic Control*, 37(9), 1992, 1442-1445.

BIOGRAPHICAL INFORMATION

Jyotirmay Gadewadikar received his Bachelor's degree in Electronics and Instrumentation Engineering from S. G. S. Institute of Technology and Science, Indore, India in 1997. He then worked for Tata Steel as a Senior Officer and was involved with installation and commissioning in Cold Rolling Mill Project. He received the Master's of Science in Electrical Engineering in 2003. He then joined Automation and Robotics Research Institute (ARRI) for- Systems & Controls Research, Prototyping & Implementation of Control Algorithms on Electromechanical Systems, taught Control System Design Capstone course, and was involved in the set up & development of undergraduate controls lab. He was also at Qualcomm, San Diego as an Intern. His research work includes H-Infinity control, Output-Feedback Control, Helicopter UAV control, Electro-Mechanical systems, and Automated Testing and Measurement tools development for Wireless Networks.